Hovedoppgave

NTNU
Norges teknisk-naturvitenskapelige universitet
Fakultet for informasjonsteknologi og elektroteknikk
Institutt for energi- og prosessteknikk

Blaszkiewicz, Robert

Green methanol

- by an offshore-onshore optimization case study

Hovedoppgave i Energi og Miljø
Veileder: Lars Olof Nord
Medveileder: Even Solbraa
Juni 2023

NTNU
Kunnskap for en bedre verden

Blaszkiewicz, Robert

Green methanol

- by an offshore-onshore optimization case study

Hovedoppgave i Energi og Miljø
Veileder: Lars Olof Nord
Medveileder: Even Solbraa
Juni 2023

Norges teknisk-naturvitenskapelige universitet
Fakultet for informasjonsteknologi og elektroteknikk
Institutt for energi- og prosessteknikk

NTNU
Kunnskap for en bedre verden

Acknowledgments

I am happy to present this thesis as the final step of my M.Sc. in Energy and Environment at the Norwegian University of Science and Technology. Embarking on this creative and as the thesis caveat itself - periodically challenging - work, I would like to thank my supervisor, Professor Lars Olof Nord for the opportunity to pursuit this endeavour from scratch in January, with the support from co-supervisor Professor Even Solbraa. I would also like to thank Sylfest Myklatun for clarification correspondences on technical possibilities and Benjamin Mitterrutzner for aid on the economical aspect. Lastly, thank you to all my fellow colleagues at the study room for all the good discussions and support, and especially for polishing my salesmanship in the ever-refining answer on: *How is it going with the thesis?*

Abstract

This research investigated the feasibility of synthesizing green methanol in light of its projections as an interesting e-fuel, by combining hydrogen and carbon dioxide by means of renewable energy sources. Therefore, three key performance indicators were to be assessed: the levelized cost of energy (LCOE), the cost of hydrogen per kg, and the cost of methanol per tonne. The project aimed at optimizing power routing, where an intermittent storage solution between the power source and the electrolyzers, was at the core of it and controlling the output. Ultimately, the goal was to produce as much – and as stable as possible. This was achieved to an extent by stage-wise sensitivity analysis with a methodology - inspired by manufacturing industry technique called parallel processing, alongside considerations for technological and economical aspects and projections, for the stipulated case studies in 2020 and 2030. The findings revealed a general trend of an increased adjusted power demand per kg of H2, accounting for power stored, with higher wind turbine capacity. This highlighted the critical role of storage technology in this process. The study also indicated that higher round-trip efficiency and cost-effective storage solutions improved system performance considerably. Moreover, power sales were introduced to make the system more cost effective and realistic. In the end, LCOE values were at large on the lower end of typical values, partially due to offsetting revenues from annual power sales and the deduction of CO2 taxes, albeit notwithstanding the simple economical modeling and great uncertainties with the large scale of the system. Consequently, impacting the hydrogen self-costs and raw methanol prices, implying great margins to the current trading prices. In conclusion, this study presented a promising potential to produce green methanol as a renewable energy source, and identified several areas for further development, such as improving the power routing model and incorporating multiple renewable energy sources for stability. The research provides both a creative and a periodical approach of the traditionally synthesizing of methanol.

Sammendrag

Denne forskinga undersøkte moglegheita for å syntetisere grøn metanol i lys av prognosene som eit interessant e-drivstoff, ved å kombinere hydrogen og karbondioksid ved hjelp av fornybare energikjelder. Dermed skulle tre nøkkel ytelsesindikatorar vurderast: den justerte energikostnaden (LCOE), kostnaden for hydrogen per kg, og kostnaden for metanol per tonn. Prosjektet sikta mot å optimalisere straumfordeling, med ei lagringsløysing mellom kraftkilden og elektrolysørene. Dette stod i kjernen kvar sistnemnde styrte produksjonen. Målet var å produsere så mykje - og så stabilt som mogleg. Dette vart oppnådd til ein viss grad ved stegvis sensitivitetsanalyse og metodikk inspirert frå parallellprosessering i produksjonsindustrien, saman med omsyn til teknologiske og økonomiske aspekt og prognoser, for dei fastsette kasusstudiene i 2020 og 2030. Funna viste ein generell trend med auka justert kraftbruk per kg H2, med omsyn til lagret straum, særleg med høgare vindturbinkapasitet. Dette framheva den kritiske rolla til lagringsteknologi i denne prosessen. Studien viste også at høgare rundtur-effektivitet og kostnadseffektive lagringsløysingar forbetra systemytelsen betydeleg. Vidare vart kraftsal implementert for å gjere systemet meir kostnadseffektivt og realistisk. Til slutt var LCOE verdiene i stor grad på den nedre enden av typiske verdier, delvis på grunn av motverkande inntekter fra årlig kraftsalg og frådrag av CO2 skatt, til tross for den enkle økonomiske modelleringa og store usikkerheiter knytta til storeleiken på systemet. Følgelig påverka dette sjølvkostnadene til hydrogen og den rå metanolprisen, noko som innebar store marginer til dei nåværande handelsprisane. Til slutt presenterte denne studien eit lovande potensial for å produsere grøn metanol frå fornybare energikjelder, og identifiserte fleire områder for vidare utvikling, som å forbetre kraftfordelingsmodellen og inkorporere ulike fornybare energikjelder for stabilitet. Forskinga gir både ein kreativ og ein periodisk tilnærming til den tradisjonelle syntesen av metanol.

Nomenclature

ADPH Adjusted Power Demand per Hydrogen [kWh/kg H2]

BE Bank of Electricity; intermittent storage solution

CH3OH Methanol

CO2 Carbon dioxide

CoC Core of the Code

DAC Direct Air Capture

FLH Full Load Hours

H2 Hydrogen

KPI Key Performance Indicator

LCOE Levelized Cost of Energy [$/MWh]

RTE Round-trip efficiency

S-DAC Solid DAC

SurpUtz Surplus Utilization Factor

UTF Utilization Factor

WACC Weighted Average Cost of Capital

Table of Contents

List of Figures

List of Tables

Chapter 1

Introduction

1.1 Motivation

In light of future fuel developments, methanol has been portrayed as a promising *e-fuel*. Especially green methanol, with virtually no carbon footprint - if produced by and with renewable energy sources [1].

A substance already known to industry, it can be further refined into kerosene, commonly known as jet fuel [2]. Hence, eligible for the aviation industry, beyond the thought long distance shipping and heavy industries, where battery electric is considered unsuitable [3]. Furthermore, whilst seaborn emissions accounted for 2.9% of 2018 global, [4], its share will only increase if not kept up with onshore developments. Despite more stringent international emission regulations [5], propulsion reduction [6],[7], more hydrodynamic ship designs [8] and solutions [9] - the emissions will not eye carbon neutrality in the end [10]. To solve this and beyond the aforementioned fields, industry majors are investigating and teaming up in ventures to facilitate solutions for renewable solutions [11]. Porsche's e-fuel facility is operative in Chile [12], and a Norwegian company called *Norsk e-Fuel* is set to start in 2024 [13]. Having to plan years ahead, shipping major A.P. Moller - Maersk has already ordered dual-fuel vessels with methanol suitability [14], one of which is to be celebrated publicly during the Fall of 2023. [15].

Besides the aspect of an e-fuel, green methanol in itself might be of interest and necessity for the industry in the long run vis-a-vis more stringent emission regulations and focus on individual product impact [16]

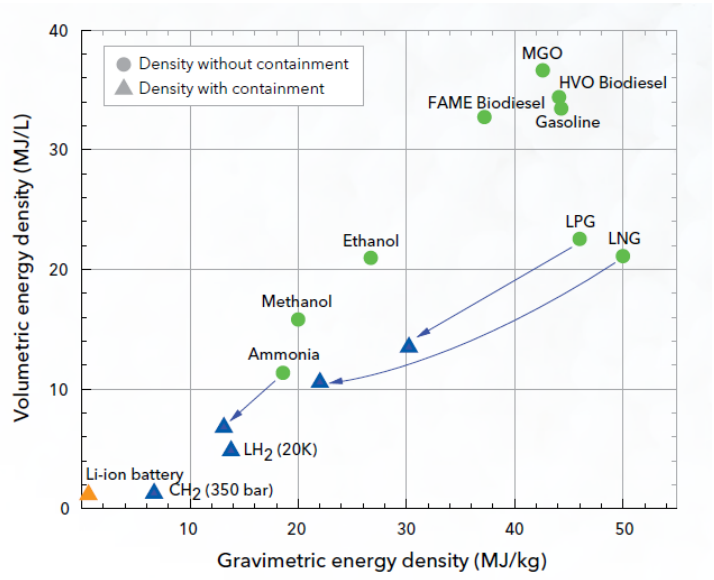

Figure 1.1: Gravimetric and Volumtric energy density chart [17]

Figure 1.1 demonstrates one significant, favourable property of methanol: **the energy density**; from which it is clear that the most anticipated e-fuels, hydrogen and ammonia, come short when accounting for their respective tank weight, as illustrated by the triangular icons. On the other hand, Figure 1.1 also depicts the decrease in both gravimetric and volumetric energy density for e-fuels as compared to traditional fuels such as gasoline.

Moreover, methanol is liquid at room temperature [18] as opposed the two counterparts being gaseous and thus more challenging handling in terms of transportation and storage; in regards to Figure 1.1 needing compression or cooling. In technical terms, methanol has lower vapour pressure and is less volatile than the two, which in turn leads to lower boil-off gas if compared on the same temperature. Additionally, methanol has a more developed infrastructure compared to hydrogen, whilst ammonia has a mature infrastructure from the fertilizer industry [17]

Ignition-wise, hydrogen [19] and methanol ignite fairly at low concentrations and energy as opposed to ammonia - which also has an environmental impact of thermal nitrogen oxides.

Lastly, ammonia [20] and methanol are toxic, where the primer, if exposed to high concentration can lead to permanent respiratory damage, whilst the latter can turn into toxic acid once inhaled. That said, the light atom weight of hydrogen impose a great safety risk of detonation. Therefore ventilation and sensors are of outermost importance here.

In sum, with emphasize on infrastructure, experience and properties - methanol seems like a viable e-fuel option.

1.2 Objectives

Therefore, the present work will investigate the possibilities of green methanol synthesis - process of combining green hydrogen with carbon dioxide; that is, carbon capture powered by renewable electricity. To combat its periodicity, stabilization by storage solutions will be at the core of the present work. In the end, the objective is to arrive at three key performance indicators:

- **the levelized cost of energy for the proposed system ($/MWh)**
- **the self-cost of hydrogen per kg ($/kg H2)**
- **The self-cost of methanol per tonne ($/MT)**

The primer being based on investment cost of the system and the total renewable power generated in a given time frame and set conditions. In turn, quantifying the latter based on one year of operation and adjustments. Thereafter, combining the latter with the price of carbon capture onshore - raw methanol price will be attained; to be synthesized in the end based on further cost estimates. [1].

Henceforth, the case study will at large be optimization-oriented around power routing and consequently hydrogen production. That is, by means of repeated sensitivity analysis, in developing phases on a method inspired by general parallel processing layout from manufacturing industries [21] - in combination with technology possibilities of the stacking structure of electrolyzers; used to produce hydrogen gas. Scenarios will be developed for an investment start in 2020 and 2030, distinguished by electrolyzer efficiency, in addition to various storage technologies, herein cost estimates and preconditions.

Nuancing further by selecting the power source location to be in Norway, based recent government concessions [22].

1.3 Challenges

At large the main the challenge will be to stabilize the periodicity of the incoming power generated by the renewable source. Thereby, develop a program to distribute this power satisfactory, upon which a handful results will be selected based on key parameters stipulating a sorting formula. Meaning, selecting it wisely in regard to the trade-offs will shape the present work. Lastly, the cost estimates for the large scale will have to be to an extent technologically realistic, whilst the economical aspect will per definition include uncertainties due to the said scale.

1.4 Contribution

To the best of author's knowledge this work is not attempted before in conjunction with the format of the case study. That is, optimization research on specific components can be readily found, e.g. on dynamic electrolyzer management [23] or optimized strategies for wind turbine placements [24].

Applying an inspired methodology onto electrolyzer management, in turn based on storage capacity is believed to be unique in this context, and more so by the incorporation of the notable periodicity onto traditionally more stable methanol synthesis from natural gas [25]. Notwithstanding the rather simple approach to model the whole system, the present work aims to shed light on a new, green methanol producing pathway.

1.5 Outline

In Chapter 2, schematic overview of the green methanol synthetization will be given together with brief introduction of DAC and electrolyzer technology. In Chapter 3, the case study will be presented, followed by its process, code and economical modeling. Thereafter, in Chapters 3.7-3.11 the format of the outputting data, the sorting formula, optimization parameters and their ranges will be stipulated. Lastly financial conditions will be presented in Chapter 3.5. In Chapter 4, the results will be presented for phase 1, and subsequently twofold for phase 2, as 2030 and 2020 scenarios with a comparison later. Next, Presenting Phase 3 results in Chapter 4.3, completing the simulation setup and providing data for the cost estimates of the sought key performance indicators in Chapter 4.4. Furthermore, general results and discussion will be done in Chapter 4.7, before concluding and shedding light on future work potential.

Chapter 2

Background

2.1 Green Methanol Synthesis Process

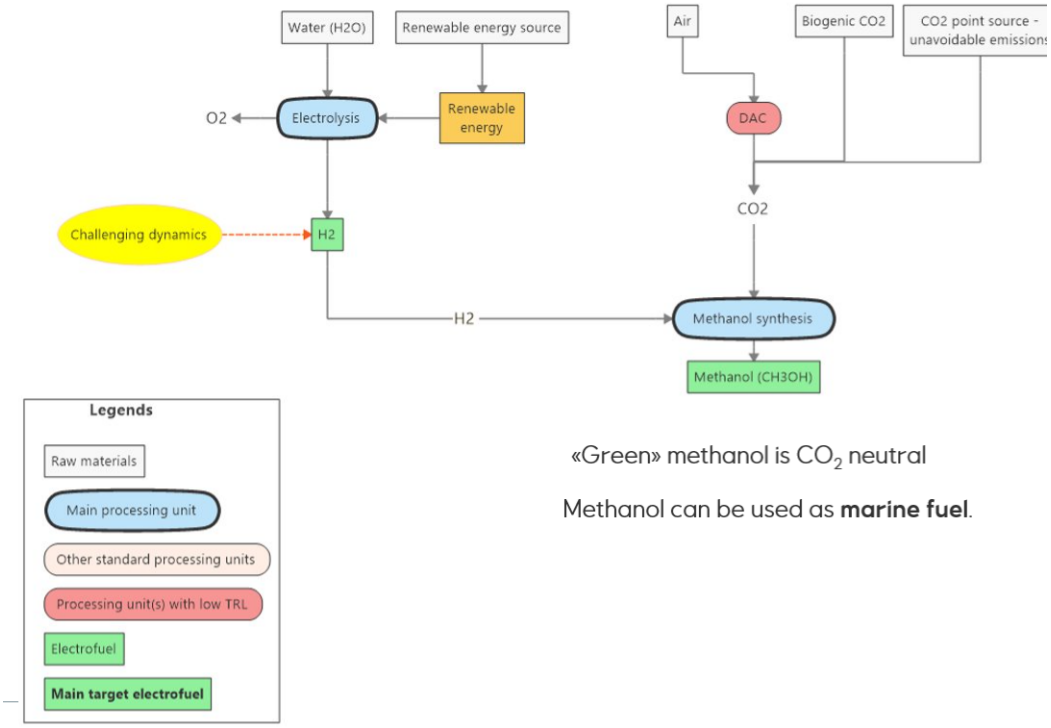

Figure 2.1: Schematic overview of green methanol production
[26] Assumed that the DAC-unit is powered by 100% renewable energy

Acknowledging that there are various approaches to synthesize methanol, Figure 2.1 shows the overview for the selected method for green methanol. Stoichiometric calculations are presented in Appendix D.

Considering Figure 2.1 as self-explanatory, worth mentioning is the water aspect; here assumed to be abundant due to the offshore location, not withstanding possible desalination problem. Moreover, a bi-product of the electrolysis - splitting water into hydrogen and

oxygen gas, described shortly in chapter 2.2 - is the oxygen itself. This is not considered in the following, albeit a possibility to capitalize on and hence offset any production costs of the primer.

Moving to the right hand side of the scheme, is the carbon capture process, of which sources can vary from point-based, biogenic or directly from air. As the names suggest, the primer is typically flue gas from chimneys being captured and the latter from combustion of decomposed biological material. Lastly, and chosen for the present work, capturing CO2 directly from the air, by technology often referred to as DAC - Direct Air Capture, described more in Chapter 2.3.

2.2 Hydrogen Electrolyzers

An addition to the *challenging dynamics* - are the hydrogen electrolyzers themselves, where the total chemical reaction is described below in equation 2.1. For simplicity, energy potential and enthalpy, in addition to anode and cathode specifics are excluded. Left and right hand side, is in liquid (l) and gaseous (g) state, respectively.

$$2H_2O\ (l) \xrightarrow{electrolysis} 2H_2(g) + O_2(g) \tag{2.1}$$

The technology is constantly evolving to operate under various pressure [27], salinity and humidity [28], and temperature [29] conditions, in addition to choosing materials carefully and cost effectively [30]. The most prominent subgroups are known as Alkaline (ALK) [31], polymer electrolyte membrane (PEM) [32] and anion exchange membrane (AEM) [33] electrolyzers.

For the problem at hand, and in regards to Figure 3.1, PEM electrolyzers are selected due to their known capability of handling dynamic conditions better than ALK, and regarding the AEM as novel technology. Since the scope is not on the equipment specifics per se, there will be no literature review on a specific PEM electrolyzer of choice, but rather using the values found for pure power production demand and projections for 2030 [34].

2.3 DAC - Direct Air Capture

Direct air capture (DAC) is a technology that captures air from the atmosphere, after which it is filtrated and compressed for further usage [35]. The most common types are differentiated by low pressure and medium temperatures (80-120℃) with a solid material used for the process, known as a S-DAC. Alternatively, are the high temperature ones operating at ranges of 300-900℃, with liquid solution material for the process, hence called a L-DAC. Moreover, the power supply is usually a combination of electrical and thermal energy [36]. The selected DAC is presented later in Subchapter 3.1.

Chapter 3

Methods

3.1 Case study

Brief overview

The starting point for the selected case study is to replicate the production of Equinor's methanol plant at Tjeldbergodden - by renewables. That is, approximately 100 tonne of methanol per hour [37], which by stoichiometry D on a mass basis is found to be **18.75 tonne hydrogen per hour**. The remaining part, carbon dioxide (CO2), is latter to be added on more simple terms (for reference: 137.5 tonne CO2 per hour). The caveat is to produce both sufficient and stable power for the electrolyzers and downstream processes. Hence, optimization by conducting sensitivity analysis in phases will be performed.

By the share size of the output and recent energy plan announcements by the Norwegian government [22],[38], wind turbines are selected as the renewable electricity source for the problem at hand. Specifically, field *Vestavind F* also known as Utsira Nord, outside the coast of Haugesund area. Here, their plan is to install three offshore wind parks each 500 MW, totalling 1.5 GW; upwards of 2.25 GW upon further investigation [39]. In addition, the geolocation of these turbines to be installed, is favourable in terms of to the significant gas refinery at Kårstø [40] and the corresponding pipeline network to Europe [41],[42]. Figure 3.1 below, depicts the wind profile for 1 GW of installed capacity at the said location [43], illustrating the *challenging dynamics* seen previously for the synthesis scheme, in Chapter 2.1. The specifics for the wind turbines are given shortly in Chapter 3.1, where they will be combined to various capacities later in Chapter 3.9.

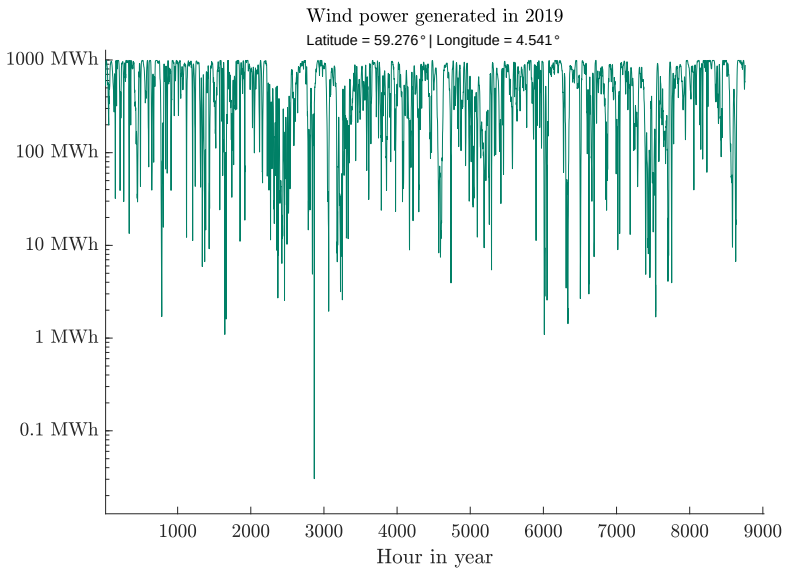

Figure 3.1: Wind profile for selected location
with 1 GW installed capacity

Next, having in mind that equipment thrives best in steady or near their design points, the periodicity shown in Figure 3.1, underscored by the downward spikes, results in a demand for an intermittent storage solution. That is, between the wind turbines and the electrolyzers. This will be called *Bank of Electricity* or *BE* in short, where the idea is to balance out the incoming power, subsequently feeding the electrolyzers more steadily and in turn produce hydrogen more predictably. Since the focus will lay primarily on optimizing the wind profile and not excluding future technologies, BE will be a black box upon receiving results - and from there discussed whether the proposed solutions are realistic today or even in the years to come - both technically and economically.

Nuancing further by having four main instances,

- Instance 1: Start in 2030, 50 kWh/kg H2 electrolyzers, strict code
- Instance 2: Start in 2030, 50 kWh/kg H2 electrolyzers, loose code

- Instance 3: Start in 2020, 60 kWh/kg H2 electrolyzers, strict code
- Instance 4: Start in 2020, 60 kWh/kg H2 electrolyzers, loose code

The scenarios will mainly be differentiated by electrolyzer technology of today and the projected in 2030 [34]. Moreover, the distinction between strict and loose code refers to the settings in the self-developed programming code, described later in Chapter 3.6. Number-wise, if the 18.750 kg of hydrogen per hour is to be produced by the said electrolyzers, it requires 937,5 and 1.125 MWh/h of installed electrolyzers at maximum load, respectively. Hence, the wind farm location is not arbitrarily chosen, and the size ranges will be given later in Chapter 3.9. All the above will be phase 1 of the optimization sequence.

Results will then be sorted out by wind turbine installment and further by selected target parameters, e.g. hydrogen output and intermittent storage peak demand, described later in Chapter 3.7. Next, one configuration for each turbine size - for each instance above, will be selected for further optimization in phase 2. There, the developed code will have mechanisms activated aiming to stabilize the intermittent storage (BE) and the hydrogen production. Hence, the parameters for these mechanisms will account for optimization parameters in phase 2, to be presented in Chapter 3.10. All the aforementioned is located offshore in this context. Additionally, power sales will be introduced if applicable.

Consequently, phase 2 results will be sorted by the same sorting formula, and once again the best configuration will be eligible for phase 3; which will be the pipeline delivery of hydrogen to onshore. There, Kårstø has been selected in light of the aforementioned. Based on distance measures [44], the pipeline will measure 56 km or more, that is, as the number of pipelines will be one of the optimization parameters, described in Chapter 3.11. Additionally, the pipeline will work as an intermittent storage in itself before delivery, aiming to replicate the line packing technique of today's natural gas pipelines [45]. The DAC will be located onshore, with an external power supply.

Finally, the end goal is to get data on key performance indicators (KPIs) such as the levelized cost of energy (LCOE) of the system, i.e., the minimal cost to generated one MWh of power, including the whole system investment. Next, the hydrogen self-cost, to be given by LCOE and APDH: how many kWh are generated relative to the total output, i.e. adjusting for the storage withholding. Lastly, as stated, cost associated with carbon capture will be factored in to get a raw methanol price; raw, as two separate self-costs of hydrogen and CO2 summed. Interested findings will be presented beyond the stated.

Wind turbine selection

Choosing a state of the art wind turbine is important for the relevancy of this text, particularly when including scenarios for 2030. Therefore, Vestas V164 - 9500 was selected [46]. As the name suggests, each turbine is capable of generating 9.5 MW per hour at full load - equivalent to powering 369 Norwegian households for an entire year - in just one hour [47]. All this, caught by the 164 meter in diameter rotor.

For the problem at hand, the technical specific of the hub height above the ocean, is set to 105 meters by literature review [48]. With the later introductions of economics, the wind turbines will have a floating structure in regards to the deep water location. Else, factors such as cut-in and cut-out wind speeds for the turbine are assumed modeled by wind profile source from renewables.ninja [43].

DAC selection

The selected DAC will be a high-temperature with aqueous solution, L-DAC, based on a pilot project [49]. Selected due to a electrical only supply [36], in light of a possible integration to the offshore system in the case study.

Scope limitations

Beyond the stated, there will be no focus on equipment specifics beyond the necessary for optimization purposes, i.e., it not mentioned then it is to be considered not included. To the extent possible, the presented technologies and estimates will be sought to be realistic, notwithstanding the large scale.

Moreover, operational aspects such as the need for preheat and purge gas to keep the electrolyzers semi-idle when coupled out - will not be modeled. Next, the compressor stage between electrolyzer output and injections to the pipeline network will omitted, i.e., hydrogen will be assumed compressed when entering the pipeline network.

Lastly, at first glance 2020 is a peculiar choice belonging to the present. However, during the first stage of literature review, projections were often presented as 2020 and 2030 scenarios. Additionally the wind profile was based on 2019 data.

3.2 Phase 1 - Energy Routing

Coefficients - c8,c6 and c4

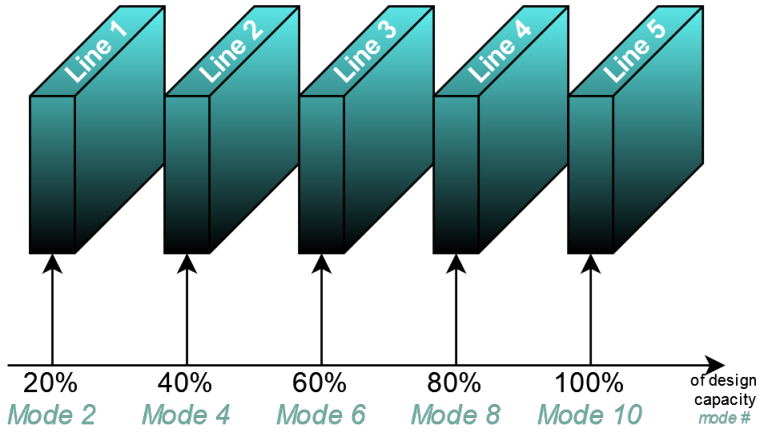

Figure 3.2: Parallel processing with electrolyzers

The initial inspiration for the energy routing was the manufacturing technique called *parallel processing*. Where in a normal series-based operation, executing step-wise until a product is made - the parallel method, spreads the different steps in parallel, each as independent process lines.

Next, the methodology was applied for the present work, with the starting foundation of having individual lines of only electrolyzers, each contributing their share of the total output capacity, as illustrated in Figure 3.2; equal shares 20%, with the corresponding names of modes 2, 4, 6, 8, and 10. Here, mode 2 represents one line, mode 4 represents two lines, each outputting 40% of capacity, and so on, up to mode 10 which equals 100% capacity. Furthermore, assumed here to not have options to run modes partially, i.e., no "mode 5".

Next, mode 2 was replaced with *mode 0* - the charging mode, in the case of insufficient wind power production. It should be noted that target production and maximum output were henceforth and subsequently used to refer to the same goal: 18.75 tonne of hydrogen per hour.

Following the optimization thread, these modes were still referred to as mode 0, 4, 6, 8, and 10 – albeit with their shares of target production - their *coefficients* – made variable. This meant that the initial shares of 20% were adjusted, except for mode 0 and 10 - which were charging and full production, respectively. For example, the coefficient associated with mode 8, was referred to as c8. While c8 had previously been fixed at 0.8 or 80%, the idea was to make it optimizable by exploring a range of values. This applied to c6 and c4 as well, with these referred to as core coefficients in the following discussion, and quantified later in Chapter 3.9.

BuT - Build up Time

Recalling the bank of electricity concept, it was set to start out empty. The next proposal was to build up a buffer before starting electrolysis, equivalent to a set number of hours that the electrolyzers could run at maximum load - without the addition of more power, i.e., in the scenario of minimal or no wind power output. This set amount of hours was one optimization parameter named *build up time* (BuT).

For instance: if BuT was set to 10 hours and the energy amount required per hour for mode 10 was 1.125 GW/h (2020), the buffer in the electricity bank would amount to 10 hours * 1.125 GW = 11.25 GWh at the start.

Margin & Thresholds

Furthermore, the previously mentioned 11.25 GWh was introduced as a **margin**. Once the margin was set, storage threshold levels were calculated by multiplying the aforementioned coefficients with the margin, as illustrated in Figure 3.3 below. In turn, based on the actual stored capacity in the bank of electricity, the thresholds determined the electrolyzer mode and consequently the hydrogen output, as illustrated on the right-hand side of Figure 3.3. Operationally, the buffering introduced with BuT and margin, was conditional. That is, one could choose to either buffer up to the margin before starting electrolysis, or let the system gradually increase the electrolyzer output from the charging state. On the other hand, it was necessary for the Matlab-code.

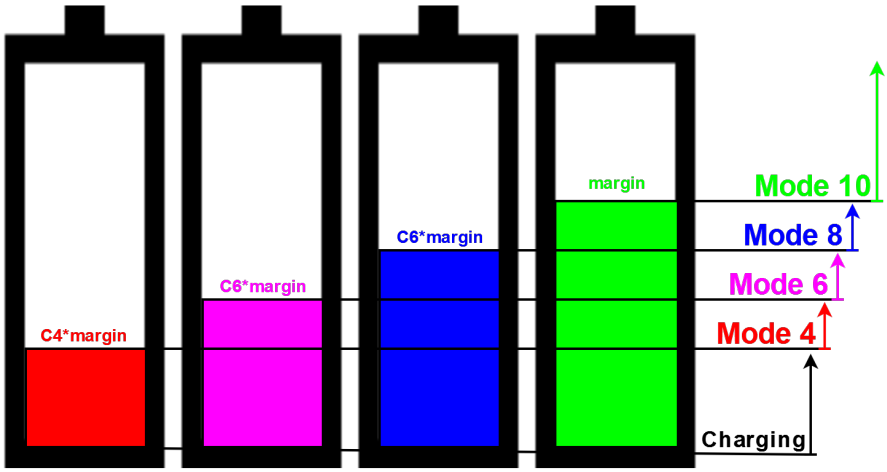

Figure 3.3: Margin and thresholds
Since c10 is per definition 1, the threshold for maximum production is the margin itself. There is no overhead to the margin, i.e. great degree of freedom potential

RTE - Round Trip Efficiency

Next, after each production hour, an indicator checked the storage level, passing on information to the following hour. Subsequently, the electrolyzer mode was selected. Then, if the

generated wind power exceeded the particular hourly demand, it was stored. Conversely, if there was not enough energy to meet the specific hourly demand for the electrolyzers, the storage was depleted by the difference between the energy produced and the energy required. In both cases, this difference was calculated and referred to as **netto**. This process is illustrated in Figure 3.4 below.

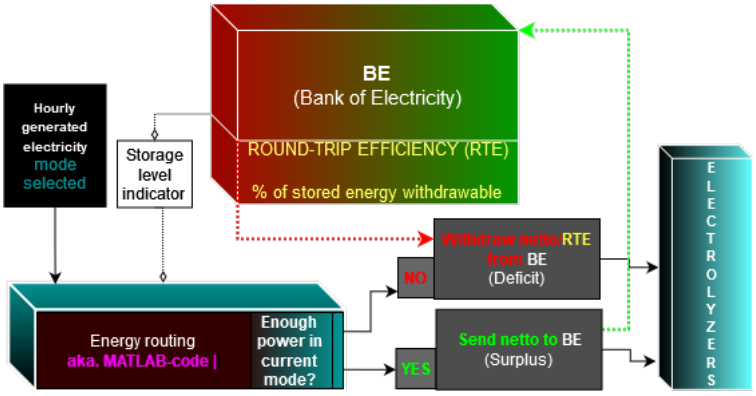

Figure 3.4: Netto and round-trip efficiency

At this point, round-trip efficiency ("**RTE**") was introduced to add detail to the basic format of the bank of electricity (BE). The concept here was twofold for surplus and deficit power. For the primer, 100% of the excess energy was directed into intermittent storage. On the other hand, for deficit power, the amount that should be withdrawn from the storage was the desired amount divided by a round-trip efficiency factor (RTE). This is usually associated with losses incurred when storing power and withdrawing it at a later point in time. Hence, various storage technologies were simulated using appropriate RTE values.

$$\text{Withdrawal amount from BE} = \frac{\text{Desired amount}}{\text{RTE}} \tag{3.1}$$

For example, if the RTE was 50%, dividing by 0.50 was equivalent to multiplying by 2, meaning that the actual storage drain was twice the desired amount as perceived by the electrolyzers' mode. Therefore, RTE was expected to be a highly impactful optimization parameter.

Lastly, acknowledging that the term "RTE" was implemented somewhat simply, as it is traditionally known to have more loss-driving elements and conversion stages from power input to output, than just the division by the factor itself. However, since the focus was on the optimization, this was deemed satisfactory.

Simulation concept

Gathering the aforementioned and building on Figure 3.4, yielded the process sketch for all phases seen in Figure 3.5. Here, Phase 2 represents the further development of the energy routing, whilst Phase 3 is the flow assurance and delivery of the hydrogen to shore.

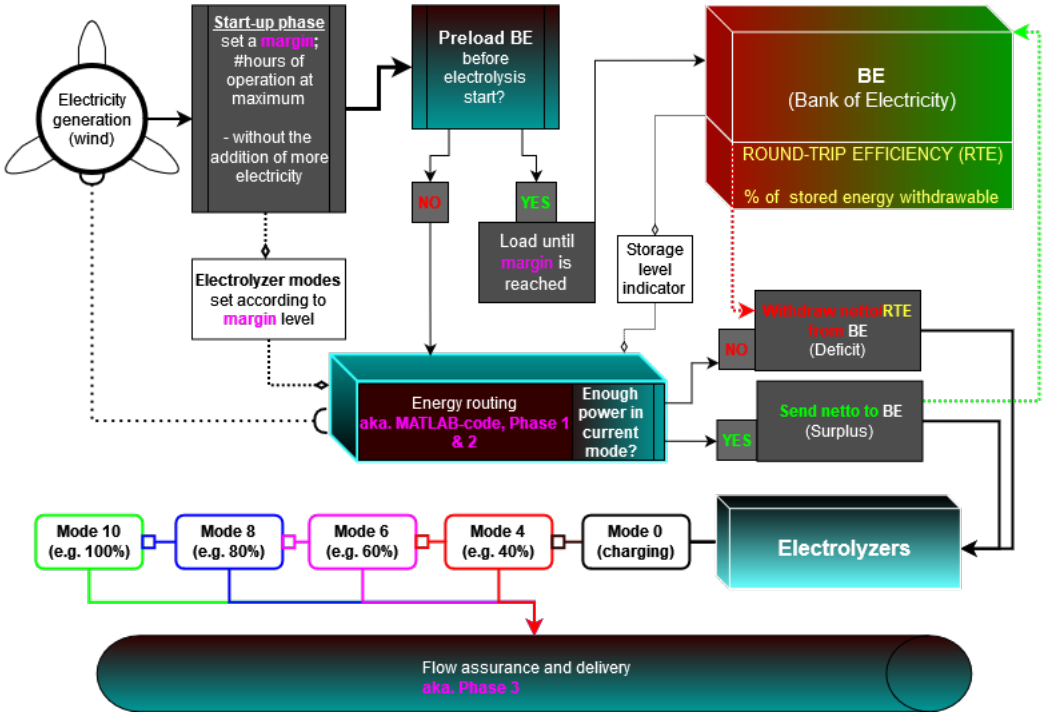

Figure 3.5: Phase 1: Concept sketch

The last optimization parameter in Phase 1 was the combined wind turbine capacity. Quantified in Chapter 3.9 by the demand and challenging demands portrayed previously in Figure 3.1 in Chapter 3.1.

3.3 Phase 2 - Implementation of Mechanisms

Based on phase 1, mechanisms were developed with a focus on stabilization and target delivery. The primary goal was to stabilize the development of intermittent storage, which on an isolated basis might reduce the overall electrolyzer output. That said, measures for the opposite effect were also put in place.

Freezemode

As the name suggests, Freezemode froze the electrolyzer mode for a certain number of hours ahead of the current one. The aim was to override the system's energy routing in favor of predictable and stable production. In and of itself, this was a realistic option with great potential for future work. Moreover, was the foundation for HillClimb and SafetyNet, described below.

HillClimb – Preventing Storage Build-up

To make use of periods of consistent surplus power rather than routing it to the intermittent storage solution - only to later withdraw it at a lower fraction (recall: RTE in Chapter 3.2) - the idea was to divert the power flow to either surplus hydrogen production or transmit it to shore. This strategy was valid for the highest electrolyzer mode; for the rest, the mechanism would increase the current electrolyzer mode.

For the first power allocation option, this would realistically require additional electrolyzer capacity, and consequently additional investments and more. Not to mention the question of implementing more capacity for the system in general. On the other hand, returning power - by means of selling it onshore via a transmission line, could provide extra revenue and consequently offset the sought KPIs. The latter was the preferred approach, while the primer will be found in the Appendices in the full versions of the coherent tables presented in Chapter 4 . It is important to acknowledge that either way, the utilization of surplus could lead to more fluctuations in storage level, as not everything would be going to the BE anymore, as was the case in phase 1.

SafetyNet - Reduction of Volatility

Conversely, SafetyNet was the proposed solution for periods of frequent withdrawal from the BE. That is, reducing the withdrawal by lowering the electrolyzer mode relative to intermittent storage thresholds and the operation suggested in phase 1. Moreover, in times of high deficit frequency, the electrolyzers would be adjusted downward accordingly until they reached charging status – if necessary.

3.4 Phase 3 - Flow Assurance and Delivery

The final phase of the simulation setup focused on the hydrogen after it had been produced, i.e., by pipeline delivery to shore. This phase was divided into two parts. Firstly, the same threshold methodology applied for the energy routing in phase 1 was used to base the flow delivery on pipe thresholds, which in turn were based on a calculated pipeline margin. For simplicity, the same coefficients from phase 1 were used, consistent with the configurations selected from phases 1 and 2. Furthermore, the number of pipes was altered, as the distance between the geographical location and Kårstø was found to be only 56 km, as described in Chapter 3.1.

Secondly, provided time and successful implementation of all the preceding phases, an attempt to replicate the line packing technique used in natural gas pipelines was to be made. This technique involved altering the pressure in the pipeline; for example, one could slow down the flow by increasing pressure while simultaneously delivering the same or more amount of hydrogen, and vice versa. In addition, an override feature of phases 1 and 2 was developed, thus prioritizing delivery over intermittent storage stability.

In Chapter 3.11, the optimization parameters of number of pipes and pipeline margin were accompanied by a *first buffer margin* - a margin to the pipeline margin - when initially buffering up the pipeline, one had the option to allow it to fill up to a set percentage higher than the margin. Therefore, unlike phases 1 and 2, the pipeline had a calculated and mandatory buffering time before delivering hydrogen

3.5 Economic Modeling

Offshore: Levelized Cost of Energy (LCOE)

The process began with a literature review, aiming to identify storage technologies suitable for the later proposed round-trip efficiencies. In addition, the estimated capital expenditures (CapEx) were sought, to later establish proportional costs in relation to phase 2 results and the system components of electrolyzers, DAC, power cables, pipelines, and wind turbines.

As a result, the total investment amounts for both startups in 2020 and 2030 were calculated in terms of present value. To do this, the first step involved determining the so-called *Weighted Average Cost of Capital* (WACC), which is based on debt (D) and equity (E) to value ratio (V), policy rate (Rd), taxes (Tc), and finally, the cost of equity for this type of investment (Re).

$$\text{WACC} = (\frac{E}{V} * Re) + (\frac{E}{V} * Rd * (1 - Tc)) \tag{3.2}$$

Subsequently, the determined WACC [50] was used to calculate the project's discount rate, given N years of project life, or the project repayment time, after which it was written off.

The shorter the project lifespan, the higher the spread costs and vice versa. The term N is typically constrained by equipment longevity or standardized accounting practices. The formula for the discount rate [36] is provided in Equation 3.3 below.

$$\text{Discount rate} = \frac{\text{WACC} * (1 + \text{WACC})^{\text{N}}}{(\text{WACC} + 1)^{\text{N}} - 1} \tag{3.3}$$

After this, the Levelized Cost of Energy (LCOE) was determined. This required accounting for full load hours or capacity factor. For example, if the total annual output of the electrolyzer was half of its annual design, the capacity factor was 50%, or 4380 hours if counted as full load hours. This meant counting all individual contributions and presenting them as one common utilization factor in regard to their CapEx size, respectively, as found in Appendix E.5 To simplify, the Direct Air Capture (DAC) technology and pipelines were assumed to have a 100% utilization degree. This was because the former's output was tailor-made in light of simplification, as can be found Chapter 3.1. Next, the latter was to the authors knowledge difficult to quantify in terms of capacity and pressure. Furthermore, the CO2 tax and the expected annual cash flows from power sales, calculated by phase 2 power return, were subtracted as tabulated in Appendix E.3. Finally, dividing everything by the aggregate wind power generation over the set lifetime yielded the formula for LCOE [36] below.

$$\text{LCOE [\$/kWh]} = \frac{\frac{\text{Total CapEx} * \text{Discount rate}}{\text{Capacity factor}} + \text{OpEx} - \text{Power revenue} - \text{CO2 tax}}{\text{Aggregated annual wind power over lifetime}} \tag{3.4}$$

The obtained LCOE was then multiplied with the adjusted hydrogen demand, resulting in a dollar-based price per kg of hydrogen. Following this, the costs to capture carbon dioxide were calculated, ultimately yielding a raw methanol price. If found in the literature, the cost of synthesis would further be applied.

Onshore: Direct air capture (DAC)

The calculation of the power consumption for carbon capture was based on the total amount captured for each case, reflecting the hydrogen output, then multiplied by the power demand per tonnage of CO2 to yield a power demand. This demand was met by purchasing power onshore at a fixed industrial-scale price.

It should be reiterated that the CapEx and OpEx of the DAC were incorporated into the LCOE, while the power consumption was treated as an exogenous variable. Although it could have been included in the LCOE, it was reasoned not to be, due to uncertainty of sufficient power delivery by the self-generated offshore power and the more distinctive separation of the onshore and offshore systems. Given that the power for the DAC was not generated by the proposed wind farm, it had to be of renewable origin to keep the work within the e-fuel framework. Since the Norwegian grid is largely hydro with the addition of other renewables [51], it was assumed to be 100% renewable electricity in the present work. On that note, it was tabulated in Appendix E.2, to illustrate the DAC power demand that of the generated.

3.6 Code architecture

The Matlab codes, or *scripts*, found in Appendix F, are based on phase 1 and were developed in accordance with the simulation outlines presented in the forgoing chapters. These include smaller scripts used for minor calculations or for visualization purposes, specifically the development of the BE and hydrogen output, henceforth referred to as the storage and hydrogen curves, respectively.

As seen in Figure 3.6, the simulations are initiated with a section of *fixed parameters*, including the methanol target, conversion factors, weather data, and option to activate the mechanisms; represented by the pink of on the right hand side. These parameters are then fed into the *core of the code* (CoC), which reads in the (scaled) power generation data given on an hourly basis in Chapter 3.1, Figure 3.1.

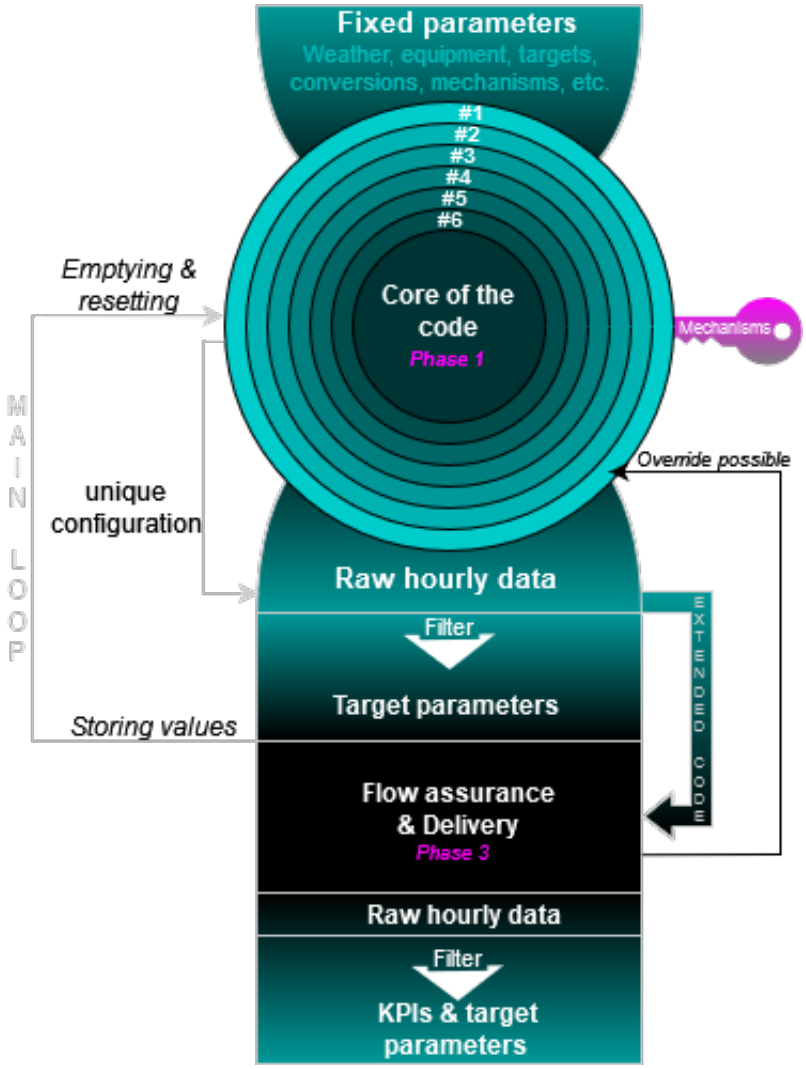

Figure 3.6: Overview of code structure

To optimize efficiently, it's crucial to streamline the CoC. This was achieved by introducing a *main loop* and outer layers (#1-6), which are the optimization parameters discussed

in Chapter 3.2 and quantified in Chapter 3.9. These layers impose a looping sequence (programming: running repeatedly over a part, until told otherwise), through a vast configuration pool determined by the range and quantity of optimization parameters selected.

The firing sequence for the optimization process begins by selecting the first range values for all layers, optimization parameters, (e.g., 1.1, 2.1,...,5.1, 6.1) and running that configuration in the main loop. It then moves to the next value in the innermost layer (i.e., 6.2 in Figure 3.6), followed by 6.3, 6.4, etc., until the entire range for layer 6.x has been covered. The code then moves to the next outer layer (in this case, layer 5) and adjusts the parameter from 5.1 to 5.2, proceeding once more through all variations for the layer below (6). This pattern continues until it reaches the outermost layer (1), at which point the sensitivity analysis is finalized.

Furthermore, the code is expanded, as seen on the lower part of Figure 3.6, to handle the hourly flow of produced hydrogen directly into the pipeline. In other words, the hydrogen curve from phase 1 is used in phase 3 as the parameter for pipe inflow and is converted from mass to volumetric terms and assumed compressed. Given a secondary optimization with mechanisms, the phase 1 parameters are transferred to the fixed parameters section and replaced by the phase 2 parameters within the CoC, as detailed in Chapter 3.9. Otherwise, the same methodology of looping sequencing and raw data handling is applied.

Core of the Code

The *core of the code* (CoC), the brain of the data handling, regulates the electrolyzers based on the BE state of charge. This task is accomplished using case-switch programming in Matlab programming language. Specifically by *case-switch* coding, one parameter, the switch, can take on a variety of values, aka. the cases. Analogy: picture an old rotary dial phone: the switch would be the rotary wheel, and the cases would be the numbers between 0 and 9. Similarly, in the code, the mode is the switch, while the cases are the various modes from M0 to M10. Each mode has its hourly electricity demand based on its coefficients relative to the target production. This is illustrated in Figure 3.7.

```
switch freezePointer % used for running normal or in FreezeMode
    case 1 % hits one - code runs normally

        switch mode
            case M10 %_______MAX MODE = TARGET___

                % netto from this hour in selected mode
                net = elProd(i) - D10;
                % deficit
                BE = BE + (net<0)*(net*(1/RTE));
                % giving mode reference if FreezeMde occurs
                modeLoad = D10;
                %hydrogen production
                H2prod = c10*mdot_h2;
                % surpluss electricity beyond the necessary
                % surpUtz = 0 by default, when mechanisms off
                surpH2el =  surpUtz*((net>0)*(net));
                % Route electricity to BE (and) power return
                BE = BE + (1-surpUtz)*((net>0)*(net));
                % surplus hydrogen production (illustration)
                surpH2prod = (surpH2el*(kilo2giga^-1))/...
                                (neta_Choice);
                %_____________________________//_____

            case M8 %____ONE LEVEL LESS OF MAX _____
```

Figure 3.7: CoC: Core of the code
selecting the electrolyzer mode based on intermittent (BE) state of charge

Once a mode is selected based on the BE level, the difference between the power generated and the specific demand yields a variable, **net**, also known as netto, indicating either a surplus or deficit (see Figure 3.7). As explained in Chapter 3.2 and shown in Figure 3.4, if the net power flow is negative, the virtual electrolyzers are supplemented by the corresponding amount from the BE. The intermittent storage is then adjusted for withdrawal and round-trip efficiency.

Conversely, if net is positive, the surplus amount is transferred to the BE. The amount of hydrogen produced in that specific hour, **H2prod**, is calculated based on the target production multiplied by the corresponding coefficient for the current electrolyzer mode. Storing the information about the current mode, so the mechanisms such as freezemode, safetyNet, or hillClimb can function appropriately. To refresh the concept of mechanisms, readers are advised to Chapter 3.3.

```
% BE level indicator:

        if BE >= M10
            mode = M10;

        elseif (BE<M10)&&(BE>= M8)
            mode = M8;

        elseif (BE<M8)&&(BE>=M6)
            mode = M6;

        elseif (BE<M6)&&(BE>=M4)
            mode = M4;
        else
          mode = M0;

        end
```

Figure 3.8: BE level indicator
part of the main Matlab-code, found in Appendix F

BE level indicator

The CoC relies on hourly BE measurements to set the electrolyzer mode for the upcoming hour of operation, which is achieved by the BE level indicator, shown in Figure 3.8. This function employs a simple IF-ELSE IF-ELSE programming approach. The code initially checks *if* the storage level is above the highest threshold (margin). If not, it checks *else if* the level falls between two set states of charge, moving down the list. If it doesn't meet any of these conditions, *else*, it must be lower than the M4 mode, causing the code to enter M0 mode or charging mode. The indicator then chooses the appropriate electrolyzer mode, as previously illustrated in Figure 3.2 in Chapter 3.2.

Code validation

Given the high degree of self-development and case study-oriented nature of the programming code, there won't be any formal code validation beyond factors of logic and reason of the presented results, in addition to the arguments and architectural build-up made prior to those.

3.7 Data handling

Given that each simulation loop is unique and represents one year of hourly data across all phases, instances, and curves (hydrogen, storage, pipeline), the process will generate a substantial amount of raw data. This data volume may require significant computational time and resources. Therefore, the code is designed to save only a select few calculated parameters from each configuration, in the following known as *target parameters*:

Run IDs

Beyond identification, these numbers are used for faster visualization purposes. By inserting these IDs, the code F automatically generates the desired curves, limiting likelihood of manual errors and time consumption. Lastly, configuration patterns can be easier to observe.

% of H2 target reached

This parameter provides a percentage corresponding to the total amount of hydrogen output throughout the year in relation to the target: 18.75 tonne hydrogen per hour. It is the first key parameter utilized in data synthesis.

BE peak [GWh]

The second key parameter is the maximum recorded storage capacity demand, also known as the BE peak. This measured extreme value is later used to calculate the storage costs and therefore a monumental aspect to the present work.

APDH: Adjusted power demand per hydrogen [kWh/kg H2]

Equally so, is the APDH parameter, accounting for the total power produces in light of hydrogen production and intermittent power storage, i.e., the process delay causing less hydrogen output. Hence, it is expected to increase parallel to energy storage and vice versa. However, this should not be confused with the impact of lower round trip efficiency, causing higher intermittent withdrawal.

Hydrogen and BE averages

The hydrogen average provides another way of showing the target reached on an hourly basis and is directly comparable to the target. The mean value for the BE is also calculated. These and the following stated target parameters are included albeit limited to illustration and future work potential. Since, their respective values demand more insight, e.g.,

understanding the relative sizes to turbine capacities, etc. Therefore, these will complete the tables presented in Chapter 4 on results, but found in the Appendix A - C.

Standard deviations of hydrogen and BE

The standard deviations of hydrogen produced and BE are crucial. Neither of these values should be high considering stabilization measures. Therefore, they constitute the last two key target parameters used in data synthesis.

Storage curve amplitude ratio

The absolute amplitude ratio of the storage curve serves as an alternative metric for evaluating the stability of the storage curve's development.

Optimization parameters

Along with the calculated values, the optimization parameters themselves will also be documented. Mostly, this is done for visualization purposes to potentially identify patterns or trends. Alternatively, one can decode the RunIDs, though this may require more time spent on spreadsheets.

3.8 Weighted sorting

Heretofore known as data synthesis, the next step involved sorting the data, and **weighted sorting** was chosen as the method for this task. This decision was made as alternatives, such as visually looking for trends or built-in sorting, e.g. within Excel spreadsheet was prone to errors and limited, respectively.

In essence, weighted sorting is a methodology consisting of **two components: normalized parameters and weights**. The primary task was to make the data comparable, as comparing percentages in one column and maximum storage capacity demand (GW) in another wouldn't have yielded a reasonable comparison. Furthermore, the data was divided into subgroups by the installed wind capacity for several reasons. Firstly, to gain more detailed information on each subgroup (GW). Secondly, the results were not expected to increase linearly with the turbine capacities.

The process began by finding the largest number in each respective column, in each subgroup. Then, the corresponding columns were divided - normalized - by their respective maximum, referred to as the *normalization factors*. As a result, the data was in a fractional format, normalized relative to the largest value encountered in that column, in that subgroup. For perspective, a table containing the normalization factors for phase 1 can be found in Appendix REEF.

Following normalization, a formula was developed based on weights and selected key parameters, as discussed in Chapter REEF. The weights, which were proportional factors between 0 and 1, were such that the total sum of the weights could not exceed 1, or 100%. These weights were then multiplied with the corresponding normalized parameters. After applying this formula to the entire normalized data set, it yielded a score for each configuration. Thus, the structure of the formula was of utmost importance, as the next step was to sort the entire data set by that score, aiming for the score to be as low as possible, since, the key parameters, such as standard deviation - which was preferred to be as low as possible for stability – and had such a format by default.

Moreover, the '% of H2 Target reached' and 'BE peak' were chosen as the heaviest weights, 40% and 30%, respectively. This choice was made based on the assumption that these factors would result in reasonable stability and hydrogen output. To complement the primary considerations, the remaining percentages were distributed among the standard deviation of the hydrogen production and the BE level. These formula suggestions were summarized in Table 3.1.

Table 3.1: Suggested sorting formulas

Paramters / Label	% of target prod	BE max need	H2 prod dev.	BE dev
Yellow	40	30	10	20
Green	40	30	0	30
Blue	40	30	30	0
Orange	40	30	20	10

Once the raw data was obtained, these formulas were tested until only one remained. This step was necessary to determine the impact of each and whether they selected the same configuration.

3.9 Phase 1 Optimization Parameters

OP1: Combined Wind Turbine Capacity

The highest demands for the electrolyzers were identified to be 937.5 and 1.125 MWh/h, respectively for 2020 and 2030 scenario. Moreover, the periodicity of the wind farm location, given as 57.8% for Utsira Nord (reference Ninja, insert screenshot of the set-up). Hence, per definition, a turbine capacity of 1 GW, displayed at the beginning of the present work would not suffice. As a result, the optimization range was calculated regarding the concessions and the utilization wind factor, yielding a range between 1 and 2.5 GW. Digression: the 1.8 GW option originated from dividing 1050 MW by 0.578 = 1.816 GW, where the electrolyzer power demand was only 55 kWh/kg in the development phase of the Matlab-code.

OP2: Round Trip Efficiency (RTE)

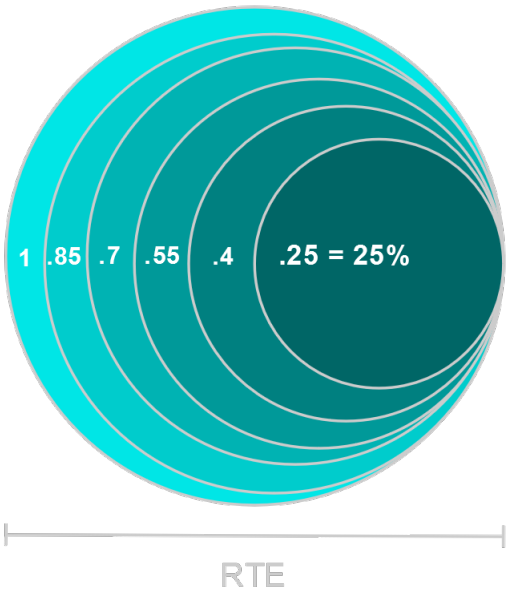

Figure 3.9: RTE, share of withdrawable energy from BE

Motivated as one of the most expected parameters to impact the energy routing, the range was set large to cover a wide range of storage technologies from 25 to 100% efficiency.

OP3: Build-Up Time (BuT)

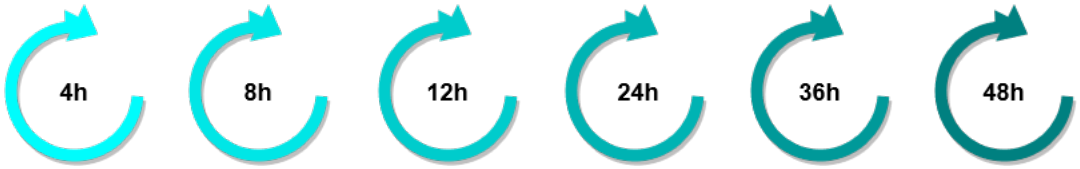

Figure 3.10: BuT

The build-up time was another crucial parameter within the code, recalling it to calculate the margin, and ultimately establishing the states of charge. The specified hours were directly related to the number of days, ranging from half a day to two days of building before initiating the process. Furthermore, two lower values of four and eight hours were supplemented to investigate the impact.

OP4-OP6: Coefficients c8, c6, & c4

The coefficient values were set to overlap in a few instances, simulating the possibility of fewer modes - from 5 to 4, or even just 3 modes. This could occur when c8 aligned with c10 = 1.0 and c6 = c4 = 0.4 or c4 = charging= 0. The possible combinations are depicted below in Figure 3.11.

Figure 3.11: Core Coefficient ranges

Note: steps of 0.1 were applied to these parameters; however, it was additionally checked if finer 0.05 steps would yield different results.

RunID identification

Since each configuration was unique, it was assigned a code indicating the range number of each optimization parameter.

Table 3.2: Phase 1 optimization parameters

showcasing the interpretation of RunID 1s. Example: 123435 = 1 GW turbine capacity, RTE = 0.4, BuT = 12, C8 = 0.7, C6 = 0.4, C4 = 0

Run ID loc.	Range #	OP1:Wind farm capacity	OP2: RTE	OP3: BuT	OP4: C8	OP5: C6	OP6: C4
Yxxxxx	1	1	0.25	4	1	0.6	0.4
xYxxxx	2	1.5	0.4	8	0.9	0.5	0.3
xxYxxx	3	1.8	0.55	12	0.8	0.4	0.2
xxxYxx	4	2	0.7	24	0.7		0.1
xxxxYx	5	2.5	0.85	36	0.6		0
xxxxxY	6		1.0	48			

3.10 Phase 2 Optimization Parameters

OP1: fuseLim - Number of Counts Before Activation

The range for this counter was set to start with 2 and end with 10 hours, increasing in steps of two, yielding five different options. There was no reasoning for the chosen range beyond experimental curiosity and the fact that the mechanisms were self-developed.

OP2: fuseLock - Iterations Locked at the Current Mode

For the coherent locking of electrolyzer mode, the range was set to at minimum to 4 hours, extending up to 12, with increments of two and thereby also yielding 5 different options. Similarly, the values were experimentally motivated.

OP3: safetyLim - Number of Counts before Activation

The range and reasoning for this parameter were the same as for fuseLim.

OP4: safetyLock - Iterations Locked at the Current Mode

The range and reasoning for this parameter were the same as for fuseLock.

OP5: SurpUtz - Surplus Utilization

The range for the de-routing of surplus power in maximum mode only was set to a minimum of 10%, followed by options of 20%, 30%, and 40%. It did not exceed the latter, due to the assumption of increased fluctuations.

3.11 Phase 3 Optimization Parameters

Number of Pipes

Given the short pipeline distance of only 56 km, the option of more than one pipe in parallel had been considered for the total range of 1-3 pipes.

Pipe Margin

Pipe margin was set between 30-80% of the calculated pipeline capacity, to have a lower and a higher bound, in turn providing operational flexibility and stability. In turn, pipeline thresholds were calculated based on this.

First Buffer Margin

As a start-up parameter, the first buffer margin was a factor multiplied with the pipeline margin, where the combined value was withing that of the latter. The primer was set between 1 and 1.25, i.e., a 25% increase.

3.12 Financial conditions

For the WACC-formula in chapter 3.5, the equity (E) to debt ((D) ratio used was 66/34, under the *low emission fuel* category, found by IEA [52]. Moreover, the cost of equity (Re) for this sector was there found to be 7%. Next, the policy rate (Rd) was set to 1% as it was virtually 0% for the Euro zone between 2014 and 2021 - and hence thought to affluence cost estimates of the found sources. At the time of writing, the current policy rate has reached 3.75% after a rapid increase [53], and arguably one could have used a higher value than 1%. This was left for further work.

Finalizing with Norwegian tax rate (Tc) of 22% [54], the WACC by equation 3.2 derived earlier, ended at 4.9% - also in line with IEA range [52].

$$\text{Discount rate} = (\frac{64}{36} * 0.07) + (\frac{36}{100} * 0.01 * (1 - 0.22)) = 4.9\% \tag{3.5}$$

In combination with a 20 year perspective, limited by DAC projected lifetime of 20 years [36] - inserting for equation 3.6 found in chapter 3.5, yielded a 7.9% discount rate; also in line with IEA numbers [52].

$$\text{Discount rate} = \frac{4.9\% * (1 + 4.9\%)^{20}}{(1 + 4.9\%)^{20} - 1} = 7.9\% \tag{3.6}$$

Next, the operational expenditure (OpEx) for the system as a whole was quantified to 3%. Firstly, this number was deemed satisfactory for novel technologies such as the direct air capture [36]. On the other hand, in the case of the wind turbines, this amount was found to be in the 1-2% area [55]. Secondly, due to the large equipment scale of the case study and hence great uncertainties, without any economics of scale factored in - a higher OpEX was reasoned for.

Storage investment costs estimates

At large, the sources of Table 3.3 where American energy government organs, European energy directives or companies acting on behalf of those. Reiterating that the 2020 values where adjusted for inflation [56] from date of publishment and currency [57], dollars to euro $\tilde{1}.1$. Subsequently, the 2030 projections were adjusted for the same rate, and thus maintaining their initial relationships between 2020 and 2030 values. With great emphasize: **the numbers were estimates and could have been already adjusted for future inflation rate.** The values to be used for capital expenditures, later in the spreadsheet calculations and subsequently for LCOE Equation 3.4 derived in Chapter 3.5 are tabulated below:

Table 3.3: Tabulated values found for equipment CapEx

Investment of	2020 $/kW	2030 $/kW	2030 LOW $/kW	2030 High $/kW
Wind turbine [55]	$5 351	$4 441	$3 478	$4 909
Electrolyzer [58], [59]	$1 500	$1 305	$1 208	$1 403
Battery [60],[61]	$198	$163	$128	$198
CAES [60]	$756	$616	$360	$930
H2/Salt cavern [60], [62]	$1 500	$1 150	$975	$1 325
DAC [36]	$815	$211	$118	$378

Some of the sources provided additional low and high estimates, or one of the said. If the latter, the counterpart was calculated by the same percentile, ratio or value. In case of no estimates, these were found by literature review on learning curves, i.e. the historical and projected cost reduction, e.g. for novel technologies such as hydrogen fuel cells [63].

2020 values were limited to baseline only, as it was thought to be of greater interest to prioritize the wider span future CapEx estimates. In addition to being past 2020 at the time of writing this report.

Pipeline

Selecting a 150 bar inlet, 60 bar outlet, with an simplified assumption of 105 bar average, which validation is found in Appendix C.3. Moreover, by a 20 inch pipeline for a distance of 56 km (34.80 miles), the following was calculated for offshore pipeline cost [64]:

$$\text{Cost (industry)} = -12.6 + 4.09 * (X^{0.5}) \tag{3.7}$$

Where X is the value for inches times miles of the pipeline. For the problem at hand, this is found to be 696. Inserting for X yields,

$$\text{Cost (industry)} = -12.6 + 4.09 * (696^{0.5}) = 95.3 \text{ [MM \$]} \tag{3.8}$$

Cable

In regard to phase 2 potential of transmitting surplus power to shore, the offshore cable of HelWin1 project [65] of 576 MW capacity, with an initial length of 130 km, and costs

of 150 and 595.3 million euros (MEUR), respectively for the line and the converters & platforms. Upon length adjustments to 56 km, the cable cost came down to 64.6 MEUR, meaning the total costs for the 2015 data, adjusted for European inflation (5.05%, [56]) amounted to $\tilde{7}63$ million dollars.

The capacity of the transmission line, 0.576 GW, was thought to be sufficient given the size of the wind turbine subgroups presented in Chapter 3.9, in addition to the energy routing mainly going to the intermittent storage.

External electricity

The surplus power of the offshore system will be sold at 96 $/MWh, reflecting the industrial spot power prices in Norway as of 2022 [66]. Additionally, the DAC power will be bought at the same price. Reiterating the minor assumption off 100% renewable energy from the Norwegian electricity grid.

CO2 tax deduction

In regards to Norwegian government projections in 2019 [67], the CO2 tax rate for 2020 was set to 60.5 USD / tonne, whilst assuming an increase to 209 USD / tonne in 2030. Acknowledging that the price in 2020 were already at 87 USD/tonne [68], the stated numbers will be applied to their respective instances to offset costs; in the form of positive, fixed cash flows based on their year of investment start.

Other

For the one scenario of H2 salt cavern storage, there is an cost associated with the up-keep/salt cavern expenses, estimated to be 2 USD/kW [62]. This will be factored into the influx of power to the intermittent storage.

Moreover, the DAC power demand was found to be 1500 kWh/tonne CO2 [36].

Lastly, incentives such as the *European Green Deal* [69], or aid from the Norwegian grant fund, *ENOVA* [70] were **not** factored in. Furthermore, that also included certificates of green energy such as *Renewable Energy Guarantees of Origin* (REGO) [71], [72] found in the United Kingdom or European guarantee of origin (GO) [73].

Chapter 4

Results and discussion

4.1 Phase 1

Table 4.1: Phase 1: Results for all instances

Run ID	Subgroup [GW]	% of target prod	BE peak [GWh]	APDH [kWh/kg H2]	Inst.#	Start
161312	1	57.08	5.59	50.04	1	2030
231333	1.5	76.52	72.65	55.99	1	2030
311433	1.8	77.65	122.55	66.20	1	2030
411533	2	82.62	206.73	69.14	1	2030
521312	2.5	99.97	1007.10	71.42	1	2030
161133	1	57.10	3.53	50.02	2	2030
231433	1.5	76.64	71.59	55.89	2	2030
311533	1.8	77.90	121.36	65.99	2	2030
411433	2	82.75	205.63	69.03	2	2030
521212	2.5	99.98	1006.16	71.42	2	2030
161312	1	47.56	4.59	60.05	3	2020
261332	1.5	71.11	37.92	60.25	3	2020
331333	1.8	76.52	87.18	67.19	3	2020
421533	2	78.89	125.97	72.40	3	2020
541422	2.5	99.96	890.32	71.43	3	2020
161234	1	47.58	2.33	60.03	4	2020
261124	1.5	71.13	36.12	60.23	4	2020
331433	1.8	76.64	85.91	67.07	4	2020
421533	2	79.13	124.56	72.19	4	2020
541131	2.5	99.97	888.13	71.42	4	2020

From the tabulated values, the general observations was heightened numbers with increasing wind turbine capacities. In itself as expected, although not to the extent as seen for the divergence between hydrogen target reached and the intermittent storage solution demand. The complete table is found in Appendix A.1 as Table A.2. Beyond this, the following was observed:

i) While Instances 1 and 3 were both strict, requiring either 50 or 60 kWh/kg H2 respectively, they both employed the same configuration in the lowest turbine capacity, with the tag number 161312. In the initial configuration, the target delivery was nearly 10% higher, albeit at the expense of an additional GWh of peak demand. This trend persisted when comparing the two loose-code instances, 2 and 4, in which the primer configuration delivered a higher target, in addition to a higher BE peak. This was rationalized by the less efficient but larger electrolyzers offsetting more off the storage demands - by a higher withdrawal at times of deficit, consequently affecting the state of charge and finally the hydrogen produced. Lastly, in regard to the high storage demands, it was clear that more optimization or different approach, viz. initially more stable power source or higher electrolyzer capacity to reach closer to target; although this could have led to higher fluctuations by up-scaled withdrawals from the BE.

Quantitatively, the BE peak differences from instance 1 to 3 were significant, e.g for the 1.5 GW subgroup: a reduction from 72.65 to 37.92 GWh. The remaining intermittent storage for the said example, is shown in Figure 4.1

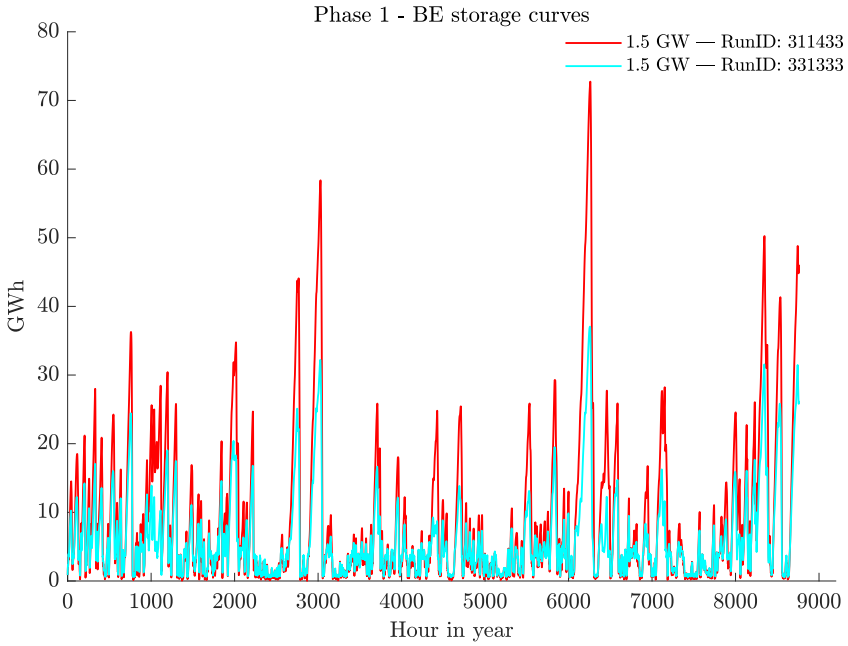

Figure 4.1: Phase 2: Comparison of 50 and 60 kWh/kg H2 electrolyzers for the subgroup of 1.5 GW

ii) The adjusted power demand per hydrogen (APDH), tended to increase with the number of turbines, and in all instances, no matter if 50 or 60 kWh/kg H2 was the starting point - and virtually attained in the lowest subgroups of 1 GW, the required power ultimately

gravitated towards 71.42 +/- 0.01 kWh/kg. Interesting, and more so, when the two instances of older electrolyzer technology, actually achieve 72.40 and 72.19 kWh/kg when looking at the subgroups of 2GW, in strict and loose mode, respectively, before lowering to ca. 71.42 for 2.5 GW. Presumably, this gravitation trend was due to the significant storage held in that subgroup.

The Adjusted Power Demand per Hydrogen (APDH) tended to increase with the number of turbines across all instances, irrespective of whether the starting point was 50 or 60 kWh/kg H2, and eventually trended towards 71.42 +/- 0.01 kWh/kg H2; presumably due to the large storage held there. An interesting observation for instance 3 and 4, was a higher APDH for 2 GW than for the 2.5 GW, opposing the said trend. This was thought to either be random occurrences or that the less efficient electrolyzers caused greater fluctuations and therefore a higher ADPH in the end, in accordance with i).

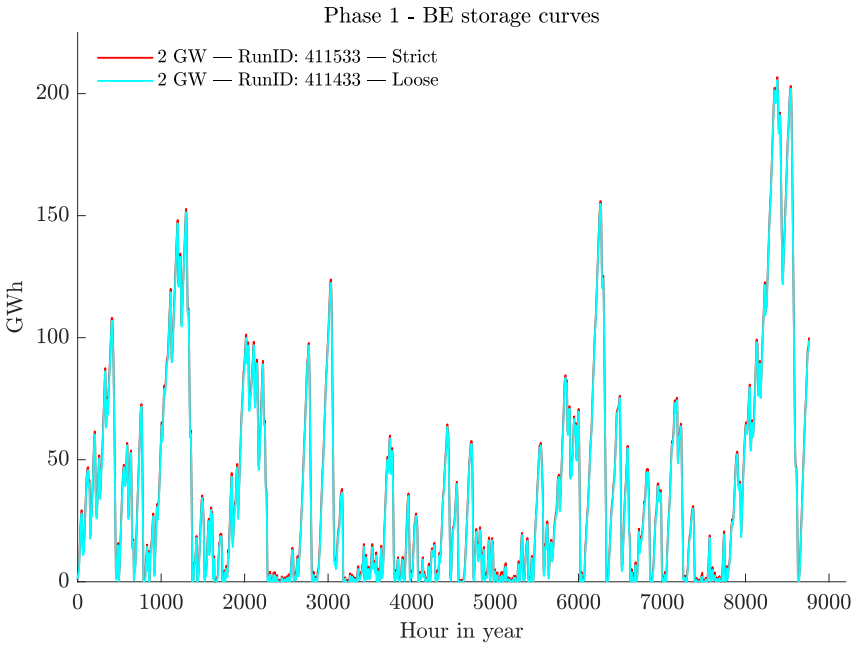

Figure 4.2: Phase 1: 2 GW 2020 and 2030
Illustrating the minor differences between strict and loose code mode within the same electrolyzer, in relations to table 4.1.

iii) The amplitude ratios of BE varied substantially, as represented in Table 4.1. When comparing strict and loose-code of 2GW for the 2030 scenario in Figure 4.2, it became evident that the amplitude parameter was of minor significance. Assumably due to the division by small numbers, likely caused by small thresholds in the first place. That is, argued by the fact that all configurations in Table 4.1 had the lowest build up time of only 4 hours; indicated by the third RunID numbers being 1, recall the deciphering Table 3.2 in Chapter 3.9.

Hence, for the selected configurations, the differences between strict and loose threshold simulations were of little significance, only notable in the lowest subgroup of 1GW, particularly when considering the BE peak. Furthermore and in regard to the lower targets

obtained with loose-code instances, 2 and 4, it was decided to proceed with only strict-coding, i.e. instance 1 and 3, corresponding to 2020 and 2030 scenarios.

iv) Lastly, the general increases in storage demands between 1 and 1.5GW was to such extent intriguing that it was ultimately decided to run the simulations anew for 1.25 GW. Results are found in table 4.3. In light with loose-code being discarded, instance 2 and 4 for illustration purposes only.

Supplementing with 1.25 GW scenarios

The results from the investigation found in Table 4.3 proved satisfactory. That is, for the 2030 scenario, target reached amounted to 71% with a BE peak of 31 GWh, i.e. a target only five percentiles short compared to 1.5 GW, whilst the storage capacity peak dropped by over 55% to 31.60 (72.65) GWh.

Discarding 2 & 2.5 GW

Having presented the simulation results and discussed a few observations, the exuberant storage demands found for 2 and 2.5 GW subgroups were not possible to reason for further inclusion. Moreover, these configurations had low round-trip efficiencies, probably due to the nature of the weight sorting formula preferring low BE peaks; had the RTE been higher, it would exceed the said numbers in Table 4.1. Meaning, it was hard to justify that the biggest turbine subgroups also had the lowest RTEs and in affect lost great shares of its harvested energy.

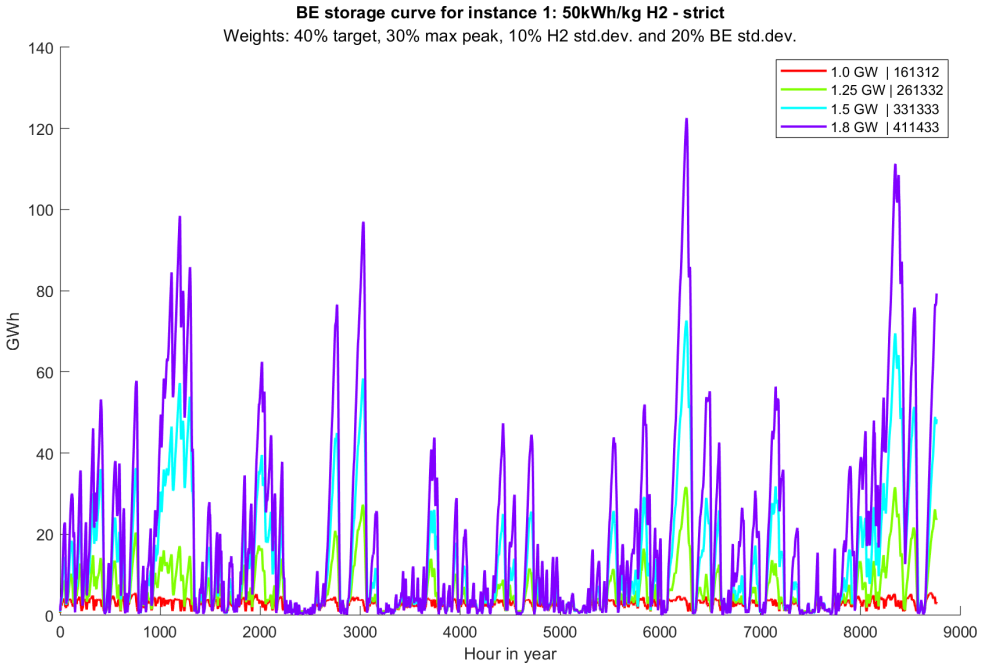

Figure 4.3: Phase 2: Selected capacities for Phase 3

To the aforementioned, from 13 500 different combinations of wind park scales, coefficients (c4,c6 & c8), build up time (BuT) and RTE - only eight configurations were selected for phase 2, of which four were presented in Figure 4.3 for instance 1 - being the preferred scenario for 2030 and to be later compared with the 2020 counterpart (instance 3, strict; standard)

It is to be noted that With the inclusion of 1.25 GW, the first RunID numbers of 1.5 and 1.8 GW subgroups, were later incremented by 1, i.e. increase of wind capacity, e.g. phase 1 results for 1.5 GW will in the following start by "3" and not by "2" - as that is now 1.25 GW.

Impact of RTE

Having discarded the subgroups of 2 and 2.5 GW, the impact of RTE on adjusted power demand of hydrogen (APDH) was investigated. After choosing a fixed case, and only varying the round-trip efficiency values, the following was obtained in Table 4.2:

Table 4.2: Phase 1: RTE impact on APDH

2030 1.5 GW with fixed BuT = 4 hours, c8,c6 and c4 = 0.7, 0.4 and 0.2.

Run ID	% of H2 target	BE peak [GWh]	ADPH [kWh/kg H2]	OP2: RTE
261433	85	107.70	50.59	1
251433	82	95.83	52.04	0.85
241433	80	83.20	53.85	0.7
231433	77	72.85	55.99	0.55
221433	73	72.79	58.53	0.4
211433	69	72.74	61.82	0.25

Here, the general trend observed with increasing RTE was increased target production and BE peak, whilst the APDH eyed reduction. Logical, as for a fixed wind capacity with a higher hydrogen output percentile, less was stored in the BE, and consequently APDH lowered; being the sum of power produced, divided by the hydrogen total output. This observation aligned with the non RTE-isolated configurations presented in Table 4.1 previously.

For reference, RTE = 55% was chosen for this particular instance and subgroup. From table 4.2, this seemed like a good trade-off, where lower RTE had yielded the same storage demand, albeit lower output and higher APDH - and vice versa - higher RTE increased the output slightly, at notably higher BE peak. In other words: the weight sorting was successful in that regard.

Table 4.3: Phase 1: 1.25 GW addition

complete table in Appendix A.3

Run ID	Subgroup [GW]	% of H2 target	BE peak [GWh]	APDH [kWh/kg H2]	Inst.#	Start
261332	1.25	71.11 %	31.60	50.20	1	2030
261332	1.25	71.12 %	30.71	50.20	2	2030
261212	1.25	59.45 %	9.74	60.05	3	2020
261122	1.25	59.47 %	7.94	60.03	4	2020

4.2 Phase 2

4.2.1 Instance 1: 50 kWh/kg H2 (2030)

Running phase two and weight sorting by the same formula as for phase 1, recall from Chapter 3.8, the following best cases were selected for phase 2, in addition to the comparison with phase 1.

Table 4.4: Phase 2: 2030 scenario results

Complete table in Appendix B.1

Subgroup [GW]	RUN ID 1	Run ID 2	% of H2 target	BE PEAK [GW]	APDH [kWh/kg H2]	Power return [GWh]	return % of generated
1	161312		57.08	5.59	50.04		
		33114	54.41	4.77	52.49	219	4.66
1.25	261332		71.11	31.60	50.20		
		33114	66.56	19.66	53.64	384	6.55
1.5	331333		76.52	72.65	55.99		
		11114	70.91	44.56	60.41	702	9.98
1.8	411433		77.65	122.55	66.20		
		11114	72.56	74.32	70.85	1139	13.49

An offset trend between target reached and the BE peak was observed, where in the case of 1 GW, the hydrogen output dropped from 57.08% to 54.41%, while the storage demand fell from 5.59 to 4.77 GWh at its maximum. In other words, these represented a relative drop of 4.7% and 14.7%, respectively. The tabulated values for all the subgroups were reported in Table 4.5 below:

Table 4.5: Phase 2: Relative changes in trade-offs between production target and maximum storage demand. Percentage point difference is calculated by dividing the storage percentage points by the target percentage points. Next, relative by elevating (1+storage points) by the inverse of the target percentage points. All values rounded to one decimal

Subgroup [GW]	-% of H2 target	-% BE peak	-%-point storage per target	-% storage per target
1	4.7	14.7	3.1	3
1.25	6.4	37.8	6	5.1
1.5	7.3	38.7	5.3	4.6
1.8	6.6	39.6	6	5.2

These offsets for storage demand were virtually identical for 1.25-1.8GW, and similar can be stated regarding their respective target reductions. Initially, it seemed like the changes in target and peak were increasing with greater capacity starting from the lowest capacity. However, the relative differences first increased from 1 to 1.25 GW, before decreasing and increasing for the cases of 1.5 and 1.8 GW, respectively, when compared to their lower prior. Since these capacities shared the same configuration for phase 2 and had almost identical target percentages initially, it appeared that the larger capacity could be a disadvantage. Despite the higher power generated, it seemed that a considerable portion of it was simply returned and not utilized for the target itself. Moreover, the 1.25 GW also initially had a relatively high target (71%), leading to a significant reduction, making it difficult to justify the options of 1.5 or 1.8 GW.

Beyond the peak shavings, the impact of the mechanisms were made visible for the storage development by Figure 4.4, comparing the subgroups of 1.8GW.

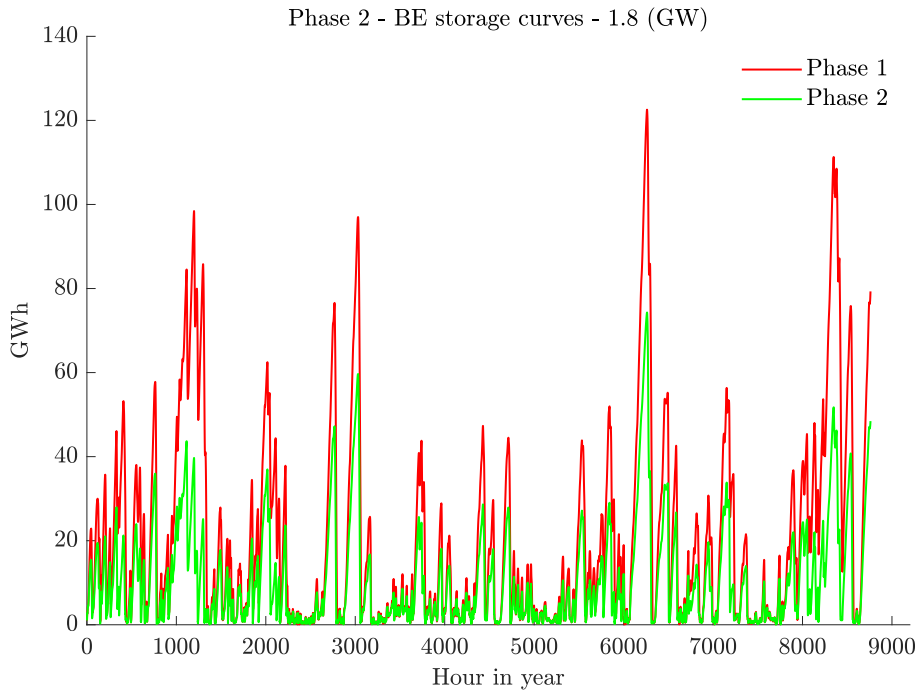

Figure 4.4: All the capacities illustrated

ii) Consequently, this affected the APDH, H2 & BE standard deviation and the averages. Interestingly, while the APDH increased despite a lower target, as expected, the average intermittent storage held by the BE was lower. This indicated that while the power output was the same, the code needed to stabilize at a lower, possibly more stable level. Despite discarding the loose-code approach, this could be compared to the loose-cases in phase 1, Table 4.1, where the price was deflated with lowered output. This further reinforced the observation made for phase 1 results, that with greater excess storage, the APDH increases, as the relative output pace was smaller than that of the storage build up.

iii) Moreover, with the option to produce excess hydrogen in maximum mode only, and wholly converting the allocated power to hydrogen based on the electrolyzer specifics and not by state of charge - virtually all the cases preferred the highest surplus fraction of 40%. One again, assumed due to the sorting formula being heavily weighted on hydrogen output. Next, a higher production deviation was encountered for the surplus hydrogen production compared to both phase 1 and phase 2 without surplus production (separate calculations) as found in the complete tables in Appendix B. These results were reasoned for with the occasional extra hydrogen output, naturally causing higher deviation. In addition, the combined APDH were the lowest encountered for each subgroup and conversely the highest target reached. Meaning, the heightened standard deviation values for a surplus hydrogen allowance yielded positive results. For the record: the calculations done for the de-routing of surplus power, were performed on separate basis in the aftermath, and hence one obtained values for the case of normal production and to compare with the power sent to shore, had it been converted to hydrogen. If so, then it could be further assumed that

the realistic values would be between phase 2 standard and surplus hydrogen, as extra electrolyzers would have an capacity limit.

Mechanism parameters selected

Table 4.6: Phase 2: 2030 complementary overview

to the results in Table 4.4

RUN ID 1	Run ID 2	Extra hours	safeLim	safeLock	hillLim	hillLock	Surp.utz. [%]
161312							
	33114	4183	6	8	2	4	40
261332							
	33114	4751	6	8	2	4	40
331333							
	11114	5593	2	4	2	4	40
411433							
	11114	6127	2	4	2	4	40

Observant readers would notice that the RunIDs for Phase 2 were only 33114 and 11114. Meaning, if looking at the safetyNet mechanism, the sorting formula favored a minimum limit of 6 counts, followed by a mode lock for 8 hours for subgroups of 1 and 1.25 GW. On the other hand, 2 counting and 4 locking hours for 1.5 and 1.8 GW, respectively. Considering the possibility of lower wind output from the lowermost subgroups, it was reasoned that the preventive mechanism, safetyNet, favored higher locking hours to ensure stability. However, the counter limit of 6, triple that of the remaining configurations, may suggest that the code was hesitant to deploy the mechanism. This could have been due to greater impact on the storage development - relative to the larger subgroups.

Next, for the hillClimb mechanism, activation hours were found to be the lowest possible: 2 hours, signaling a potentially very active intervention mechanism. In terms of locking hours, these were all the lowest possible: 4 hours, which in turn suggested a more cautious code. Put differently: active mechanism, but little impact per activation.

4.2.2 Instance 3: 60 kWh/kg H2 (2020)

Table 4.7: Phase 2: 2020 scenario results

Complete table in Appendix B.2

Subgroup [GW]	RUN ID 1	Run ID 2	% of H2 target	BE PEAK [GW]	APDH [kWh/kg H2]	Power return [GWh]	return % of generated
1	161312		47.56	4.59	60.05		
		11111	47.56	4.59	60.05	43	0.92
1.25	261212		59.45	9.74	60.05		
		11114	56.60	7.35	63.08	280	4.78
1.5	361332		71.11	37.92	60.25		
		33114	66.56	23.59	64.37	461	6.55
1.8	431333		76.52	87.18	67.19		
		11114	70.91	53.48	72.49	842	9.98

Before examining the relative trade-off between the target and BE demand reduction, focus was shifted to the 1GW subgroup. In this context, no impact on the results was observed after phase two, and a look at the complementary table 4.8 revealed no surplus hours, implying no power return.

Table 4.8: Phase 2: 2030 complementary overview

to the results in Table 4.7

RUN ID 1	Run ID 2	Extra hours	safeLim	safeLock	hillLim	hillLock	Surp.utz. [%]
161312							
	11111	0	2	4	2	4	10
261212							
	11114	4281	2	4	2	4	40
361332							
	33114	4751	6	8	2	4	40
431333							
	11114	5593	2	4	2	4	40

Additionally, Table 4.8 depicted the halved limits and locking hours for the safetyNet mechanism for 1 and 1.25 GW, when compared to instance 1, as previously shown in Table 4.8. One possible interpretation could be that electrolyzers for this scenario were less efficient, and consequently demanded more power for the same wind power profile, as

compared to instance 1. This led to less usable surplus, or in the case of 1 GW, none at all.

Else, the 1.5 GW saw an increase in both locking hours and counter limit, equal to those found for 1 and 1.25 GW found for instance 1 in Table 4.6. No further reasoning was made her beyond reason of code dynamics.

Table 4.9: Phase 2: 2020 Relative trade-offs

Subgroup [GW]	-% of H2 target	-% BE peak	-%-point storage per target	-% storage per target
1	-	-	-	-
1.25	4.8	24.5	5,1	4,6
1.5	6.4	37.8	5,9	5,1
1.8	7.3	38.7	5,3	4,6

This time, however, the 1.5GW subgroup experienced the greatest trade-off effect, with corresponding values to the found in instance 1, for 1.25 and 1.8 GW, respectively. Moreover, this mirror observation was also applicable for the remaining values. Assumably random, albeit mentioned for the pattern-interested reader.

Beyond the maximum peak savings, the impact of phase 2 is illustrated by Figure 4.5 with respective states of charge; from which one can see the hydrogen production of target, in addition to max (BE peak) and minimum amplitudes.

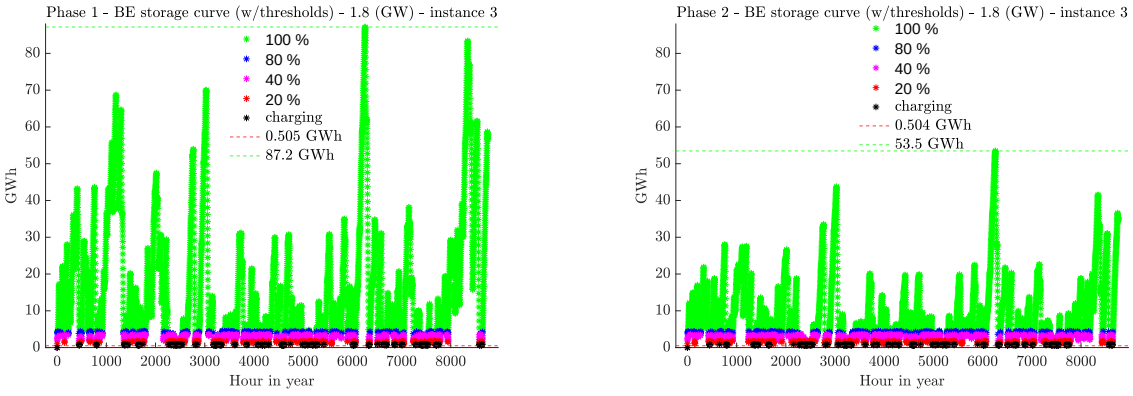

Phase 1 Phase 2

Figure 4.5: Phase 2: 2020 1.8 GW, Threshold plot before and after mechanism impact

Significantly and satisfactorily, the two subplots highlight the effect of optimization and that further potential could be unlocked, as seen by the over-representation of maximum state of charge (green) way above its threshold level.

Conversely, a major weakness of the code is the disproportionate allocation of BE capacity. Seen from the lowermost region of the plot in Figure 4.5, approximately 5 GWh and below, does not noticeably improve with the mechanisms introduced in phase 2. A potential solution would require more years of data, an predictive model of wind conditions combined with real-time weather data; simulated here with hourly input read. This would enable a more accurate assessment of production and storage, thereby spreading the stored capacity evenly throughout the year. That being said, phase 2 surprisingly handled the first 3000 hours of the year quite effectively, particularly around hour 1000 and 3000, were the spikes were significantly truncated. Moreover, the largest spike, at about 6000 hours into the year, saw a reduction of approximately 35 GWh.

Investigation of increased *SurpUtz* to 80%

Therefore a test was performed on the 1.8GW 2020 scenario (instance 3), raising the surplus utilization overhead range from 40 to 80% by 10% increments, while keeping other parameters fixed. The highest percentile, 80, was selected from the extra 5000 configurations. However, it is to be mentioned that 144 configurations produced the same score, highlighting the potential for a more nuanced optimization strategy. The preferred configuration was RunID 2 of 1111x (where x ranged from 60-80%).

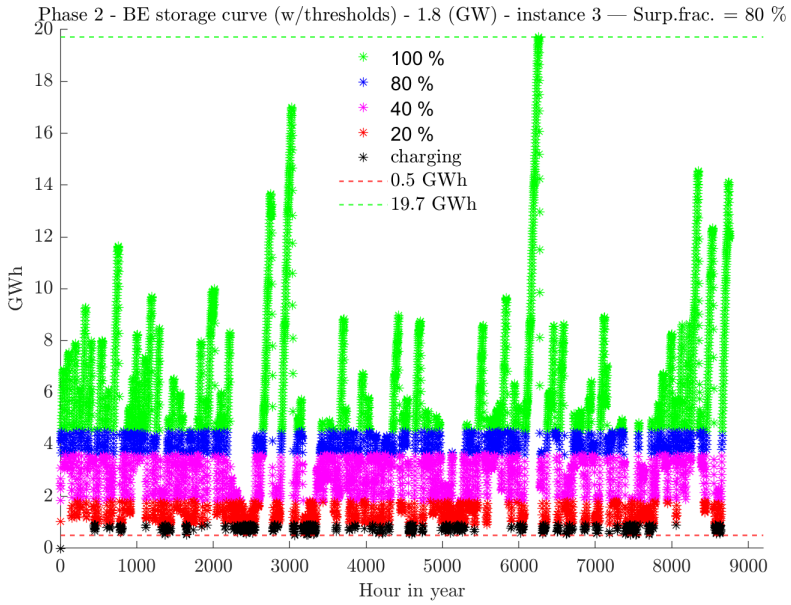

Figure 4.6: Phase 2: 2020 1.8GW with allowed surplus utilization of 80%

The key effects of this change were seen in the green region of the plot. Doubling surplus utilization led to a 170% power return increase (842 to 2272 GWh) and reduced the BE peak to 19.71 GWh, as tabulated in Appendix B.3. However, this came with an 11 percentage point target reduction and a 19% increase in hydrogen cost to 86.23 kWh/kg. For the combined option, the target rose by 3 percentile points, and the cost dropped by 4%. These results underscored the need for further code stabilization, vis-a-vis a stable storage

curve development, where the over-charging should be utilized for the aforementioned lower region.

Correlation of 2020 and 2030 scenarios

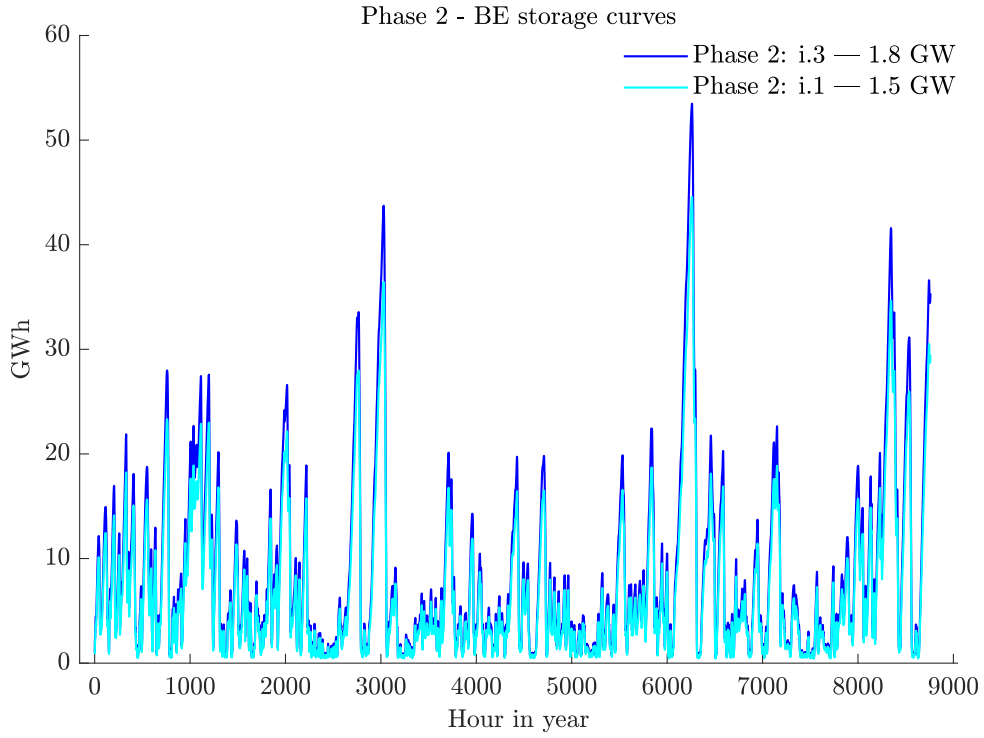

Figure 4.7: Phase 2: Comparison of 2020 and 2030

Whilst the present electrolyzer technology had a considerably lower BE peak, trading off lower targets reached. For the observant reader, results tabulated in Tables 4.7 and 4.8, the target reached (and consequently, its standard deviation) was identical for the selected 2020 1.8 GW and 2030 1.5GW scenarios, in Figure 4.7. Moreover, this was also found true for 1.5GW and 1.25 GW, and almost for 1.25 and 1 GW, respectively for 2020 and 2030. Assumed due to to mathematics: the present electrolyzers demanded $60/50 = 1.2$ (or electrolyzer capacity: $1.125/937.5 = 1.2$), i.e. 20% more power than their future counterpart. Next, dividing 1.8 by 1.5, and 1.5 by 1.25 both yield 1.2. In other words: reasonable to assume that mathematics impacted at large. Additionally, this observed for the fraction of returned power. On the other hand, with all the optimization parameters and variables involved - one would assume greater nuance than such. However, as mentioned, the build up time (BuT) of all configurations was 4 hours. Hence, the margin and states of charge where calculated accordingly, that is, parallel shifted since both the electrolyzer and and turbine capacity had the same number-wise increase.

Conversely, the adjusted power demand per hydrogen and storage parameters where not identical - as it should given different electrolyzer efficiencies of 2020 and 2030. Unless it would stabilize around a number as seen in phase 1 for the 1.8 GW cases in Table 4.1. That said, those were without any activated mechanisms. Meaning, had the unique parameter

values been identical - then the code would most certainly be majorly faulty, except in the off chance of a small mathematical possibility.

Regarding power returned, values of 702 and 842 GWh were reported for 1.5 and 1.8 GW, respectively, for the configurations shown in Figure 4.7. Interestingly, a 20% increase in turbine installation resulted in a proportional 20% increase in power return. Interested readers will find these and related tables in Appendix E.3

4.3 Phase 3

After continuous refining of the Matlab-code for the two first phases and simultaneously developing an economical aspect, phase 3 was limited to a threshold approach. That is, the valve openings on the delivery side were based on the hourly capacity of the pipeline(-s) - analogical to state of charge and the electrolyzer output logic in phase 1 & 2. The reason was the trial progress of adding so-called pipeline override - which sought to prioritize delivery over phase 2 stabilization measures. Meaning, if safetyNet or hillClimb was activated - those - and BE indicator selecting state of charge - would be overruled in favour of a minimum pipeline level, hence imposing a greater hydrogen production. Simultaneously, the valve openings would be decreased, resulting in a double pipeline build-up effect as such, and consequently a increased flow delivery in the long run. Moreover, these adjustments were to be in a gradually increasing fashion, followed by a period of incremental valve opening release, where the mechanisms or phase 1 logic would steer the power routing again. On an isolate basis, this override feature was successfully developed, albeit since the code was overly performance-focused vis-a-vis keeping everything in one script - not advisable - the stacked layers of override features summed to high; clouding the code readability. As a result, phase 3 operated independently, managing only hydrogen pipeline flow. The final simulation results are found in Table 4.10.

Table 4.10: Phase 3: Results

Complete table in Appendix C

RunID 3	Subgroup [GW]	% of H2 target, phase 2	% of H2 target, phase 3	ADPH [kWh/kg H2]
111	1	57.08	54.41	52.49
112	1.25	71.11	66.53	53.66
111	1.5	76.52	70.92	60.41
112	1.8	77.65	72.51	70.90
111	1	47.56	47.12	60.61
111	1.25	59.45	56.60	63.07
112	1.5	71.11	66.53	64.39
111	1.8	76.52	70.92	72.49

Here, it was evident that phase 3 reduced the target delivery furthermore - as expected - due to initial pipeline build-up, similar to the BE level buffering in phase 1 and 2. Consequently, this elevated the APDH, i.e. per definition increasing the hydrogen production price later on. Equivalent to the aforementioned of BE build-up increasing APDH in the forgoing phases.

One solution could be to adjust the valve openings closer to the actual targets reached in phase 2. Meaning, in the said configuration, as shown in Table 4.10, the hydrogen output was 77.65% of the target and since the maximum valve opening (coefficients inherited)

was equivalent to 100% of target - it would per definition not be able to delivery maximum throughout the year. Therefore, delivery fluctuations were seen in Figure 4.8 below, presenting the highest hydrogen target among all the configurations.

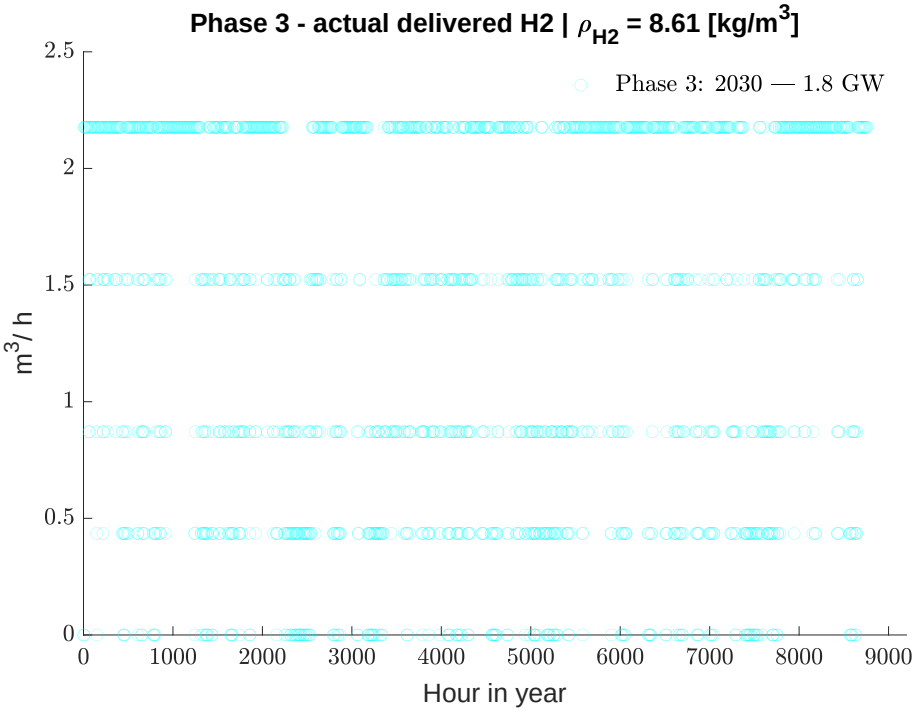

Figure 4.8: Phase 3: 2030 1.8 GW flow delivered

Interestingly, for 1.5 GW case for the same scenario, a 1.6% target reduction yielded a APDH reduction of 10 kW/kg. Hence, selecting the overall subgroup beyond target reached is important. Moreover, for future work it should be investigated whether the adjustment of valve openings to the results of phase 2 would ensure greater stability of the delivery flow, and possibly a lower APDH, that is, independent of a line packing implementation.

Prior to discarding its development, it was investigated whether compressed hydrogen had a linear pressure development. This was found by CoolProp software integration in Matlab to be true, as can be found in Appendix C.3. Meaning, this simplifies the development of a comprehensive line packing approach if to be attempted in future work. **Additionally, this validated the 105 bar average pressure utilized for the threshold approach.**

Lastly, configuration for phase 3 is found in Appendix C.2, where all the eight configurations preferred a pipeline margin of 30%, with virtually no extra margin to the pipeline for the initial buffering, having three cases selecting a mere 5%, and no in the remaining. Presumably and in light of previous observations: due to the sorting formula at large.

4.4 Key performance indicators

LCOE

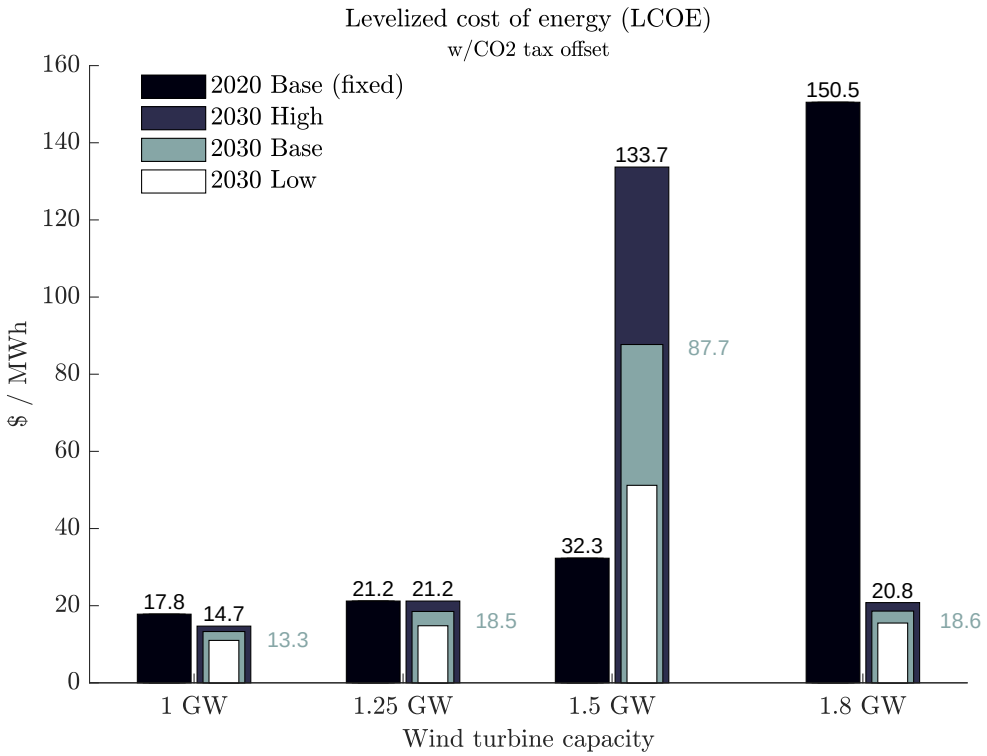

Figure 4.9: LCOE w/CO2 adv.

The integration of estimated costs and simulation data resulted in low values of typical levelized costs of energy (LCOE), as seen in Figure 4.9. That is, not unrealistic had the 1 and 1.25 GW subgroups solely represented onshore (here: offshore, expected: 3-4 times higher) wind turbines for a low-cost scenario; albeit with a lower utilization factor and consequently higher LCOE [55].

To an extent, the low values were assumed due to the offset effect of power sales revenue and CO2 tax deductions, found in Appendix E.3, Table E.3, where the latter accounted for roughly 1.1-1.5 and 0.3-0.4 $ offset per MWh, for the 2030 and 2020 scenario, respectively; with decreasing offset towards higher turbine capacity, assumably an effect from the storage build-up. As expected, the 2030 had higher offset with a higher modeled carbon tax. Given a relatively small offsets for the CO2 tax deduction, all the remaining results are presented in a CO2 tax deducted format in the following. Moreover, the 20 years of payback time could have lowered the costs beyond the necessary.

Conversely, the values had been lower with a lower discount factor, which in itself was modest of 7.9% and as previously stated in line with IEA calculations. Therefore, it was reasoned to rout in too low cost projections and/or faulty LCOE formula, where one possible explanation was the division by aggregate wind for 20 years, and not one year. Had it been so, then the presented values would by mathematics have been 20 times higher

(20 times lower denominator).

Else, the overall decaying trend for the future base scenarios compared to the costs of the present, were in line with the lower cost projections for 2030.

Interestingly, the high future estimate of 1.25 GW subgroup equalled its current counterpart. This discrepancy can be attributed to two key factors: the cost of the battery remained constant for the 2020 base and 2030 high. Secondly, the full load hours (FLH) for all future capacities, except the 1 GW subgroup, were found to be lower than their 2020 counterparts, as tabulated in Appendix E.5. This implies that the efficiency gains from the 2030 electrolyzer, coupled with its reduced size, led to fewer full load hours, thereby increasing the adjusted present value of the investment.

Notably, were the two configurations: the scenarios for both compressed air storage of the 1.5 GW in 2030 and 1.8 GW in 2020; labelled as "towers" in the following. One explanation was the considerably high capital expenditures for these storage choices, as found in Appendix E.1. Subsequently, a “battery-only” case was investigated for the two cases, in addition to the 1.8GW 2030 having hydrogen as storage medium. This is described later in Chapter 4.5.

Hydrogen production cost

The second key performance indicator (KPI) under consideration, price per kilogram of hydrogen, is essentially a reflection of the LCOE, demonstrated by Figure 4.9 previously. On the other hand, nuanced by the APDH, the resulting values, projected in Figure 4.10, were consequently low, but to an lesser degree than the LCOE itself. For perspective, in regards to IEA hydrogen price projections, the found values were seemingly corresponding to those with natural gas or coal origin, where by renewables it should have been in the 3-8$ range [74] by 2018 projections.

Moreover, novel hydrogen companies such NEL, are aiming for 1.5$ per kilogram of hydrogen by 2025 [75]. That said, on less capital intensive grounds than for the proposed system. Hence, the found values can be stated as low, notwithstanding that 2030 is five years ahead of the said company target.

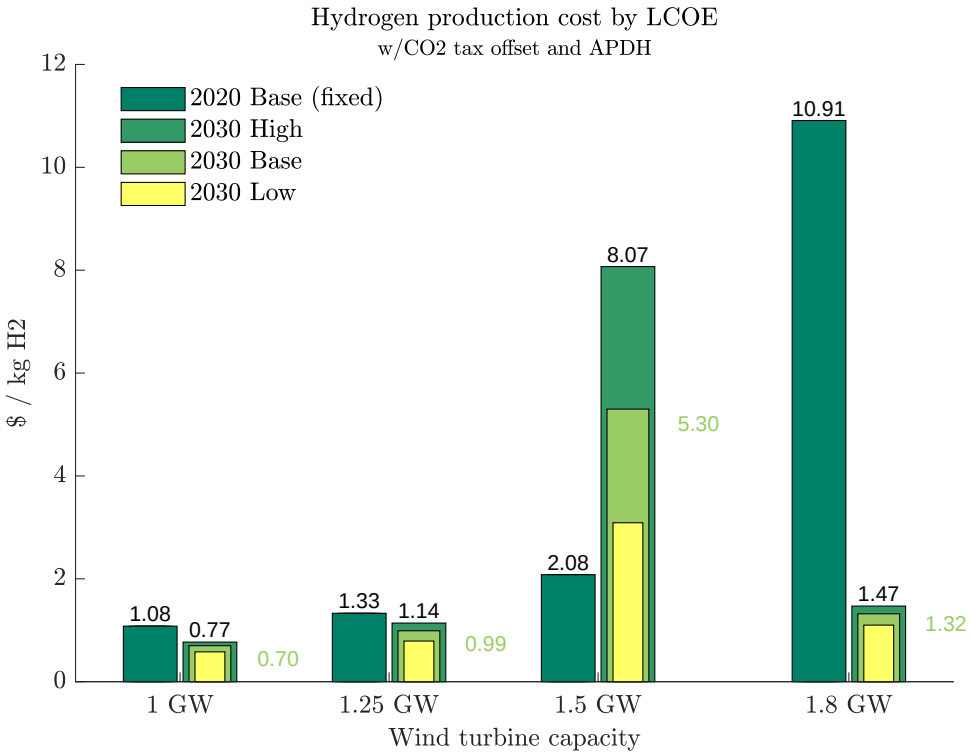

Figure 4.10: H2 cost

For the observant reader, the trend of decreasing values for future scenarios was clearer. Recall that the LCOE for the 1.25 GW scenario in 2030 was equal to its 2020 counterpart. This discrepancy was no longer the case when the latter was found to have an 66.53 versus 56.6 kWh/kg H2 demand, found in Appendix C

Moreover, while the 1.25 GW and 1.8 GW scenarios for 2030 had similar LCOEs, the higher APDH for the latter drove the future base prices apart to 1.02 to 1.36 $/kg, respectively, shown on the right-hand side of the bar plots for these respective capacities.

Methanol RAW production cost

Following the LCOE and hydrogen results, the cost sum of the green hydrogen and onshore DAC-captured CO2, with a power purchase at 96$ /MWh, is plotted below in Figure 4.11.

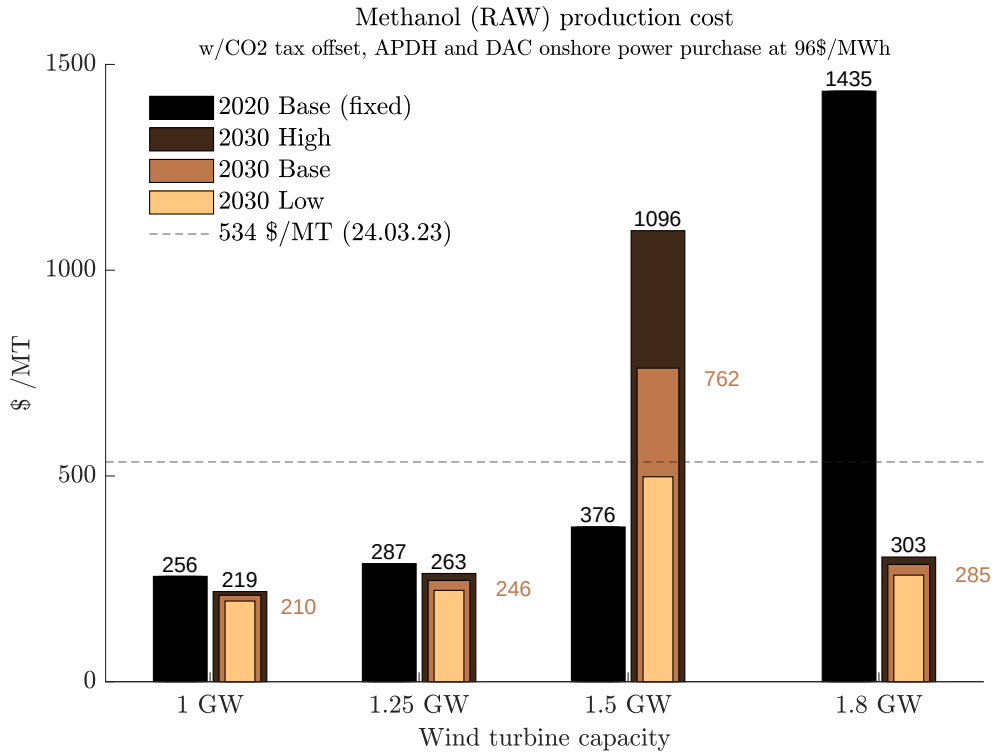

Figure 4.11: KPI RAW Methanol w/onshore DAC

As a more mature product, the trading price for methanol was found to be 534 $ / MT as of 24.03.23 [76]. Meaning, all the raw prices apart from the two said configurations of high LCOE, had production cost lower than its price today, implying profitable production of the suggested system. That said, without the cost of compressors, incoming hydrogen storage and the synthesis itself. The latter being marked up by a factor from literature review [1], to portray slightly more realistic results later, in Chapter 4.6.

4.5 Battery-only

Encouraged by the high values in the "tower" instances, a scenario with batteries only was formulated. This began with three cases having a round-trip efficiency (RTE) less than 100%, to which a battery solution was virtually assigned. Specifically, for the two cases with RTE = 55%, their new BE peak was reduced to 55% of the initial demand, as it now represented a 1:1 withdrawal/deposit technology. Resulting in a twofold cost reduction: first, lowered capacity demand, and second, in terms of price, since the battery solution had a lower tabulated cost than compressed air. Next, the 1.8 GW 2030 case had its original hydrogen storage "replaced" by a battery solution, thus demanding only 25% of the original share.

Further, the remaining power fractions, 45% and 75% respectively, were sold as power to shore, in the following as "extra power", constrained by the cable capacity of 576 MWh. Alternatively, one could have dissipated the energy, e.g. by higher resistance in the wind turbine rotors, effectively reducing their rotations. Power influxes larger than 576 MWh were not included, although retrospectively, their fraction upwards of the cable limitation could have been utilized.

In terms of energy, the extra power amounted to a staggering 1045, 1672, and 1235 GWh for the configurations, driving down the system costs further by the subsequent extra power sales. For perspective, this was the equivalent of 6.7, 14.9 and 6.6% as found in Table E.8 in Appendix E.8. **Moreover, combined with phase 2 return power, the total power sold was 16.7, 28.3 and 16.6% of the generated.**

Acknowledging no validation of the actual storage development was conducted with the virtual battery-only investigation. Assuming the new (lower) storage peaks exceeding the largest calculated BE threshold, they would, by definition, not affect the states of charge, and therefore, the storage development directly. On the other hand, the storage development as a whole could have been altered.

In essence, the changes presented subsequently will only be applicable to the specific cases where the remaining instances remain unchanged, as their RTE was 100%, i.e., they initially had battery storage. In addition: these demonstrate an intermittent storage overhead, where complete tabulated data is found in Appendix E.7.

LCOE - battery only

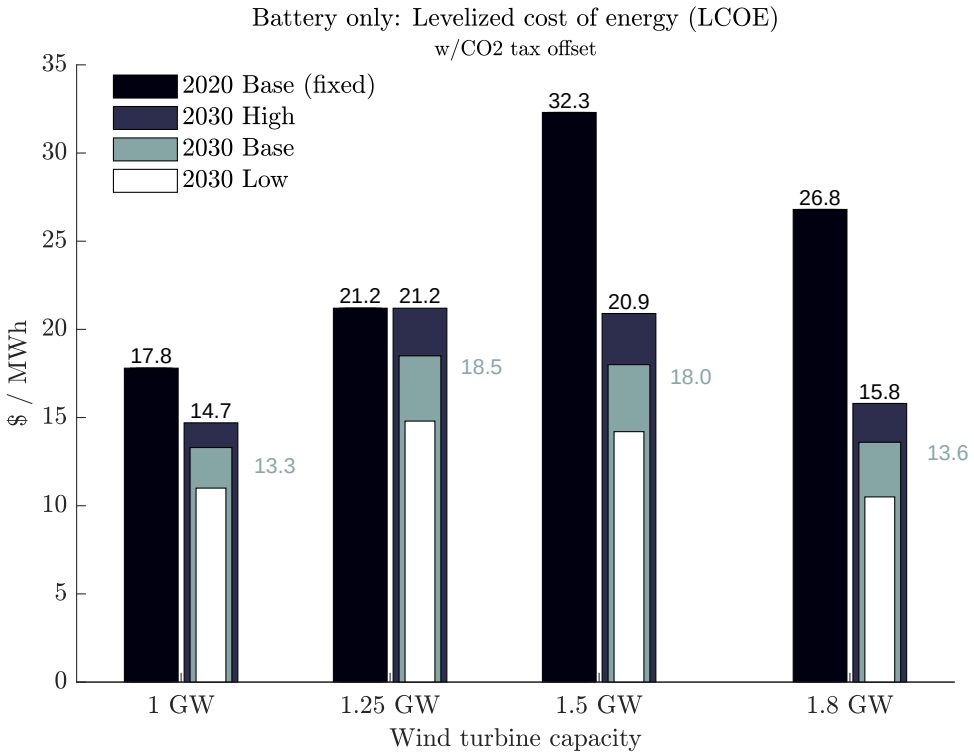

Figure 4.12: Battery-only: LCOE w/CO2 advantage
The battery-only effects are limited to the three rightmost barplots for 1.5 GW 2030, 1.5 & 1.8 GW

Quantitatively, this led to changes in LCOE of -79.5%, -82.2%, and -26.9%, respectively, from left to right. As expected, the first two cases saw the largest changes, achieved by replacing the compressed air storage. For the initial hydrogen storage, at the rightmost, despite being relatively cost-effective as shown in Appendix E.1, also experienced a reduction, presumably at large due to increased power sales revenue, also found in Appendix E.8.

Moreover, now the 2020 1.5 GW turned more capital intensive than the 2030 option, whilst the relation remained the same for the subgroup of 1.8GW, in line with the expected.

Hydrogen production cost - battery only

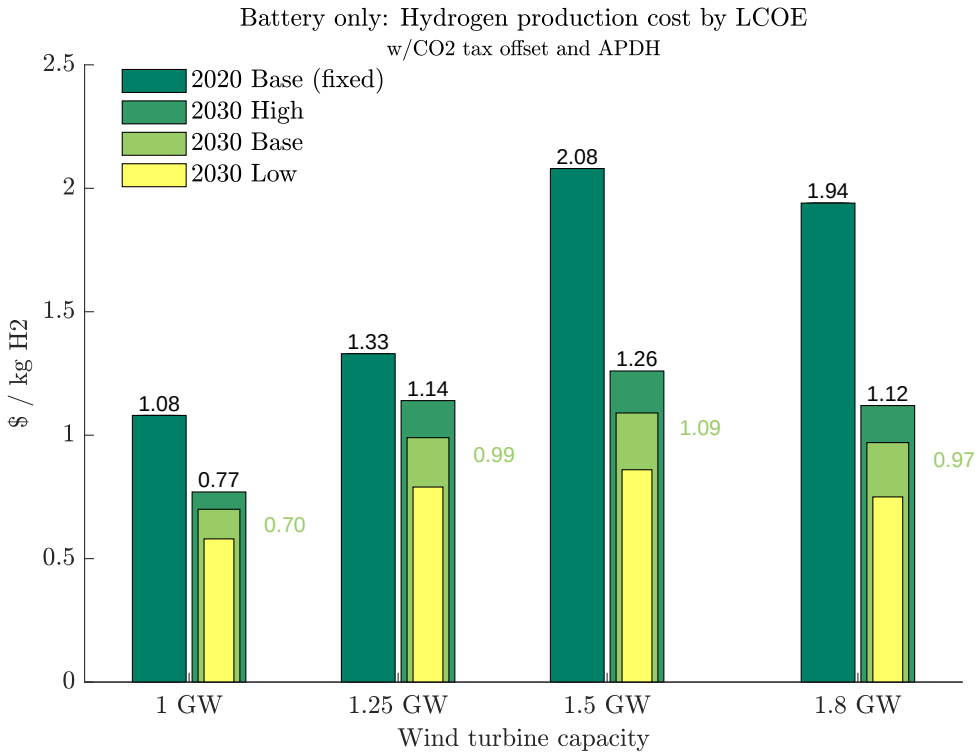

Figure 4.13: KPI: Hydrogen self cost (battery-only)

From the plot in Figure 4.13, it appears that the 1.5 GW is somewhat of a turning point for the 2030 values, with the 1.25 and 1.8 GW options being more cost-effective. For the 2020 values, the cost increases with capacity until the largest subgroup. The results themselves yielded more conservative estimates than their counterparts with less than 1$ per kilogram. Meaning, these results were satisfactory relative to each other, but as discussed on the lower end.

That said, whilst the larger subgroups had a trend of increased self-cost, their output share is greater, which in sum may yield larger operational profits. This an aspect for further work.

Methanol (RAW) production cost - battery only

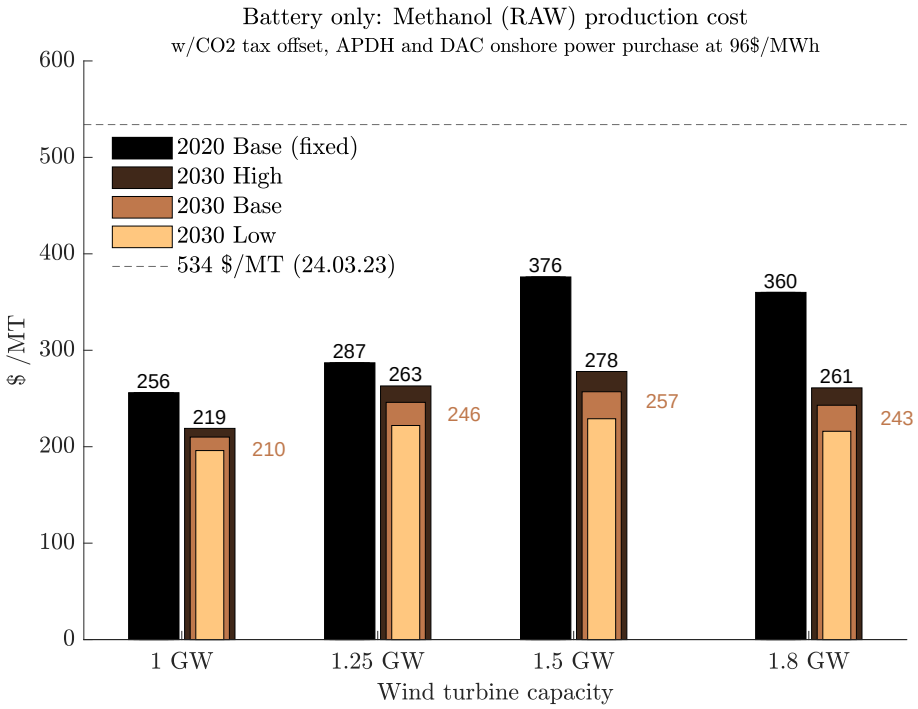

Figure 4.14: KPI: RAW Methanol

Similar to the reductions seen for the hydrogen self-cost, subsequently this yielded changes of -70%, -78% and -17%, respectfully, left to right. Additionally, now all cases below the found methanol trading price of 534$ per metric tonne.

4.6 Methanol estimates w/markup

Consequently, from a report on e-fuels towards 2050 [1], visually, the synthesize process was estimated to 10-15% of the total e-methanol price. Hence, by selecting a 25% markup factor, to virtually include additional system costs neglected, for instance compressors and/or intermittent hydrogen storage solution onshore, the following plots have been made in Figure 4.15 and 4.16, for the standard and battery-only scenarios.

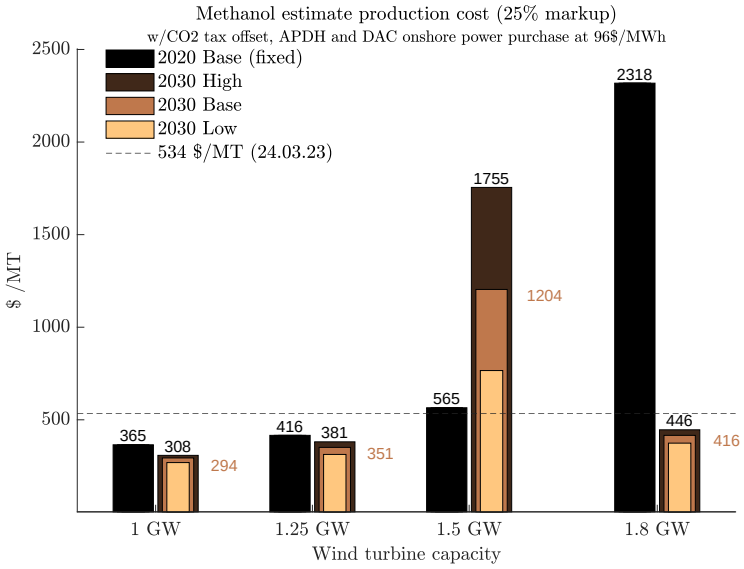

Figure 4.15: Methanol estimate w/markup 25%

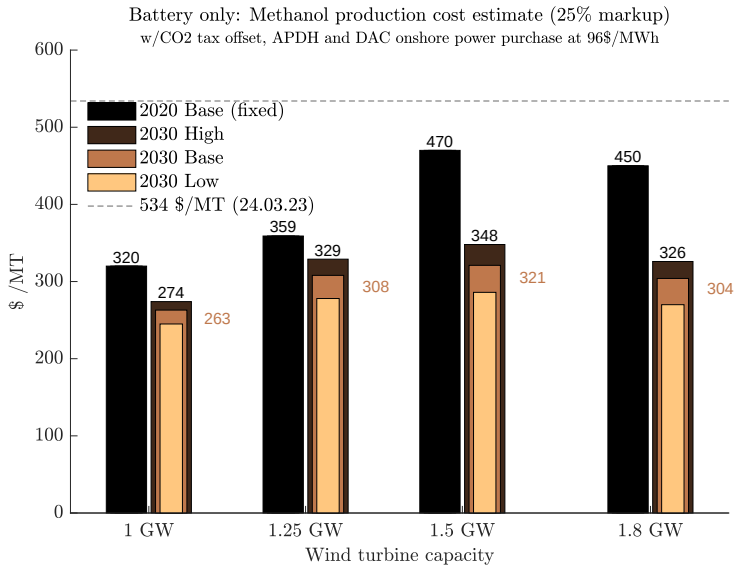

Figure 4.16: Battery only: Methanol estimate w/markup 25%

Focusing on the latter, all the self-cost estimates were still found to be below methanol prices of today. Moreover, if there would be a green methanol premium and/or more offset possibilities beyond the factored CO2 tax - the profit margins would be even greater.

On the other hand, whilst these are only estimates, more capital expenditures would have to take place for equipment such as the aforementioned compressors, intermittent storage facilities, purge gas systems for the electrolyzers and more.

4.7 Other results & discussions

Limited uniqueness of sorting

The chosen configurations and parameters for phases 2 and 3 were preferred by the weighted formula score. However, for each phase, the results became increasingly over-optimized. That is, the configurations selected were often among the best (lowest) 50 100, or even 200 identical scores. Herein, the selected options were automatically sorted by the lowest RunID and if not – assumably based on the heaviest formula weights, since there was a mathematical possibility of having lower targets and a higher BE peak, compensating by very lower standard deviations and in sum yielding the same score.

In essence, it was a positive indication that the system did not need to operate on a single specific configuration, i.e., being hyper-optimized. For instance, if the locking hours of mechanisms could be extended from 2 to 10 hours without impacting the output, it could provide flexibility.

Sorting formula

Given that both the code and the weight formula were self-developed, there was a combined subjective and mathematical probability that the chosen weight formula could have prevented the identification of the best optimization in terms of trade-offs. Additional parameters could have been incorporated into the formula, such as the fluctuation of the electrolyzer mode.

Simulation step size

In regards to figure 3.11 in Chapter 3.9, it was discussed whether halved step sizes of 0.05 would be required. This was not case, as the finer sensitivity analysis of 52 500 as opposed to 13 500, did not yield more unique results. Meaning, step sizes of 0.1 were chosen for all instances subsequently to the testing of instance 1, phase 1. Moreover, this was underscored by the limited sorting uniqueness.

Counters for mechanisms

Recalling that prior to activating the mechanisms, a counter had to reach a limit, set by the sensitivity analysis. These, were disclosed to not be in a consecutive fashion, e.g. if the safetyNet limit was set to 2 hours, and the netto power was deficit, surplus and lastly deficit - the counter would not reset by the second hour - when there was a surplus, but rather activate the mechanism for the third hour. In retrospect, this could have been implemented upon testing whether it would reduce excess interventions. That is, by comparing target parameters such as standard deviations and the hydrogen output, with the BE peak in mind.

On the other hand, during fluctuations between deficit and surplus - relative to the power demand in that particular electrolyzer mode, then per chance this implementation is correct after all, as it would then activate the mechanism mentioned, i.e. lower one electrolyzer mode for a lock-number of hours.

Extra surplus utilization

The initial assumption that the surplus utilization parameter should be on the lower end (10-40%), proved to be irrelevant, when investigating successfully upwards of 80%. Meaning, further optimization potential is possible. Moreover, if to be combined with battery-only scenario (or a equivalently high RTE solution) with an higher surplus utilization could potentially return incredible amounts power. Consequently, the re-inclusion of larger sub-groups could be of interest.

Power revenue

Having modeled purchase and selling price based on larger industry spot contracts of 96$/MWh - in perspective, the assumption of no impact on the power grid, is emphasized as an simplification. That is, in light of the 2030 1.8GW setup, yielding 1.1 TWh power return, and 2.4 TWh for the same case in battery only scope (inc. phase 2). These numbers were equivalent to 0.75% and 1.64 % of the produced power in Norway in 2022, respectively. Additionally, the maximum purchase power was for the same scenario, demanding 953 MW. On the other hand, the average major power consuming price could be modeled at half the price, had one chosen to fixate the contracts. In other words: one could argue that the impact on the grid was reflected to an certain degree.

Re-adjustments of APDH

In hindsight, having obtained the APDH based on the hydrogen output in light of the total wind produced - the returned power sold to shore, was not subtracted from the overall production. Meaning, the APDH could have been lowered, as all of the power was not solely oriented around the hydrogen production no more. Hence, the APDH could be lowered, and possibly the overall self-costs.

On the other hand, the LCOE was adjusted by the power sales itself, hence lowering the hydrogen and methanol costs as such.

Learning curves and economics of scale

There was not applied a learning curve for the DAC power demand of 1500 kWh/MT CO2, due to limited knowledge and the technology itself maturing. Moreover, the number presented was fairly low in the first place, being based on a novel company with reference to a pilot project. On the other hand, the DAC learning curve was significantly projected,

hence, one could argue that if not the CapEx itself would arrive at the lowered, future costs, then indirectly power savings could accounted for the remaining fraction; i.e. a reduced power demand per annum could represent an part of the levelized CapEx costs spread over a given lifetime.

In addition, economics of scale was not applied due to limited literature found for the large scales at hand, e.g. if it would even be possible, especially for the storage solutions such as batteries.

Cable Capacity Check

The preliminary estimate for the returned power demand, 576 MWh, was deemed satisfactory, given that the maximum value observed was 560 MW per hour in the 2030 1.8 GW scenario. Consequently, the cable costs for all scenarios were scaled based on this configuration and assumed to have 100% full load hours: per definition potential for further cost reduction by individual cable capacity and utilization factors less than 100%.

Visualization Errors

Following phase 2, the RunIDs of 2-61332 and 3-61332, for 1.25 GW 2030 and 1.5 GW 2020 respectively, the Matlab-script designed to plot the actual differences indicated by the raw data failed to do so. However, had the code been faulty, the remaining plots shown in phase 2 results would not have been generated either. The source of the error remained a mystery. Intriguingly, the cases shared the same ID, excluding the first digit - differentiated by the first digit corresponding to 1.25 and 1.5 GW, respectively.

Conclusion

In the first simulation phase, with increased wind turbine capacity, the general trend was increased adjusted power demand per kg of H2 (APDH), a parameter accounting for power withheld in the intermittent storage (BE), due to the divergence between hydrogen output and the unrealistic storage demands; not being limited. Consequently the 2 and 2.5 GW options were discarded. Additionally, as intended, round-trip efficiency (RTE) significantly influenced APDH: a higher RTE increased target production and BE peak while lowering APDH. Lastly, an intriguing increase in the storage demand (peak) from 1 to 1.5GW motivate the inclusion of a 1.25 GW subgroup, resulting in a halved storage peak to that of the 1.5 GW subgroup, whilst nearly matching the target of it.

With the activation of mechanisms in phase 2, the observed trade-off in both 2020 and 2030, was that storage demands decreased more than the reductions of hydrogen production. In turn, increasing the APDH contrary to the findings from phase 1. That said, not accounting for the power sold, where in hindsight APDH could have been lowered. Meaning, power sales was enabled by a hillClimb mechanism, where virtually all the scenarios preferred to transmit 40% (largest share in range) of the hourly surplus, once in the maximum production mode. It was further demonstrated that doubling this surplus utilization factor to 80% for the 1.8 GW 2020 configuration, increased the power amount sold by 170% and considerably reduced the BE peak to 19.71 (53.48) GWh. However, it also resulted in a decreased target and higher ADPH. In the end, the challenge of stabilizing the incoming power was not solved, with a disproportionate allocation of intermittent storage capacity.

Phase 3 was limited to threshold methodology and subsequently lowering the the output target, due to the buffering and strategy of the pipeline. Consequently, this heightened the APDH. It was proposed that lowering the settings of the delivery valves could have led to more stable pipeline levels and thereby delivery. The linear pressure assumption of the hydrogen was validated by CoolProp software, simplifying future work on a comprehensive line packing approach.

With the economic modeling, the study arrived at the sought key performance indicators. Firstly, the levelized costs of energy (LCOE) values fell on the lower end of typical values, that is, 17.8-32.3 (150.5) $/MWh for the 2020 base scenario, and 13.3-18.6 (87.7) for the 2030 base. Partly due to the offsetting revenues from annual power sales and the deduction of CO2 taxes. Notably, the discount factor 7.9% was on the higher end, which should have made the overall costs less competitive, especially with a fixed for all 3% OpEx and the combined system utilization factors found to be in the 25-50% range. Hence, the system

was assumed modeled incorrectly and/or with incomplete cost estimates.

In terms of discrepancies, the 1.25 GW 2030 High scenario surpassed the 2020 base costs due to conservative battery cost reductions projected and smaller utilization factor. Moreover, the 1.8 GW in 2020 and 1.5 GW in 2030 configurations, already denoted by the parenthesized values above and in the following, respectively, were close to and above the onshore power purchase price of 96$/MWh, i.e., in this context high LCOE values. The 1.8 GW 2030 scenario had hydrogen storage, which proved comparable to those of 1.25 GW, having battery storage.

Upon factoring in the adjusted power demand per hydrogen (APDH), the second KPI: hydrogen self-cost, was found slightly less consistent with the low LCOE, yielding 1.08-2.09 (10.91) $/kg H2 for the 2020 base scenario, and 0.7-1.32 (5.30) $/kg H2 for the 2030 base. That is, due to increased APDH with higher subgroup capacity, as stated.

For the third KPI: raw methanol prices, were found with good margin below the present trading (534 $/MT) prices, when yielding 256-376 (1435) $/MT for the 2020 base scenario, and 210-285 (762) $/MT for the 2030 base. Motivated by the pursuit of a final, synthesized methanol price – the raw methanol cost estimates were marked up by 25%. Subsequently, yielding cost projections closer to the present trading price. That is, still with a reasonable, profitable margin.

Lastly, for the three configurations not having a battery solution, an assessment of a battery-only scenario was conducted, i.e. by virtually replacing their storage solutions. Resulting in substantially more power sold and and lowering of storage costs. Consequently, the LCOE got reduced by over 80% and 20% for the initial compressed air and hydrogen storage solutions, with the more efficient battery storage. In concluding remarks, this underscored the large potential of power optimization for the problem at hand.

Further work

Current Structure of the Code

Having demonstrated the potential of power return in phase 2, and furthermore in the case of 80% surplus utilization in Chapter 3.3 – the code should be enhanced to yield a better power spread of the stored energy throughout the year, avoiding the highs and lows.

Moreover, upon investigating the battery-only scenario, the proposed system should clearly be evaluated to focus more on the power aspect, as opposed to hydrogen only, with power sales as a side benefits.

Dynamic flow to the electrolyzers

Regarding the assumption of full capacity utilization of the power cable, one could also consider expanding the scope to deliver electricity from the shore to the electrolyzers. That is, either by hourly demand and/or once within certain power prices onshore. Moreover, in light of the low LCOE attained as compared to the fixed purchase price, one could focus on power sales during the daytime, and retrieving power by the night time, possible at more stable rates with the Norwegian hydro production, in turn better suited for the electrolyzers offshore. In other words: stabilize the whole system by grid balancing. For the intermittent storage offshore, it could then be charged during daytime by the amount not transmitted to shore, i.e., by selecting a base load of sales.

Multiple Power Sources and/or Hot Spot

The initial selection of wind as the sole power source should be reconsidered given the great optimization potential left; if possible, to solve by the system proposed. That is, the combination of wind and solar are portrayed [77] to as solution for higher base loads of power generation, that in turn should simplify the optimization challenge, as it per definition would yield a more stable input. Herein, a comparison with a so-called *Hot spot* — a location with more stable and/or superior weather conditions, should be included, if not made as main location.

Number of Threshold Modes

The methodology, derived from a simple inspiration, is suitable for further investigation of the number of states of charge. That is, beyond the five (three in some configurations) modeled here. Acknowledging that more BE thresholds could lead to higher state of charge fluctuations, and consequently more deviation. Conversely, an optimal number of modes could cause the intermittent storage to stabilize around a few modes throughout the year, making the downstream processes more predictable.

Data input & predictive modeling

Having the scripts only read one year of weather data on an hourly basis, there is, by definition, room for optimization by prediction.

For starters, feeding the developed scripts with 2019 data, and then developing the code to use it as backbone. Next, once simulating with the same 2019 data and knowing the hours ahead, one could make a simple prediction mechanism based on that, in addition to the felt wind conditions together with the BE state of charge for the next hours. At the core of it, operational security would be the overruling feature of the current conditions, effectively turning the prediction impact of in necessary.

Furthermore, refined by using real-time machine learning, allowing the code to continuously learn the patterns. For instance, identifying similarities between the hourly input and the pre-loaded data, calculating parameters such as standard deviation, and thus determining the degree of freedom for the predictive model.

Herein, if a significant difference were to exist between the current and the pre-loaded conditions, e.g. based on predictions impact or a new year of data, the primary focus would be on the former, while more predictive approaches would be allowed if conditions were more similar and within the learned material. Lastly, with more years of data, the model would get more accurate. If successful, this could solve some of the disproportionate energy management in the intermittent storage, seen in the present work.

Green power certificates

In addition to the CO2 offset applied, the Renewable Energy Guarantees of Origin (REGO) in the United Kingdom saw average prices of 3£ (approximately 3.7$) per MWh in July 2022. This was equivalent to over 20% of the found LCOE for 1 GW in 2020.

In essence, an industrial player would purchase this certificate to offset their emissions, in line with given legislation or climate goals. From the producer's perspective, it would consequently offset the LCOE by the said premium. It is worth noting that such a combination with a CO2 tax might be an overestimation, but it demonstrates an additional incentive, once there is a market for such.

Further to this, even without a carbon offset modelled here, the REGO equivalent in the

EU region, known as *Guarantees of Origin*, were estimated to reach 6-8 € per MWh in 2023. Moreover, it was found that the peak of the GO in 2022 totaled 10 € per MWh, which constituted over 50% of the self-cost of 1 GW in 2020.

Appendix A

Phase 1

A.1 Complete table 2030

Table A.1: Phase 1: Full table 2030

1: 50 kWh/kg H2, strict threshold; 2: 50 kWh/kg H2, loose threshold; 3: 60 kWh/kg H2, strict threshold; 4: 60 kWh/kg H2, loose threshold

Run ID	% of target prod	BE peak [GWh]	APDH [kWh/kg H2]	H2 avg [tonne/h]	H2 prod dev. [tonne]	BE amp. [ratio]	BE avg. [GWh/h]	BE dev. [GWh]	Inst.#
161312	57.08	5.59	50.04	10.70	6.25	6.59	2.65	1.14	1
231333	76.52	72.65	55.99	14.35	6.57	172.63	12.84	14.32	1
311433	77.65	122.55	66.20	14.56	6.68	1969.03	20.79	23.95	1
411533	82.62	206.73	69.14	15.49	6.11	8495.37	37.72	43.00	1
521312	99.97	1007.10	71.42	18.74	0.27	701.28	610.00	192.83	1
161133	57.10	3.53	50.02	10.71	7.00	19.32	1.21	0.76	2
231433	76.64	71.59	55.89	14.37	6.55	222.15	11.85	14.31	2
311533	77.90	121.36	65.99	14.61	6.73	114.33	19.69	23.87	2
411433	82.75	205.63	69.03	15.52	6.13	217.77	36.65	42.92	2
521212	99.98	1006.16	71.42	18.75	0.22	700.63	609.07	192.83	2

A.2 Complete table 2020

Table A.2: Phase 1: Full table 2020

1: 50 kWh/kg H2, strict threshold; 2: 50 kWh/kg H2, loose threshold; 3: 60 kWh/kg H2, strict threshold; 4: 60 kWh/kg H2, loose threshold

Run ID	% of target prod	BE peak [GWh]	APDH [kWh/kg H2]	H2 avg [tonne/h]	H2 prod dev. [tonne]	BE amp. [ratio]	BE avg. [GWh/h]	BE dev. [GWh]	Inst.#
161312	47.56	4.59	60.05	8.92	5.32	4.50	2.75	1.08	3
261332	71.11	37.92	60.25	13.33	6.60	37.13	7.15	6.75	3
331333	76.52	87.18	67.19	14.35	6.57	172.63	15.41	17.19	3
421533	78.89	125.97	72.40	14.79	6.41	348.02	23.19	26.40	3
541422	99.96	890.32	71.43	18.74	0.31	619.96	535.29	164.84	3
161234	47.58	2.33	60.03	8.92	5.94	21.39	1.21	0.76	4
261124	71.13	36.12	60.23	13.34	6.82	345.26	5.42	6.63	4
331433	76.64	85.91	67.07	14.37	6.55	222.15	14.22	17.17	4
421533	79.13	124.56	72.19	14.84	6.48	226.40	21.77	26.29	4
541131	99.97	888.13	71.42	18.75	0.26	593.03	533.10	164.84	4

A.3 1.25 GW full table

Table A.3: Phase 1: Full 1.25 GW table

Run ID	% of target prod	BE peak [GWh]	a.kWh/ kg H2	H2 avg [t]	H2 prod dev. [t]	BE amp. [GWh]	BE avg. [GWh]	BE dev [GWh]	Instance #
261332	71.11 %	31.60	50.20	13.33	6.60	37.13	5.96	5.62	1
261332	71.12 %	30.71	50.20	13.33	6.57	111.79	4.89	5.68	2
261212	59.45 %	9.74	60.05	11.15	6.43	9.49	3.49	1.72	3
261122	59.47 %	7.94	60.03	11.15	6.78	24.84	1.90	1.48	4

Instance 1 - Phase 1 -normalization factors

Table A.4: Phase 1: 2030 normalization factors

CAP	% of target prod	BE max need	Hours in max	r.kWh/ kg H2	H2 avg	H2 prod dev.	BE max/min	BE avg. Held	BE dev
1	57.1 %	47.22	3371	68.80	10.70	7.49	1388	39.23	13.01
1.5	84.7 %	149.61	6888	68.54	15.88	7.91	8640	63.16	28.09
1.8	99.5 %	477.72	8688	70.55	18.65	7.31	85570	222.78	103.26
2	100.0 %	1195.59	8753	72.31	18.74	6.69	17816	672.80	228.04
2.5	100.0 %	3536.97	8756	78.12	18.74	4.57	29333	1857.07	854.97

Appendix B

PHASE 2

B.1 2030

Table B.1: Phase 2 results tabulated for instance 1

comparing phase 1 and phase 2 results directly. Headers with "comb" refer to a surplus hydrogen production, if all the allocated surplus electricity once ran in maximum mode.

RUN ID 1	Run ID 2	% of H2 target	% of target prod COMB	BE PEAK [GW]	APDH [kWh/kg H2]	adj. kWh / kg H2[C]	H2 prod dev. [t]	H2 prod dev.[C, t]	BE avg. [GWh]	BE dev [GWh]
16131		57.08		5.59	50.04		6.25		2.65	1.14
	33114	54.41	57.08	4.77	52.49	50.03	6.04	6.10	2.53	1.05
261332		71.11		31.60	50.20		6.60		5.96	5.62
	33114	66.56	71.22	19.66	53.64	50.12	6.63	6.94	4.20	3.26
33133		76.52		72.65	55.99		6.57		12.84	14.32
	11114	70.91	79.48	44.56	60.41	53.90	6.84	7.55	7.04	7.28
411433		77.65		122.55	66.20		6.68		20.79	23.95
	11114	72.56	86.43	74.32	70.85	59.48	6.98	8.39	10.73	12.21

B.2 2020

Table B.2: Phase 2 instance 3, best weight sorted combinations.

RUN ID 1	Run ID 2	% of target prod	% of target prod COMB	BE PEAK [GW]	adj. kWh / kg H2	adj. kWh / kg H2[C]	H2 prod dev. [t]	H2 prod dev.[C, t]	BE avg. [GWh]	BE dev [GWh]
16131		47.56		4.59	60.05		5.32		2.75	1.08
	11111	47.56	47.56	4.59	60.05	60.05	5.32	5.32	2.75	1.08
261212		59.45		9.74	60.05		6.43		3.49	1.72
	11114	56.60	59.46	7.35	63.08	60.04	6.26	6.31	3.23	1.42
36133		71.11		37.92	60.25		6.60		7.15	6.75
	33114	66.56	71.22	23.59	64.37	60.15	6.63	6.94	5.04	3.91
431333		76.52		87.18	67.19		6.57		15.41	17.19
	11114	70.91	79.48	53.48	72.49	64.68	6.84	7.55	8.45	8.73

B.3 80% surplus complete table

Table B.3: Phase 2 instance 3, 80% surplus

Run ID	% of H2 target prod	% of target prod COMB	BE PEAK	a.kWh/ kg H2	a.kWh/ kg H2 [COMB]	H2 prod dev.	H2 prod dev. [COMB]	BE avg. Held	BE dev
11118	60	83	19.71	86.23	62.12	6.75	8.69	4.07	3.04

Appendix C

Phase 3

C.1 Full table phase 3

Table C.1: Phase 3: All results

RunID 3	% of H2 target, Phase 2	% of H2 target, Phase 3]	ADPH [kWh/kg H2]	Flow avg [m3/h].	flow std.dev.	Pipe avg.	Pipe std.dev.
111	57.08	54.41	52.49	1.18	0.70	2.31	0.93
112	71.11	66.53	53.66	1.45	0.76	2.70	1.10
111	76.52	70.92	60.41	1.54	0.79	2.69	1.08
112	77.65	72.51	70.90	1.58	0.80	2.77	1.20
111	47.56	47.12	60.61	1.03	0.61	2.13	0.85
111	59.45	56.60	63.07	1.23	0.72	2.37	0.95
112	71.11	66.53	64.39	1.45	0.76	2.70	1.10
111	76.52	70.92	72.49	1.54	0.79	2.69	1.08

C.2 Phase 3: RunID

Table C.2: Phase 3: ID table

complementing Table 4.10

RunID 2	RunID 3	# Pipes	Pipe margin [%]	First buffer margin [%]
33114	111	1	30	0
33114	112	1	30	5
11114	111	1	30	0
11114	112	1	30	5
-	-	-	-	-
11111	111	1	30	0
11114	111	1	30	0
33114	112	1	30	5
11114	111	1	30	0

C.3 CoolProp

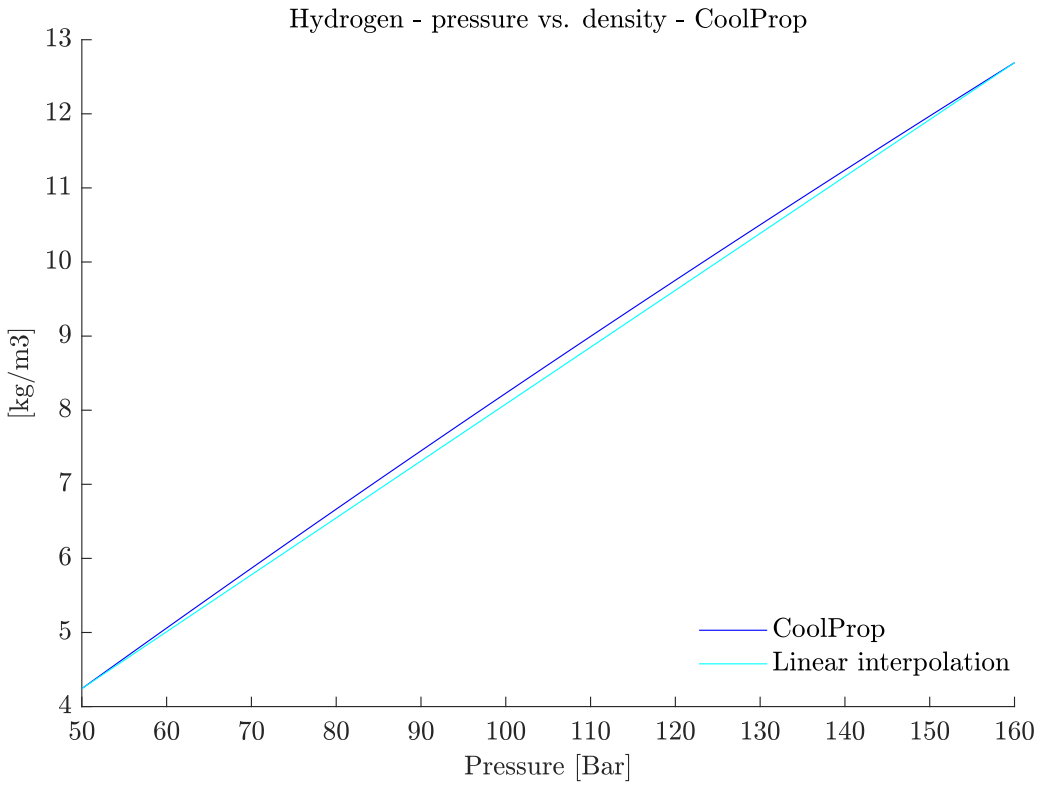

Figure C.1: Hydrogen: finding the relationship between density and pressure w/CoolProp

Figure C.1 gives valuable information. Firstly, it validates the linear assumption made for the threshold approach by setting the average of 50 and 160 bar, i.e. 105 bar for the whole pipeline - to determine the capacity.

Secondly, in terms of future work, and the possible implementation of line packing - one could alter the code from adjusting the delivery valve openings - to increase or decrease the pressurization inside the pipe, i.e. slowing down the flow, but at the same time hold - and subsequently deliver a higher amount of hydrogen per hour. Whilst it would be limited by the actual hydrogen produced, the amount received on the other side would be more stable and predictable as such.

Appendix D

Methanol synthesis reaction

The stoichiometric reaction for green methanol synthesis used [78]:

$$\mathrm{CO_2} + 3\,\mathrm{H_2} \longrightarrow \mathrm{CH_3OH} + \mathrm{H_{20}} \tag{D.1}$$

In terms of molecular weights, we have:

- CO_2: 44 g/mol
- H_2: 2 g/mol
- CH_3OH: 32 g/mol
- H_2O: 18 g/mol

Converting to mass:

$$(44\frac{kg}{kmol} * 1 \text{ kmol } \mathrm{CO_2}) + (2\frac{kg}{kmol} * 3 \text{ kmol } \mathrm{CO_2}) \tag{D.2}$$

$$= \tag{D.3}$$

$$(32\frac{kg}{kmol} * 1 \text{ kmol } \mathrm{CH_3OH}) + (18\frac{kg}{kmol} * 1 \text{ kmol } \mathrm{H_2O}) \tag{D.4}$$

Mass basis:

$$44kg\mathrm{CO_2} + 6kg\mathrm{H_2} = 32kg\mathrm{CH_3OH} + 18kg\mathrm{H_2O} \tag{D.5}$$

Dividing by 32:

$$1.375kg\mathrm{CO_2} + 0.1875kg\mathrm{H_2} = 1kg\mathrm{CH_3OH} + 0.563kg\mathrm{H_2O} \tag{D.6}$$

Resulting in 0.1875 kilogram of hydrogen needed per kilogram of methanol.

Appendix E

Economy

E.1 CapEx cost distribution

Table E.1: CapEx cost distribution

GW	year	Turbines [%]	Electrolyzers [%]	Pipeline [%]	Storage [%]	DAC CapEx [%]	Cable [%]
1	2030	60.0	16.5	1.3	10.5	1.4	10.3
1.25	2030	50.7	11.2	0.9	29.2	1.1	7.0
1.5	2030	18.3	3.4	0.3	75.6	0.4	2.1
1.8	2030	52.0	8.0	0.6	33.6	0.9	5.0
1	2020	58.6	18.5	1.0	9.9	3.7	8.3
1.25	2020	49.5	12.5	0.7	28.7	3.0	5.6
1.5	2020	40.4	8.5	0.5	44.4	2.4	3.8
1.8	2020	14.0	2.5	0.1	81.6	0.7	1.1

E.2 Phase 2 power returned & DAC demand

Table E.2: Phase 2: Power returned & DAC demand

CAPACITY	INSTANCE	Generated [GWh]	Returned [GWh]	Return RATE	DAC Power
1	1	4691	219	4.66 %	20.96 %
1.25	1	5864	384	6.55 %	20.50 %
1.5	1	7037	702	9.98 %	18.21 %
1.8	1	8444	1139	13.49 %	15.51 %
1	3	4691	43	0.92 %	18.15 %
1.25	3	5864	280	4.78 %	17.44 %
1.5	3	7037	461	6.55 %	17.08 %
1.8	3	8444	842	9.98 %	15.17 %

E.3 Annual revenues

Table E.3: Annual revenues

Subgroup [GW]	Instance	Power revenue [MM $]	CO2 tax deduction [MM $]
1	1	21.0	137.0
1.25	1	36.9	167.5
1.5	1	67.4	178.5
1.8	1	109.4	182.5
1	3	4.1	34.3
1.25	3	26.9	41.2
1.5	3	44.2	48.5
1.8	3	80.9	51.7

E.4 Utilization factors

Table E.4: Utilization factors

Storage	YEAR	[GW]	W.Turbine [%]	Elec. [%]	Battery [%]	CAES [%]	H2 [%]	CABLE [%]	DAC [%]	Pipe [%]
BATTERY	2030	1	54	54	53	-	-	4	100	100
BATTERY	2030	1.25	54	67	19	-	-	8	100	100
CompAir	2030	1.5	54	71	-	16	-	14	100	100
H2 storage	2030	1.8	54	73	-	-	14	23	100	100
-	-	-	-	-	-	-	-	-	-	-
BATTERY	2020	1	54	47	60	-	-	1	100	100
BATTERY	2020	1.25	54	57	44	-	-	6	100	100
BATTERY	2020	1.5	54	67	19	-	-	9	100	100
CompAir	2020	1.8	54	71	-	16	-	17	100	100

E.5 Utilization factors adjusted for CapEx share

Table E.5: Utilization factors adjusted for CapEx share

Storage	Year	[GW]	WIND [%]	Elec [%]	Battery [%]	CAES [%]	H2 [%]	CABLE [%]	DAC [%]	Pipe [%]	FLH [%]
Battery	2030	1	32	9	6	-	-	0.4	2	1	50
Battery	2030	1.25	27	7	5	-	-	0.5	2	1	43
CAES	2030	1.5	10	2	-	12	-	0.3	0	0	25
H2 storage	2030	1.8	28	6	-	-	5	1.1	1	1	41
-	-	-	-	-	-	-	-	-	-	-	-
Battery	2020	1	31	9	6	-	-	0	5	1	51
Battery	2020	1.25	26	7	13	-	-	0	4	1	51
Battery	2020	1.5	21	6	8	-	-	0	3	0	39
CAES	2020	1.8	7	2	-	13	-	0	1	0	23

E.6 LCOE with and without CO2 tax [Battery-only]

Table E.6: LCOE with and without CO2 tax [BAT]

Year	CAPACITY	LCOE [$ /MWh]	LCOE (w/CO2 tax adv.)	Difference [$ /MWh]
2030	1	14.7	13.3	1.5
2030	1.25	19.9	18.5	1.4
2030	1.5	89.0	87.7	1.3
2030	1.8	19.7	18.6	1.1
-	-	-	-	-
2020	1	18.2	17.8	0.4
2020	1.25	21.5	21.2	0.4
2020	1.5	32.6	32.3	0.3
2020	1.8	150.8	150.5	0.3

E.7 CapEx cost distributions [Battery-only]

Table E.7: CapEx cost distributions [BAT]

Subgroup [GW]	Instance	Turbines start	Electrolyzers	PipeLine	Storage	DAC CAPEX	CABLE
1	1	59.7	16.4	1.3	10.4	1.9	10.3
1.25	1	50.5	11.1	0.9	29.1	1.5	6.9
1.5	1	51.6	9.5	0.7	30.9	1.4	5.9
1.8	1	60.2	9.2	0.7	22.8	1.4	5.7
1	3	57.8	18.2	1.0	9.8	5.0	8.2
1.25	3	48.9	12.3	0.7	28.4	4.1	5.6
1.5	3	40.1	8.4	0.5	44.0	3.3	3.8
1.8	3	46.0	8.1	0.5	38.6	3.3	3.6

E.8 Phase 2 & DAC demand + extra power returned [Battery-only]

Table E.8: Phase 2 power return + extra power [BAT]

Subgroup	Instance	Generated [GWh]	Phase 2 return [GWh]	Return rate [%]	DAC [GWh]	extra [GWh]	extra sold [GWh]	extra return [%]	Total return [%]
1	1	4691	219	4.7	21.0				
1.25	1	5864	384	6.5	20.5				
1.5	1	7037	702	10.0	18.2	1045	470	6.7	16.7
1.8	1	8444	1139	13.5	15.5	1672	1254	14.9	28.3
1	3	4691	43	0.9	18.1			0.0	0.9
1.25	3	5864	280	4.8	17.4			0.0	4.8
1.5	3	7037	461	6.5	17.1			0.0	6.5
1.8	3	8444	842	10.0	15.2	1235	556	6.6	16.6

E.9 Annual revenues [Battery-only]

Table E.9: Annual revenues [BAT]

Subgroup [GW]	INSTANCE	Power revenue [MM $]	CO2 tax deduction [MM $]
1	1	21.0	137.0
1.25	1	36.9	167.5
1.5	1	112.5	178.5
1.8	1	229.8	182.5
1	3	4.1	34.3
1.25	3	26.9	41.2
1.5	3	44.2	48.5
1.8	3	134.2	51.7

E.10 Utilization factors adjusted for CapEx share [Battery-only]

Table E.10: Utilization factors adjusted for CapEx (battery only)

Where the non-adjusted were equal to those in standard study.

Year	Subgroup [GW]	WIND [%]	Electrolyzers [%]	Battery [%]	CAES [%]	H2 [%]	Cable [%]	DAC [%]	Pipeline [%]	UTF [%]
2030	1	32	9	6	-	-	0.4	2	1	50
2030	1.25	27	7	5	-	-	0.5	2	1	43
2030	1.5	28	7	-	5	-	0.8	1	1	42
2030	1.8	32	7	-	-	3	1.3	1	1	46
-	-	-	-	-	-	-	-	-	-	-
2020	1	31	9	6	-	-	0	5	1	51
2020	1.25	26	7	13	-	-	0	4	1	51
2020	1.5	21	6	8	-	-	0	3	0	39
2020	1.8	25	6	-	6	-	1	3	0	41

E.11 LCOE with and without CO2 tax deduction [Battery-only]

Table E.11: LCOE with and without CO2 tax deduction [BAT]

Year	Subgroup [GW]	LCOE [$ /MWh]	LCOE (w/CO2 tax adv.)	Difference = CO2 offset in $ /MWh
2030	1	14.7	13.3	1.5
2030	1.25	19.9	18.5	1.4
2030	1.5	19.2	18.0	1.3
2030	1.8	14.7	13.6	1.1
-	-	-	-	-
2020	1	18.2	17.8	0.4
2020	1.25	21.5	21.2	0.4
2020	1.5	32.6	32.3	0.3
2020	1.8	27.1	26.8	0.3

Appendix F

Matlab-script

```
clear all
close all
clc
% script version RAW

%% Data read
% 2019-01-10 16:00,2019-01-10 17:00,1618507.606 (GW)
% is the format to read inn the data
tic
fullFileName = 'YOUR FILE LOCATION OF THIS ---->\
    Vestas_V164_8000_140.csv';

t = readtable(fullFileName);  % copy this one out for speeeed
    processing
toc
%
% startHours  = t{:,1};
% endHours    = t{:,2};
electricity = t{:,3};

tic



%% Important info
% this script is the sensitivity version, i.e. it does not
    provide plots.



pointer = 1;
```

```
hoursOfData = length(electricity);
jpoint = pointer:1:hoursOfData; % length of remaining hours


%% CODE START : input paramters  [FIXED THROUGHOUT]

% Hourly methanol production target
mdot_methanol = 100000; %100 000 kg/h

H2perM = 0.1875; % hydrogen per methanol (mass basis)| 18 750 kg
mdot_h2 = mdot_methanol*H2perM; %Kg H2/h


%_______________
% electrolyzers
neta_PEM = 60 % kWh/kg H2

neta_Choice = neta_PEM;

%_______________
% Conversion factors

kilo2giga= 10^-6;
kilo2ton = 10^-3;

% Flow control
% standard for zero (charging mode) and full production = 100%
    load
%_____________________
c0  = 0;              %|
c10 = 100 / 100;      %|
%_____________________|

targetValues = 16; %i.e we will have one row, with 16 filtered
    variables
                   %per simulation setup
%
    ::::::::::::::::::::::::::::::::::::::::::::::::::::::::::::::::::::::::::::::::

%% Pre_calc

%H2 kg/H * kWh/ kg H2  * (1/10^6) = GWh/h
powerPEM = neta_PEM*mdot_h2*kilo2giga;
```

```
% Scaling from kWh to GWh
elProdFull = electricity.*kilo2giga;

%% Choice of code mechanisms (CCM)

% Build up in pipeline
PreLoad = 'off'; %NB! Has to be "off" exactly; "Off" does not
    work:)

% freezeMode
freezeInterval = 0; % off when zero, do not remove anyway!

% surpluss utilization
surpUtz = 0 / 100; % surpluss utilization for extra electrolyzer
    output


% safetyNet
%____________________|
safetyNet = 'on';%|
%>>>>>>>>>>>>>>>>>>>>|


% hillClimb
%____________________|
hillClimb = 'on';%|
%>>>>>>>>>>>>>>>>>>>>|

%NB! the counters and more for safetyNet and hillClimb are being
    handled
%automatically in the main code!

%% INPUT RUN ID

RunID = [1 6 1 3 1 2];

%% Phase 1 INPUT: USE RANGES FROM PHASE 1 and selected
    configurations


%************ MANUAL INPUT FROM PHASE 1*************
Phase1_selected_OP1 = [1 1.25 1.5 1.8 2 2.5];
Phase1_selected_OP2 = linspace(0.25,1.0,6);
Phase1_selected_OP3 = [4 8 12 24 36 48];
```

```
Phase1_selected_OP4 = linspace(1,0.6,5);
Phase1_selected_OP5 = linspace(0.6,0.4,3);
Phase1_selected_OP6 = linspace(0.4,0,5);


elProd = elProdFull.*Phase1_selected_OP1(RunID(1)); %scaleFactor;
    %     /(kilo2giga))/1816600;
RTE = Phase1_selected_OP2(RunID(2));
BuT = Phase1_selected_OP3(RunID(3));
c8 = Phase1_selected_OP4(RunID(4));
c6 = Phase1_selected_OP5(RunID(5));
c4 = Phase1_selected_OP6(RunID(6));


coeffList = [c10,c8,c6,c4,c0];
margin = BuT*powerPEM;


M10 = c10*margin;
D10 = c10*powerPEM;
% Mode 8
M8  = c8*margin;
D8  = c8*powerPEM;
% Mode 6
M6  = c6*margin;
D6  = c6*powerPEM;
% Mode 4
M4  = c4*margin;
D4  = c4*powerPEM;
% Mode 0/Charging
M0 = c0*margin;
D0 = c0*powerPEM;
%::::::::::::::::::
modeLoadSelection = [D10,D8,D6,D4,D0];
modeSelection = [M10,M8,M6,M4,M0];
% modeSelectionTXT = split(num2str(modeSelection));
modeSelectionTXT = {'M10','M8','M6','M4','M0'};



%% PHASE 2 input - USE RANGES FROM PHASE 2 and selected
    configurations
% i.e., it is using the previous phase ranges, similar to those
    found lower
```

```
% in  %% THE SENSITIVITY ANALYSIS SIMULATION SETUP     [PHASE 3]

RunID2 = [2  1  1  1  1];

Phase2_selected_OP1 = linspace(2, 10, 5);    % fuseLim
Phase2_selected_OP2 = linspace(4,12,5);      % fuseFreezeRef
Phase2_selected_OP3 = linspace(2, 10, 5);    % hillLim
Phase2_selected_OP4 = linspace(4,12,5);      % hillFreezeRef
Phase2_selected_OP5 = linspace(10,40,4);     % surtpUtzHillClimb

fuseLim           = Phase2_selected_OP1(RunID2(1));
fuseFreezeRef     = Phase2_selected_OP2(RunID2(2));
hillLim           = Phase2_selected_OP3(RunID2(3));
hillFreezeRef     = Phase2_selected_OP4(RunID2(4));
surpUtzHillClimb = Phase2_selected_OP5(RunID2(5));
%::::::::::::::::::::::::::::::::::::::::::::::::::

%% PHASE 3 settings

% Hydrogen properties ~ in the pipeline

rhoH2 = 8.6136;% kg/m3 % 7.057 engineering toolbox, nederst, 100
    bara
hydrogenTarget = mdot_h2/rhoH2; % 18 750 [kg/h] /
%                                       rho [kg/m3] = flow [m3/h]

m3ToTCM = 10^-3;
hydrogenTargetTCM = hydrogenTarget*m3ToTCM;


pipeLength = 56;%km
km2m = 1000;
pipeDiameter = 0.508; % m; 20 inch pipe

counterDelta = 5; % manualy set the intervals of the counters


%___________DELIVERY VALVE
    Openings_____________________________________________
Valve10 = c10*hydrogenTargetTCM; % should not be adjusted as it
    has to
                                 % match max production in case
                                     of overfill
Valve0 = c0*hydrogenTargetTCM;   % Per definition zero _ closed
```

```
    valve
%
    ________________________________________________________________________________


Valve8 = c8*hydrogenTargetTCM;
Valve6 = c6*hydrogenTargetTCM;
Valve4 = c4*hydrogenTargetTCM;
%
    ****************************************************************************


% List of the above valves
ValveLoadSelection = [Valve10,Valve8,Valve6,Valve4,Valve0];
% Length of list; # unique valves
ValveModes = size(ValveLoadSelection,2);


 %% THE SENSITIVITY ANALYSIS SIMULATION SETUP      [PHASE 3]


OP1 = [c4,c6,c8]; % MAKE SHURE THE UPSHIFT CAN HANDLE IT
OP1steps = length(OP1);

OP1 = c4; OP1steps = 1;
%------------------------------------------------------------

%-----------------------------OP2----------------------------- # of pipes
OP2Low = 1; OP2High = 3; OP2steps = 1;%3
OP2 = linspace(OP2Low,OP2High,OP2steps);

OP2 = 1; OP2steps = 1;
%------------------------------------------------------------

%-----------------------------OP3----------------------------- pipeMarginFrac
OP3Low = 0.3; OP3High = 0.8; OP3steps = 1; %5
OP3 = linspace(OP3Low,OP3High,OP3steps);
%------------------------------------------------------------

%-----------------------------OP4----------------------------- firstBufferMargin
OP4Low = 1; OP4High = 1.25; OP4steps = 1;% 6
OP4 = linspace(OP4Low,OP4High,OP4steps);
%------------------------------------------------------------
```

```
% Number of configurations
codeRowLength = OP1steps*OP2steps*OP3steps*OP4steps;

% codeRowCounter = 1:1:codeRowLenght;
fprintf('Selected optimization ranges yield %.0f configurations
    to run!\n', codeRowLength)
fprintf('Initializing!\n')

% Counter for the row number
codeRowCounter = 1;

% The rows will represent the OP1-parameters:)
codeOutPut    = zeros(codeRowLength,targetValues);

% ____________________THE SENSITIVITY ANALYSIS SIMULATION SETUP
    _________________
%
    ____________________________________________________________________________

%% ______________________________CORE CODE
    LOOP_____________________________________

for OpOne = 1:OP1steps
    % selecting the treshold value activating the underFill
        mechanism based
    % on one of the coefficients (c8,c6,c4)
    riskCoeff = OP1(OpOne);
    % consequently, the said upshift mechanism can only shift one
        modi down
    % or up per "upshift", this mainted by valveUpshiftRisk
    valveUpshiftRisk = find(riskCoeff == coeffList,1); % 1 is
        needed here to avoid duplicates

    for OpTwo = 1:OP2steps
        pipes = OP2(OpTwo);

        for OpThree = 1:OP3steps
            pipeMarginFrac = OP3(OpThree);

            for OpFour = 1:OP4steps
                firstBufferMargin = OP4(OpFour);

%% ________________RESETTING DUMMIES AND FETCHING
```

```
    VALUES_______________________

%start with charging and from zero preLoad per iteration

mode = M0;
BE = 0;
H2prod = 0;
net = 0;

BEvector = [];
H2vec =       [];
% BE = BEdummy; % copied out: starts from zero anyway

%_____________________
%code 3.0
extraH2vec  = [];
surpH2el    =  0;
surpH2prod  =  0;

fuseCounter = 0;
fuseBlown = 0;
fuseFreeze = fuseFreezeRef;

%____________
% code 3.0 - hill climb + overProduction
hillCounter = 0;
hillBreak = 0;
hillFreeze = hillFreezeRef;



surp = surpUtz; % can use normally surpluss production with
    hillClimb mode
%
    ::::::::::::::::::::::::::::::::::::::::::::::::::::::::::::::::::::::::::::


%_________________________RESETTING DUMMIES / FETCHING
    VARIABELS____________________________
%
    ____________________________________________________________________________________________

%% OLD AND NEW RESTART BEFORE CODE _ OUTER LOOP
```

```
% In thousand cubic meters (TCM)
pipeCapacityTCM = pipes*(pipeLength*km2m)*(pi*(pipeDiameter*0.5)
    ^2)...
                    *m3ToTCM;

pipeStorageMargin = pipeMarginFrac.*pipeCapacityTCM;


%_____________________________
% Pipeline & delivery mechanisms and vectors|
%_____________________________________________|
firstBuffer = "not reached";%|
% pipeOverride = "false";      %|    % hydrogen produced in a
    specific hour
%>>>>>>>>>>>>>>>>>>>>>>>>>>>>>>>>>>>>>>>>>>>|
dummySkip = -1;                %|       % Dummy needed for start-up
                               %|
pipeStorageVec =[];            %|
flowDelivered = [];            %|
                               %|
flowDiff = 0;                      %|
pipeStorage = 0;               %|
valveOpen = Valve0;            %|       % delivery valve closed @
    start
%-------------------------------|

% UNCLEARED VARIBLES _ what do they do?

tankCount = 0;
safeReleaseRelay = 0;



%_______________
% Pipeline risks

riskOverfill = pipeCapacityTCM-(1*hydrogenTargetTCM);%|
riskUnderfill =(riskCoeff)*pipeCapacityTCM;          %|
%-----------------------------------------------------------

%_____________________________________________________
% Valve tresholds                                     |
%_____________________________________________________|
Valve5t = c10*pipeStorageMargin;
```

```
Valve4t = c8*pipeStorageMargin;
Valve3t = c6*pipeStorageMargin;
Valve2t = c4*pipeStorageMargin;
Valve1t = c0*pipeStorageMargin;
%
    <<<<<<<<<<<<<<<<<<<<<<<<<<<<<<<<<<<<<<<<<<<<<<<<<<<<<<<<<<<<<<<<<<<<<<<<<<<<<|

tresholdLoadSelection    = [Valve5t,Valve4t,Valve3t,Valve2t,
    Valve1t];%|

%
    --------------------------------------------------------------------------|

% the load selections above are containers for selected variables
        |
%
    --------------------------------------------------------------------------|


startUpBuffer = pipeStorageMargin*firstBufferMargin;        %|
marginUpShiftEnd = tresholdLoadSelection(valveUpshiftRisk);


%*****
%___________________RESETTING DUMMIES / FETCHING
    VARIABELS_____________________
%
    ___________________________________________________________________________________

%% ____________________________CORE of the
    CODE________________________________

for i = jpoint % (MAIN LOOP)


  % Standard code no matter  Freezing(on  | off)
  %                                    :       :
  %                          safetyNet(off | on)
  %
  % NB! modes have to be linked (:) in this way

  % Should this be copied as well=??

              freezePointer = rem(i,freezeInterval);
```

```
            if isnan(freezePointer) % quick fix when NaN;
            freezePointer = 1;          % the case when freezing
               is off
            end

  %
     _______________________________________________________________________________

  %___________________________FUZE CHECK
     _______________________________________
  %
     _______________________________________________________________________________


if fuseBlown == 1
     if fuseFreeze == 1 % code goes back to normal

           fuseBlown = 0;
           fuseFreeze = fuseLim;
           fuseCounter = 0;

           % oversteer the freezPointer one last time
           freezePointer = 0;


     elseif (fuseFreeze<=fuseLim) && (fuseFreeze>1)
            % freezing goes on
            fuseFreeze = fuseFreeze -1;
            freezePointer = 0;

     end % of FUZE CHECK

end % of fuseBlown

 %
    _________________________________________________________________________________

 %____________________________ hillCLIMB
    check______________________________________
 %
    _________________________________________________________________________________
```

```
 if hillBreak == 1

          if hillFreeze == 1 % LAST HILL RUN

                  hillBreak = 0;
                  hillFreeze = hillLim;
                  hillCounter = 0;
%                   disp('Last run') % test


                  freezePointer = 0;% oversteer the freezPointer
                     one last time


          elseif (hillFreeze<=hillLim) && (hillFreeze >1)

                   hillFreeze = hillFreeze-1;
                   freezePointer = 0;
%                       disp('Still hill locked') test

          end % of hillCLIMB check


    %% COPY BACK-IN IN PHASE 3

% %  else
% %          surpUtz = surp; % reset the extra production
% % %          disp('Normal run') test
%_____________________________________
%_____________________________________


 end
%
    ____________________________________________________________________

%% SWITCH freezePointer ( MAIN INTERNAL LOOP )
% CASE 1: normal run
% Case "else" : looping locks into a certain mode
%             : depending on weather safetyNET or hillCLIMB is
    activated
%
    ____________________________________________________________________
```

```
switch freezePointer

    case 1 % hits one - code runs normally - unfrozen

        switch mode

            case M10
                % netto from this hour in selected mode
                net = elProd(i) - D10;
                %too litle
                BE = BE + (net<0)*(net*(1/RTE));

                modeLoad = D10;

                %hydrogen production

                H2prod = c10*mdot_h2;

                % code 3.0

                % extra - in case - with variable
                    surpluss usage

                surpH2el =  surpUtz*((net>0)*(net));
                BE = BE + (1-surpUtz)*((net>0)*(net));

                % Electricity , [GWh--> kWh] ,[kWh/(kWh/kg)
                    = kg H2
                                                        %
                                                          -->

                                                        ton

                                                        H2

                surpH2prod = (surpH2el*(kilo2giga^-1))
                    /...
                                (neta_Choice);



            case M8
```

```
%                           fprintf(['Iteration ',num2str(i),'net
    ', num2str(net) ,...
%                                   ' M8 |  BE: ',num2str(BE),' \n
    '])

                            net = elProd(i) - D8;
                            %too litle
                            BE = BE + (net<0)*(net*(1/RTE));
                            % too much

                            modeLoad = D8;

                            %hydrogen production

                            H2prod = c8*mdot_h2;

                            % code 3.0

                            % extra - in case

                            surpH2el =  surpUtz*((net>0)*(net));
                            BE = BE + (1-surpUtz)*((net>0)*(net));

                            % Electricity, [GWh--> kWh],[kWh/(kWh/kg)
                                = kg H2
                                                                  %
                                                                    -->

                                                                  ton

                                                                  H2

                            surpH2prod = (surpH2el*(kilo2giga^-1))
                                /...
                                            (neta_Choice);


                        case M6

%                           fprintf(['Iteration ',num2str(i),'net
    ', num2str(net) ,...
%                                   ' M6 |  BE: ',num2str(BE),' \n
    '])
```

```
                net = elProd(i) - D6;

                %to litle
                BE = BE + (net<0)*(net*(1/RTE));
                % to much

                modeLoad = D6;

                %hydrogen production

                H2prod = c6*mdot_h2;

                % code 3.0

                % extra - in case

                surpH2el =  surpUtz*((net>0)*(net));
                BE = BE + (1-surpUtz)*((net>0)*(net));

                % Electricity , [GWh--> kWh] ,[kWh/(kWh/kg)
                    = kg H2
                                                        %
                                                          -->

                                                        ton

                                                        H2

                surpH2prod = (surpH2el*(kilo2giga^-1))
                    /...
                                (neta_Choice);


            case M4

%                   fprintf(['Iteration ',num2str(i),'net
    ', num2str(net) ,...
%                           ' M4 |  BE: ',num2str(BE),' \n
    '])
%
                net = elProd(i) - D4;
                %to litle
                BE = BE + (net<0)*(net*(1/RTE));
```

```
                % to much

                modeLoad = D4;

                %hydrogen production

                H2prod = c4*mdot_h2;

                % code 3.0

                % extra - in case

               surpH2el =  surpUtz*((net>0)*(net));
                BE = BE + (1-surpUtz)*((net>0)*(net));

               % Electricity, [GWh--> kWh],[kWh/(kWh/kg)
                  = kg H2
                                                        %
                                                          -->

                                                        ton

                                                        H2

                surpH2prod = (surpH2el*(kilo2giga^-1))
                    /...
                                (neta_Choice);


            otherwise %direct all to storage - STOP THE
               PLANT!
                BE = BE + elProd(i);


                H2prod = c0*mdot_h2;

                 modeLoad = D0;

        end

%
    ------------------------------------------------------------------------

%_____________________ safetyNET control panel
```

```
%_____________________________
%_____________________________________________________________________

        if safetyNet == "on" || safetyNet == "On"

                fuseCounter = fuseCounter + (net<0)*(1);

                fuseBlown = (fuseCounter>=fuseLim)*1;

                %
                    ..................................................

                if fuseBlown == 1

                safetyMode = find(modeLoadSelection ==
                    modeLoad);
                %_____________PATCH : if modes are merged
                    _____________
                safetyMode = safetyMode(1);
                %
                    ____________________________________________________


                            if safetyMode == 5 % can not go
                                below charging mode!
                                 modeLoad = modeLoadSelection
                                     (5);
                            else
                                 modeLoad = modeLoadSelection(
                                     safetyMode+1);
                            end
                end

        end
%
_____________________________________________________________________

%_____________________ hillCLIMB control panel
_____________________________
%
_____________________________________________________________________
```

```
if hillClimb == "on" || hillClimb == "On"

          hillCounter = hillCounter + (net>0)*(1);

          hillBreak = (hillCounter>=hillLim)*1;
                       % if yes : then SafetyNet deploys
                           via FuzeCheck next round
                       % and is consequently locked into
                           freezeMode for a given
                       % number of times (here:
                          fuzeFreeze = fuseLim for
                          starters)
          %only happens once fuse goes off, else the
             safetyNet jumps over this
          %part



          %
             ...................................................

          if hillBreak == 1

             safetyMode = find(modeLoadSelection ==
                modeLoad);
             %---------------PATCH : if modes are merged
               ---------------
               safetyMode = safetyMode(1);
            %
              ------------------------------------------------------------


                       if safetyMode == 1
                           surpUtz = surpUtzHillClimb;
                       elseif safetyMode == 5
%                              disp('Still charging')
                       else
                           modeLoad = modeLoadSelection(
                               safetyMode-1);
                       end


          end
          %
```

```
                    ...........................................
        end

    %___________________________Froozen
    ____________________________________________

        otherwise % freeze mode selected

                    % the net production is locked in by
                        modeLoad
                    net = elProd(i) - modeLoad;

                    %to litle
                    BE = BE + (net<0)*(net*(1/RTE));


                    %hydrogen production

                    H2prod = modeLoad*mdot_h2;

                    % code 3.0

                    % extra - in case

                  surpH2el =  surpUtz*((net>0)*(net));
                    BE = BE + (1-surpUtz)*((net>0)*(net));

                   % Electricity , [GWh--> kWh],[kWh/(kWh/kg)
                      = kg H2

                    surpH2prod = (surpH2el*(kilo2giga^-1))
                        /...
                                    (neta_Choice);

        end % FREEZE POINTER

%
   ______________________________________________________________________

%__________ BE level indicator: swtich freezePointer
   _______________
%
   ______________________________________________________________________
```

```
%STRICT


        if BE >= M10
            mode = M10;

        elseif (BE<M10)&&(BE>= M8)
            mode = M8;

        elseif (BE<M8)&&(BE>=M6)
            mode = M6;

        elseif (BE<M6)&&(BE>=M4)
            mode = M4;
        else
          mode = M0;

        end

%
    ------------------------------------------------------------------------

%_____________ UPDATE STORAGE LEVEL AND HYDROGEN OUTPUT
    ____________
%
    ------------------------------------------------------------------------


    BEvector(end+1) = BE;
    H2vec(end+1) = H2prod;
    extraH2vec(end+1) = surpH2prod;


end %of MAIN LOOP


%
%% FILTER THE DATA ------------------------> STORE
```

```
%_________________
% targetValue 1 : run ID

id = str2double(sprintf('%d', OpOne, OpTwo, OpThree, ...
                                OpFour, OpFive));
%........
codeOutPut(codeRowCounter,1) = id;


%_________________
% targetValue 2 : sum of all hydrogen produced vs target (TON
    )

totH2 = sum(H2vec);

fracOfTarget = (totH2) / (hoursOfData*mdot_h2);

%......
codeOutPut(codeRowCounter,2) =fracOfTarget;

%_________________
% targetValue 3 : sum of normal + extra hydrogen produced vs
    target (TON)

combH2vec = H2vec + extraH2vec;
totTOTH2 = sum(combH2vec);
fracOfTargetTOT = (totTOTH2) / (hoursOfData*mdot_h2);
codeOutPut(codeRowCounter,3) =fracOfTargetTOT;

%_________________
%     targetValue 4 : Bank of Electricity: max amp

firstPModeReached = find(BEvector>=M4,~0,'first');


minAmp = min(BEvector(firstPModeReached:end));
maxAmp = max(BEvector(firstPModeReached:end));

codeOutPut(codeRowCounter,4) = maxAmp;
```

```
    %__________________
    % targetValue 5 : PRODUCED KPI: kg H2 / kWh

    totPower = sum(elProd)/kilo2giga;

%     kgPerKwh = totH2/totPower;
    kWhPerkg = totPower/totH2;

    %......
    codeOutPut(codeRowCounter,5) = kWhPerkg;

        %__________________
    % targetValue 6 : PRODUCED w/extra KPI: kg H2 / kWh

    totPower = sum(elProd)/kilo2giga;

%     kgPerKwh = totH2/totPower;
    kWhPerkgX = totPower/totTOTH2;

    %......
    codeOutPut(codeRowCounter,6) = kWhPerkgX;



  %:::::::::::::::::::::::::

    %______
    %convert kg to Ton
    H2vec = H2vec./1000;
    extraH2vec = extraH2vec./1000;
    combH2vec = combH2vec./1000;


          %__________________
    % targetValue 7 : Standard deviation H2 normal


    diffH2 = H2vec-mean(H2vec);

    diffH2Squared = diffH2.^2;

    diffH2sum = sum(diffH2Squared);

    deviation = diffH2sum/length(H2vec);
```

```
standardDeviationH2 = sqrt(deviation);

codeOutPut(codeRowCounter,7) = standardDeviationH2;

%_____________________
% targetValue 8 : Standard deviation H2 normal  + EXTRA

diffH2comb = combH2vec-mean(combH2vec);

diffH2combSquared = diffH2comb.^2;

diffH2combsum = sum(diffH2combSquared);

deviation = diffH2combsum/length(combH2vec);

standardDeviationH2comb = sqrt(deviation);

codeOutPut(codeRowCounter,8) = standardDeviationH2comb;



%_____________________
 % targetValue 8 : Bank of Electricity: ampRatio
 ampRatBE = abs(maxAmp/minAmp);
 codeOutPut(codeRowCounter,9) = ampRatBE;

 %_____________________
 % targetValue 9: Bank of Electricity: mean

 meanBE = mean(BEvector);
 codeOutPut(codeRowCounter,9) = meanBE;


  %_____________________
  % targetValue 10: Bank of Electricity: standard deviation

 diffBE = BEvector - meanBE;

 diffBESquared = diffBE.^2;

 diffBEsum = sum(diffBESquared);
```

```
    deviation = diffBEsum/length(BEvector);

    standardDeviationBE = sqrt(deviation);


    codeOutPut(codeRowCounter,10) = standardDeviationBE;



     %__________________
     % targetValue 11: hours when having surpluss
    extraHours= sum(extraH2vec>0);

    codeOutPut(codeRowCounter,11) = extraHours;

% %
    %_____________________ PRINT OUT THE OP's for easier
       read_____

    codeOutPut(codeRowCounter, 12) = OP1(OpOne);
    codeOutPut(codeRowCounter, 13) = OP2(OpTwo);
    codeOutPut(codeRowCounter, 14) = OP3(OpThree);
    codeOutPut(codeRowCounter, 15) = OP4(OpFour);
    codeOutPut(codeRowCounter, 16) = OP5(OpFive);




    % Making a list of
    %         T1  T2 T3 T4  T5  T6.... T16 # amount of Target
       variabels
    %          :  :  :  :   :   :       :


   codeRowCounter = codeRowCounter+1;


%% STORING THE FILTERED DATA

            end %of optimalization paramter 4 : C8
        end %of optimalization paramter 3 : BuT (margin)
    end %of optimalization paramter 2 : RTE
end %of optimalization paramter 1 : wind capacity
```

```
% PRINT OUT
T = table(codeOutPut);
filename = 'Phase 3 results.xlsx';
writetable(T,filename,'Sheet','SensitivityAnalysisRAW','
    WriteVariableNames',true);



toc % end of timer
```

References

[1] Alba Soler et al. 'E-Fuels: A techno- economic assessment of European domestic production and imports towards 2050'. en. In: 17 (). URL: https://www.concawe.eu/wp-content/uploads/Rpt_22-17.pdf.

[2] Jenna Ruokonen et al. 'Modelling and Cost Estimation for Conversion of Green Methanol to Renewable Liquid Transport Fuels via Olefin Oligomerisation'. en. In: *Processes* 9.6 (June 2021). Number: 6 Publisher: Multidisciplinary Digital Publishing Institute, p. 1046. ISSN: 2227-9717. DOI: 10.3390/pr9061046. URL: https://www.mdpi.com/2227-9717/9/6/1046 (visited on 1st June 2023).

[3] Jessica Kersey, Natalie D. Popovich and Amol A. Phadke. 'Rapid battery cost declines accelerate the prospects of all-electric interregional container shipping'. en. In: *Nature Energy* 7.7 (July 2022). Number: 7 Publisher: Nature Publishing Group, pp. 664–674. ISSN: 2058-7546. DOI: 10.1038/s41560-022-01065-y. URL: https://www.nature.com/articles/s41560-022-01065-y (visited on 7th June 2023).

[4] *Reducing emissions from the shipping sector*. en. URL: https://climate.ec.europa.eu/eu-action/transport-emissions/reducing-emissions-shipping-sector_en (visited on 1st June 2023).

[5] *Decarbonize shipping*. en. URL: https://www.dnv.com/maritime/hub/decarbonize-shipping/resources/index.html (visited on 1st June 2023).

[6] Mina Tadros et al. 'Effect of different speed reduction strategies on ship fuel consumption in realistic weather conditions'. In: May 2022, pp. 553–561. ISBN: 978-1-00-332027-2. DOI: 10.1201/9781003320272-62.

[7] Ahmed G. Elkafas, Massimo Rivarolo and Aristide F. Massardo. 'Environmental economic analysis of speed reduction measure onboard container ships'. en. In: *Environmental Science and Pollution Research* 30.21 (May 2023), pp. 59645–59659. ISSN: 1614-7499. DOI: 10.1007/s11356-023-26745-4. URL: https://doi.org/10.1007/s11356-023-26745-4 (visited on 1st June 2023).

[8] Elizabeth Lindstad et al. 'Decarbonizing bulk shipping combining ship design and alternative power'. en. In: *Ocean Engineering* 266 (Dec. 2022), p. 112798. ISSN: 0029-8018. DOI: 10.1016/j.oceaneng.2022.112798. URL: https://www.sciencedirect.com/science/article/pii/S0029801822020819 (visited on 1st June 2023).

[9] *A brief introduction to air lubrication systems (ALS)*. en. URL: https://www.tmc.com/blog/article/brief-introduction-air-lubrication-systems-als (visited on 1st June 2023).

[10] *Maritime Forecast to 2050*. en. URL: https://www.dnv.com/Default (visited on 1st June 2023).

[11] *Energy giants BP and Iberdrola team up to build about 6GW of green hydrogen projects in Europe*. en. Section: energy_transition. July 2022. URL: https://www.rechargenews.com/energy-transition/energy-giants-bp-and-iberdrola-team-up-to-build-about-6gw-of-green-hydrogen-projects-in-europe/2-1-1268028 (visited on 1st June 2023).

[12] *eFuels pilot plant in Chile officially opened*. en. Dec. 2022. URL: https://newsroom.porsche.com/en/2022/company/porsche-highly-innovative-fuels-hif-opening-efuels-pilot-plant-haru-oni-chile-synthetic-fuels-30732.html (visited on 1st June 2023).

[13] *Norwegian tar eierandel i Norsk e-Fuel*. Apr. 2023. URL: https://www.tu.no/artikler/norwegian-gar-inn-i-e-fuel-fabrikk/529952 (visited on 1st June 2023).

[14] *A.P. Moller - Maersk continues green transformation with six additional large container vessels*. en. URL: https://www.maersk.com/news/articles/2022/10/05/maersk-continues-green-transformation (visited on 1st June 2023).

[15] *A.P. Moller – Maersk welcomes landmark green methanol vessel in Copenhagen this fall*. en. URL: https://www.maersk.com/news/articles/2023/04/26/maersk-welcomes-landmark-green-methanol-vessel-in-copenhagen-this-fall (visited on 1st June 2023).

[16] *The Paris Agreement | UNFCCC*. URL: https://unfccc.int/process-and-meetings/the-paris-agreement (visited on 7th June 2023).

[17] *Ammonia as a marine fuel DNV*. en. URL: https://www.dnv.com/Publications/ammonia-as-a-marine-fuel-191385 (visited on 1st June 2023).

[18] PubChem. *Methanol*. en. URL: https://pubchem.ncbi.nlm.nih.gov/compound/887 (visited on 1st June 2023).

[19] PubChem. *Hydrogen*. en. URL: https://pubchem.ncbi.nlm.nih.gov/compound/783 (visited on 1st June 2023).

[20] PubChem. *Ammonia*. en. URL: https://pubchem.ncbi.nlm.nih.gov/compound/222 (visited on 1st June 2023).

[21] Gürsel Süer. 'Designing parallel assembly lines'. In: *Computers & Industrial Engineering* 35 (Dec. 1998), pp. 467–470. DOI: 10.1016/S0360-8352(98)00135-1.

[22] Olje-og energidepartementet. *Nye områder for havvind på norsk sokkel*. no. Pressemelding. Publisher: regjeringen.no. Apr. 2023. URL: https://www.regjeringen.no/no/aktuelt/nye-omrader-for-havvind-pa-norsk-sokkel/id2973609/ (visited on 7th June 2023).

[23] Benjamin Flamm et al. 'Electrolyzer modeling and real-time control for optimized production of hydrogen gas'. en. In: *Applied Energy* 281 (Jan. 2021), p. 116031. ISSN: 0306-2619. DOI: 10.1016/j.apenergy.2020.116031. URL: https://www.sciencedirect.com/science/article/pii/S0306261920314690 (visited on 7th June 2023).

[24] G. Mosetti, C. Poloni and B. Diviacco. 'Optimization of wind turbine positioning in large windfarms by means of a genetic algorithm'. en. In: *Journal of Wind Engineering and Industrial Aerodynamics* 51.1 (Jan. 1994), pp. 105–116. ISSN: 0167-6105. DOI: 10.1016/0167-6105(94)90080-9. URL: https://www.sciencedirect.com/science/article/pii/0167610594900809 (visited on 7th June 2023).

[25] J. W. M. H. Geerts, J. H. B. J. Hoebink and K. van der Wiele. 'Methanol from natural gas. Proven and new technologies.' en. In: *Catalysis Today* 6.4 (Feb. 1990), pp. 613–620. ISSN: 0920-5861. DOI: 10.1016/0920-5861(90)85059-W. URL: https://www.sciencedirect.com/science/article/pii/092058619085059W (visited on 7th June 2023).

[26] *Green methanol schematic overview, correspondence Sylfest Myklatun.*

[27] Ragnhild Hancke, Thomas Holm and Øystein Ulleberg. 'The case for high-pressure PEM water electrolysis'. en. In: *Energy Conversion and Management* 261 (June 2022), p. 115642. ISSN: 0196-8904. DOI: 10.1016/j.enconman.2022.115642. URL: https://www.sciencedirect.com/science/article/pii/S0196890422004381 (visited on 7th June 2023).

[28] Shaolong Yang et al. '-Performance Modelling of Seawater Electrolysis in an Undivided Cell: Effects of Current Density and Seawater Salinity'. In: *Chemical Engineering Research and Design* 143 (Mar. 2019). DOI: 10.1016/j.cherd.2019.01.009.

[29] Annabelle Brisse, Josef Schefold and Aline Léon. 'Chapter 7 - High-temperature steam electrolysis'. en. In: *Electrochemical Power Sources: Fundamentals, Systems, and Applications*. Ed. by Tom Smolinka and Jurgen Garche. Elsevier, Jan. 2022, pp. 229–280. ISBN: 978-0-12-819424-9. DOI: 10.1016/B978-0-12-819424-9.00009-4. URL: https://www.sciencedirect.com/science/article/pii/B9780128194249000094 (visited on 7th June 2023).

[30] *Manufacturing Cost Analysis for Proton Exchange Membrane Water Electrolyzers*. URL: https://www.nrel.gov/wind/assets/pdfs/02_2_ning_aning_optimization.pdf.

[31] R. M. Navarro, R. Guil and J. L. G. Fierro. '2 - Introduction to hydrogen production'. en. In: *Compendium of Hydrogen Energy*. Ed. by Velu Subramani, Angelo Basile and T. Nejat Veziroğlu. Woodhead Publishing Series in Energy. Oxford: Woodhead Publishing, Jan. 2015, pp. 21–61. ISBN: 978-1-78242-361-4. DOI: 10.1016/B978-1-78242-361-4.00002-9. URL: https://www.sciencedirect.com/science/article/pii/B9781782423614000029 (visited on 7th June 2023).

[32] S. Shiva Kumar and V. Himabindu. 'Hydrogen production by PEM water electrolysis – A review'. en. In: *Materials Science for Energy Technologies* 2.3 (Dec. 2019), pp. 442–454. ISSN: 2589-2991. DOI: 10.1016/j.mset.2019.03.002. URL: https://www.sciencedirect.com/science/article/pii/S2589299119300035 (visited on 7th June 2023).

[33] Mandar Risbud et al. 'Chapter 14 - Electrolyzer technologies for hydrogen economy'. en. In: *Hydrogen Economy (Second Edition)*. Ed. by Antonio Scipioni, Alessandro Manzardo and Jingzheng Ren. Academic Press, Jan. 2023, pp. 459–485. ISBN: 978-0-323-99514-6. DOI: 10.1016/B978-0-323-99514-6.00003-0. URL: https://www.

sciencedirect.com/science/article/pii/B9780323995146000030 (visited on 7th June 2023).

[34] *Fueling the future of mobility: hydrogen electrolyzers*. URL: https://www2.deloitte.com/content/dam/Deloitte/cn/Documents/finance/deloitte-cn-fueling-the-future-of-mobility-en-200101.pdf.

[35] *AIR TO FUELS™ Technology*. en. URL: https://carbonengineering.com/air-to-fuels/ (visited on 7th June 2023).

[36] Mahdi Fasihi, Olga Efimova and Christian Breyer. 'Techno-economic assessment of CO2 direct air capture plants'. en. In: *Journal of Cleaner Production* 224 (July 2019), pp. 957–980. ISSN: 0959-6526. DOI: 10.1016/j.jclepro.2019.03.086. URL: https://www.sciencedirect.com/science/article/pii/S0959652619307772 (visited on 31st May 2023).

[37] URL: https://www.equinor.com/content/dam/statoil/documents/what-we-do/terminals-and-refineries/equinor-tjeldbergodden-2019.pdf.

[38] *Foreslår å utrede disse 20 områdene for havvind - NVE*. no. URL: https://nve.no/nytt-fra-nve/nyheter-energi/foreslaar-aa-utrede-disse-20-omraadene-for-havvind/ (visited on 7th June 2023).

[39] Office of the Prime Minister. *Announces the first competitions for offshore wind*. en-GB. Pressemelding. Publisher: regjeringen.no. Mar. 2023. URL: https://www.regjeringen.no/en/aktuelt/announces-the-first-competitions-for-offshore-wind/id2969473/ (visited on 7th June 2023).

[40] *Landanlegg*. no. URL: https://www.equinor.com/no/energi/landanlegg (visited on 7th June 2023).

[41] *Europipe II*. en. URL: https://www.gassco.no/en/our-activities/pipelines-and-platforms/europipe-II/ (visited on 7th June 2023).

[42] *Statpipe Dry Gas*. en. URL: https://www.gassco.no/en/our-activities/pipelines-and-platforms/statpipe-dry-gas/ (visited on 7th June 2023).

[43] *Renewables.ninja*. URL: https://www.renewables.ninja/ (visited on 7th June 2023).

[44] *Distance calculator - Calculate the distance online!* en-us. URL: https://www.distance.to/ (visited on 7th June 2023).

[45] harry budiharjo harry et al. *Increasing of Gas Capacity in Pipeline Using Line Packing Technique for Sustaining Gas Supply to Consumers*. June 2006.

[46] *V164-9.5 MW™*. en-US. URL: https://us.vestas.com/en-us/products/offshore/V164-9-5-MW (visited on 7th June 2023).

[47] *Normalt strømforbruk*. no. URL: https://www.elvia.no/smart-forbruk/forbruk-og-sparing/normalt-stromforbruk/ (visited on 7th June 2023).

[48] Florin Onea, Eugen Rusu and Liliana Rusu. 'Assessment of the Offshore Wind Energy Potential in the Romanian Exclusive Economic Zone'. en. In: *Journal of Marine Science and Engineering* 9.5 (May 2021). Number: 5 Publisher: Multidisciplinary Digital Publishing Institute, p. 531. ISSN: 2077-1312. DOI: 10.3390/jmse9050531. URL: https://www.mdpi.com/2077-1312/9/5/531 (visited on 7th June 2023).

[49] Natural Resources Canada. *Air-to-Fuels Development, Feasibility, and pre-FEED Study for First Commercial-Scale Demonstration Plant*. eng. Last Modified: 2019-03-22 Publisher: Natural Resources Canada. Dec. 2017. URL: https://natural-resources.canada.ca/science-and-data/funding-partnerships/funding-opportunities/current-investments/air-fuels-development-feasibility-and-pre-feed-study-for-first-commercial-scale-demon/20430 (visited on 7th June 2023).

[50] *Weighted Average Cost of Capital (WACC) Explained with Formula and Example*. en. URL: https://www.investopedia.com/terms/w/wacc.asp (visited on 7th June 2023).

[51] *Electricity production*. en. URL: https://energifaktanorge.no/en/norsk-energiforsyning/kraftproduksjon/ (visited on 7th June 2023).

[52] *The cost of capital in clean energy transitions – Analysis*. en-GB. URL: https://www.iea.org/articles/the-cost-of-capital-in-clean-energy-transitions (visited on 31st May 2023).

[53] *Euro Area Interest Rate - 2023 Data - 1998-2022 Historical - 2024 Forecast - Calendar*. URL: https://tradingeconomics.com/euro-area/interest-rate (visited on 31st May 2023).

[54] *Norway Corporate Tax Rate - 2022 Data - 2023 Forecast - 1981-2021 Historical - Chart*. URL: https://tradingeconomics.com/norway/corporate-tax-rate (visited on 31st May 2023).

[55] Tyler Stehly and Patrick Duffy. '2020 Cost of Wind Energy Review'. en. In: *Renewable Energy* (2022). URL: https://www.nrel.gov/docs/fy22osti/81209.pdf.

[56] *EUR Inflation Calculator - Euro (1991-2023)*. URL: https://www.inflationtool.com/euro (visited on 31st May 2023).

[57] European Central Bank. *ECB euro reference exchange rate: US dollar (USD)*. en. May 2023. URL: https://www.ecb.europa.eu/stats/policy_and_exchange_rates/euro_reference_exchange_rates/html/eurofxref-graph-usd.en.html (visited on 31st May 2023).

[58] *Final Report Summary - MEGASTACK (Stack design for a Megawatt scale PEM electrolyser.) | FP7*. en. download: https://www.sintef.no/contentassets/f8060684df6f459da532cb3aec6b cost-benefit-analysis-and-cost-and-performance-target-for-large-scale-pem-electrolyser-stack.pdf. URL: https://cordis.europa.eu/project/id/621233/reporting (visited on 31st May 2023).

[59] *Electrolysers – Analysis*. en-GB. URL: https://www.iea.org/reports/electrolysers (visited on 31st May 2023).

[60] Johan Carlsson et al. *ETRI 2014 Energy Technology Reference Indicator projections for 2010-2050*. Dec. 2014. DOI: 10.2790/057687.

[61] Wesley Cole, A Will Frazier and Chad Augustine. 'Cost Projections for Utility-Scale Battery Storage: 2021 Update'. en. In: *Renewable Energy* (2021). URL: https://www.nrel.gov/docs/fy21osti/79236.pdf.

[62] Kendall Mongird et al. '2020 Grid Energy Storage Technology Cost and Performance Assessment'. en. In: (2020). URL: https://www.energy.gov/energy-storage-grand-challenge/articles/2020-grid-energy-storage-technology-cost-and-performance.

[63] *Green hydrogen cost reduction*. en. Dec. 2020. URL: https://www.irena.org/publications/2020/Dec/Green-hydrogen-cost-reduction (visited on 31st May 2023).

[64] *UCEC 2020 upstream cost engineering committee, correspondence Even Solbraa.*

[65] Philipp Härtel et al. 'Review of investment model cost parameters for VSC HVDC transmission infrastructure'. en. In: *Electric Power Systems Research* 151 (Oct. 2017), pp. 419–431. ISSN: 03787796. DOI: 10.1016/j.epsr.2017.06.008. URL: https://linkinghub.elsevier.com/retrieve/pii/S0378779617302572 (visited on 31st May 2023).

[66] *09366: Kraftpriser i sluttbrukermarkedet, etter kontraktstype (øre/kWh) 2012 - 2022. Statistikkbanken*. no. URL: https://www.ssb.no/system/ (visited on 9th June 2023).

[67] Ministry of Climate and Environment. *Norway's comprehensive climate action plan*. en-GB. Nyhet. Publisher: regjeringen.no. Jan. 2021. URL: https://www.regjeringen.no/en/historical-archive/solbergs-government/Ministries/kld/news/2021/heilskapeleg-plan-for-a-na-klimamalet/id2827600/ (visited on 31st May 2023).

[68] Sean Bray. *Carbon Taxes in Europe*. en-US. Section: Business Taxes. June 2022. URL: https://taxfoundation.org/carbon-taxes-in-europe-2022/ (visited on 31st May 2023).

[69] *A European Green Deal*. en. July 2021. URL: https://commission.europa.eu/strategy-and-policy/priorities-2019-2024/european-green-deal_en (visited on 31st May 2023).

[70] *Havvind 2035 – Søk om støtte*. nb-NO. URL: https://www.enova.no/bedrift/industri-og-anlegg/havvind-2035/ (visited on 31st May 2023).

[71] *Renewable Energy Guarantees of Origin (REGO)*. en. URL: https://www.ofgem.gov.uk/environmental-and-social-schemes/renewable-energy-guarantees-origin-rego (visited on 31st May 2023).

[72] *REGO Index update – August 2022 - Renewable Exchange*. en-US. Aug. 2022. URL: https://renewable.exchange/blog/rego-index-update-august-2022/ (visited on 31st May 2023).

[73] *GO prices to trade for EUR 6-8/MWh in 2023 – Greenfact*. en. URL: https://www.montelnews.com/news/1405147/go-prices-to-trade-for-eur-6-8mwh-in-2023--greenfact- (visited on 31st May 2023).

[74] *The Future of Hydrogen – Analysis*. en-GB. URL: https://www.iea.org/reports/the-future-of-hydrogen (visited on 11th June 2023).

[75] *Nel CMD 2021: Launches 1.5 USD/kg target for green renewable hydrogen to outcompete fossil alternatives*. en-GB. Jan. 2021. URL: https://nelhydrogen.com/press-release/nel-cmd-2021-launches-1-5-usd-kg-target-for-green-renewable-hydrogen-to-outcompete-fossil-alternatives/ (visited on 8th June 2023).

[76] *Pricing*. en-CA. URL: https://www.methanex.com/about-methanol/pricing/ (visited on 8th June 2023).

[77] S. Mertens. 'Design of wind and solar energy supply, to match energy demand'. en. In: *Cleaner Engineering and Technology* 6 (Feb. 2022), p. 100402. ISSN: 2666-7908. DOI: 10.1016/j.clet.2022.100402. URL: https://www.sciencedirect.com/science/article/pii/S2666790822000076 (visited on 9th June 2023).

[78] *Methanol synthesis, correspondence Lars O. Nord.*

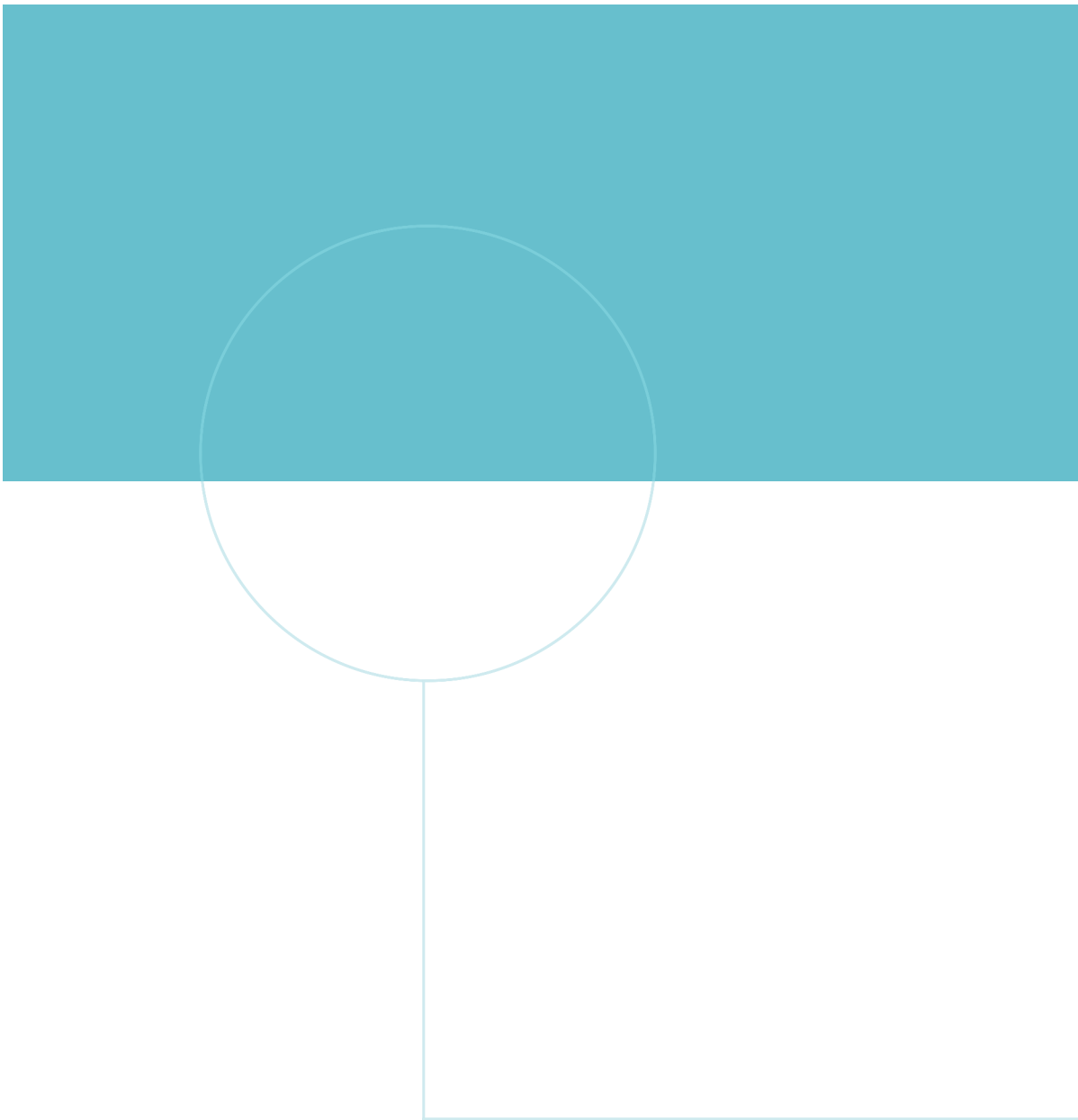

NTNU

Kunnskap for en bedre verden